ACR No. L6D17

NATIONAL ADVISORY COMMITTEE FOR AERONAUTICS

WARTIME REPORT

ORIGINALLY ISSUED
June 1946 as
Advance Confidential Report L6D17

PARAMETERS DETERMINING PERFORMANCE OF SUPERSONIC PILOTLESS AIRPLANES POWERED BY RAM-COMPRESSION POWER PLANTS

By Paul R. Hill

Langley Memorial Aeronautical Laboratory
Langley Field, Va.

NACA

WASHINGTON

Barrow

NACA ACR No. L6D17

NATIONAL ADVISORY COMMITTEE FOR AERONAUTICS

ADVANCE CONFIDENTIAL REPORT

PARAMETERS DETERMINING PERFORMANCE OF SUPERSONIC PILOTLESS AIRPLANES POWERED BY RAM-COMPRESSION POWER PLANTS

By Paul R. Hill

SUMMARY

The dimensional parameters of ram-compression power plants are related in this analysis to their thrust and economy performance, and the speed and range performance possibilities of a family of pilotless airplanes powered with such a power plant are investigated.

The performance calculations were made for a power plant in which the air enters the nose at stream velocity, a normal shock occurs inside the nose, the subsonic flow expands through an expanding diffuser to the velocity at the entrance of the combustion chamber, fuel is added and burning takes place in a constant-area tube, and the air expands to supersonic velocity through a contracting and expanding nozzle to stream pressure. A specific fuel consumption of 0.46 pound per thrust-horsepower-hour and a thrust of 3750 pounds per square foot of combustion-chamber area appears possible at sea level at a fuel-air ratio of 0.035.

In the study of pilotless-airplane performance, a body with a conical nose and a cylindrical afterbody was mounted on circular-arc-section wings that had a thickness ratio of 5 percent in the stream direction. All the lift was considered to be carried on the wings. The lift and drag were calculated by the Ackeret theory for two-dimensional flow at supersonic speeds. Performance was calculated for wide ranges of the basic parameters of power-plant size, gross weight, and wing area. A range of 1200 miles appears possible and speeds up to 3000 miles per hour (Mach number of 4) were calculated.

The calculated motor characteristics of subsonic ram-compression engines, the constants used in the computations, and the equations used in computing performance are given in appendixes. An example showing the method of computing thrust is included.

INTRODUCTION

Jet-propulsion systems using atmospheric air for combustion are the ram-compression engine of the intermittent-flow type and the jet-propulsion unit employing a blower, both of which have proved useful at subsonic velocities. Both these systems have maximum pressures greater than ram compression. As flight speed is increased, more pressure is available from ram compression and less reliance needs to be placed on auxiliary devices for obtaining high pressures. At supersonic velocities the continuous-flow ram-compression unit has a compression high enough for good efficiency and has a large mass flow of air per unit frontal area, which gives high power output.

In the present paper performance computations are made covering the speed range from a Mach number of 1.5 to one of 4.0. (Calculated engine characteristics of subsonic ram-compression engines are given in appendix A.) The ram-jet engine performance is treated as an aerodynamic and thermodynamic problem and the performance of the engines is given as a function of the areas, velocities, and temperatures involved in the design of such a unit. The engine performance is presented as the thrust per unit combustion-chamber area.

The airplanes upon which the computations are carried out consist of: (1) a fuselage housing the engine unit with a frontal area equal to the frontal area of the engine; (2) wings of circular-arc and diamond-wedge types, 5 percent or less in thickness ratio and with areas varying with the wing loading; (3) tail surfaces of the same types as the wing. The external lift and drag of the wing, body, and tail surfaces are based on the theoretical work of Ackeret and Busemann (references 1 to 3), which has experimental verification and is sufficiently accurate for high fineness ratios. Speed and range performances are

computed for wide ranges of the basic parameters of weight, power-plant area, wing area, and altitude.

There are numerous major problems to be encountered in the successful design and operation of a ram-jet powered airplane that are beyond the scope of this paper. Among these problems are take-off or launching, landing, structural design, stability, control, burner design, and cooling. These problems will take considerable time and ingenuity to surmount.

ANALYSIS OF SUPERSONIC RAM-COMPRESSION POWER PLANTS

The following analysis is devoted to a description of the power-plant configurations, a description of the power-plant cycle, and an analysis of the power and economy performance.

Power-Plant Configuration

The power plant is a duct consisting of an entrance or compression region, a combustion chamber, and an exhaust nozzle. Schematic drawings showing the configurations of the ducts upon which the calculations of this paper are based are shown in figure 1. The leading edge is a sharp ring formed by the intersection of the conical external surface with the internal surface of the duct.

Computations are presented for three configurations of the compression region of the ducts. In figure 1(a) the compression region consists of a gradually expanding cone, or diffuser, which begins at the leading edge and extends to the combustion chamber. In figure 1(b) the compression region begins as a circular cylinder, or pipe. Behind the pipe follows the expanding cone leading to the combustion chamber. The purpose of introducing the pipe is to form a cargo space between the inner and outer shells ahead of the combustion chamber. In figure 1(c) the compression region begins as a short contracting cone giving a small reduction in duct area. The contracting part is followed by an expanding cone extending to the combustion chamber. The purpose of adding the contracting cone, or supersonic diffuser, is to decrease the stream velocity before the occurrence

of normal shock. Test data for this type of entrance for the part of the duct from station 1 to station 4 were obtained from reference 4.

The combustion chamber is simply a circular cylinder. Fuel is added at the beginning of the combustion chamber. The cross-sectional area of the combustion chamber is used herein as a reference area.

The exhaust nozzle, of the Laval type, consists of a contracting section to speed up the gases to the local velocity of sound at the throat and an expanding section for obtaining supersonic gas speeds.

Aerodynamic and Thermodynamic Cycle

The cycle of the supersonic ram-jet motor operating at design conditions is described for the entrance-region configuration of figure 1(b), which is a more general case than the configuration of figure 1(a). The cycle is illustrated by a diagram showing the variation of pressure, velocity, and temperature (fig. 2(a)) and a pressure-volume diagram (fig. 2(b)). The air enters the duct at free-stream velocity. Immediately inside the duct a normal shock wave reduces the velocity to a subsonic value and creates a sudden rise in pressure. This compression is shown in figure 2(a) as a vertical line at station 2 and in figure 2(b) as a line connecting stations 1 and 2. After the shock wave the air flows through the cylindrical part of the duct at subsonic velocity and a friction pressure drop from stations 2 to 3 results. A further compression is then obtained by a reduction in air velocity through the diffuser cone, stations 3 to 4.

Station 4 is at the entrance to the combustion chamber. Here the velocity is at its minimum value and the pressure at its maximum. At this point the fuel is added. As the burning progresses, an expansion takes place together with a proportionate speeding up of the gases because the cross-sectional area of the combustion chamber is constant. The acceleration of the gases and the friction losses produce a drop in pressure from stations 4 to 5, as shown in figure 2(b). Part of the diagrams where the curves are not clearly defined are dashed.

The exhaust nozzle, stations 5 to 7, accelerates the gases from subsonic to supersonic velocity as it expands the gases from the pressure at the end of combustion to atmospheric pressure at the end of the nozzle.

Constants Used in Power-Plant Computations

The constants used in the power-plant analysis are listed below. A complete list of the conditions assumed for the analysis is given in appendix B, and the symbols are defined in appendix C.

(1) The friction factor is 0.0030 in the entrance pipe. This value can be obtained only in a smooth, polished pipe.

(2) The subsonic diffuser has an efficiency of 90 percent.

(3) The lower heating value of fuel is 19,000 British thermal units per pound.

(4) Incomplete combustion and heat transfer through the combustion-chamber walls are accounted for by a combustion efficiency factor shown in figure 16.

(5) The ratio of specific heats varies with temperature and fuel-air ratio (figs. 15(a) and 15(b)).

(6) The friction pressure loss in the combustion chamber is 10 percent of the average dynamic pressure.

(7) The exhaust-gas velocity at the nozzle exit is 97 percent of the value for isentropic expansion to the pressure at the nozzle exit.

Power-Plant Performance

Figures 3(a) to 3(d) give power-plant data for ram-jet units with a cylindrical-pipe entrance. The pipe has sufficient length to make the over-all length-diameter ratio of the airplane fuselage 10. Figures 3(e) and 3(f) are for ram-jet units with supersonic-diffuser entrances. The stream Mach number 1.673 was chosen because experimental data are available for this value. Figure 3 is for a fuel-air ratio of 0.033 and an altitude

of 35,500 feet. This altitude was chosen because it is in the lower edge of the stratosphere, or constant-temperature region. Figure 3 shows the thrust per square foot of combustion-chamber area F/A_4, maximum temperature occurring in the cycle t_5, and the ratio of three important areas to the combustion-chamber area: entrance area A_2/A_4, nozzle-throat area A_6/A_4, and nozzle-exit area A_7/A_4, all expressed as functions of the velocity at entrance to the combustion chamber v_4.

The combustion-chamber entrance velocity is a significant parameter because, for any given flight Mach number and compression efficiency, this velocity determines the mass flow per unit combustion-chamber area and the compression ratio and influences the frictional losses. Both power and economy are therefore affected by the combustion-chamber velocity. The ratio of nose-entrance area to combustion-chamber area determines, for given initial stream condition and compression efficiency, the velocity at entrance to the combustion chamber. The lower limit of the combustion-chamber velocity is zero, which corresponds to a nose area of zero. An upper limit is the value that produces the speed of sound at the combustion-chamber exit and chokes the flow.

Inasmuch as the thrust per square foot of combustion-chamber area is given, the thrust of any size unit may be obtained by multiplying the thrust per unit area by the combustion-chamber area. Also, if such small effects as the change in friction factor with a change in Reynolds number are neglected and all independent parameters except density are held constant, the thrust obtainable at a given atmospheric temperature is proportional to atmospheric density. Since standard atmospheric temperature is constant above the altitude for which the charts are constructed, 35,500 feet, the power at any higher altitude can be obtained by multiplying the power as read from figure 3 by the relative-density ratio. Likewise, the areas given are also valid for standard conditions at any higher altitude.

When A_7 is larger than A_4, A_7 becomes the effective drag area. In order to locate the maximum thrust per unit effective drag area for complete

expansion nozzles, a curve of F/A_7 is introduced for the range where A_7 is larger than A_4. The negative slope of this curve shows that the complete expansion nozzle gives a reduction in thrust-drag ratio in this range. A vertical line is drawn on figure 3(a) at the value of v_4 making A_7/A_4 equal to unity. Schematic drawings on figure 3 illustrate the proportions of the ducts.

Stream Mach number has a marked effect on maximum flame temperature; t_5 is increased from 1990° F to 3125° F by an increase in stream Mach number from 1.5 to 4.0 (figs. 3(a) and 3(d)). Also, figure 3 shows that at the lower Mach numbers the combustion-chamber velocity has an appreciable effect on temperature. For example, at a Mach number of 1.5, the temperature drops 150° F for an increase in v_4 of 40 feet per second. At a Mach number of 4.0 the drop is only 6° F for an equal change in v_4.

Figure 3(g) gives a comparison of the design thrust at a fuel-air ratio of 0.035 of the ram-compression engines treated herein with the static thrust per square foot of frontal area of a turbocompressor jet-propulsion unit in current use, designed for high thrust output. The thrust of the turbojet unit is seen to be between the thrusts of subsonic and supersonic ram-compression units.

Figure 3(h) shows the temperature and pressure of the air at the entrance to the combustion chamber. The purpose of this figure is to give information pertinent to the ignition problem. For a stream Mach number of 4.0, the temperature of the air is above the ignition temperature for many fuels at the pressure obtained. The figure is made for pipe entrances for an over-all length-diameter ratio of 10 and a velocity at entrance to combustion chamber of 250 feet per second. A change in the length-diameter ratio or entrance velocity has a negligible effect on ignition qualities. Stream Mach number and altitude have a significant effect.

In figure 4(a) are shown cross plots of the basic thrusts obtained in figure 3 as functions of stream Mach number. In addition, the thrust with entrance pipes for an over-all length-diameter ratio of 15 and the thrust for the case in which the pipe length is zero are also

shown. The thrust increases rapidly to a Mach number of 3. At a Mach number of 4 the thrust begins to decrease because of the decreased efficiency of pressure recovery across the shock wave.

The supersonic-diffuser entrance gives the greatest thrusts and the longest pipes the lowest thrusts, although there is not a great difference. The object of changing the proportions (over-all length-diameter ratio) is to investigate cases with different amounts of cargo space forward of the combustion chamber. The fuel capacity of the wing tanks of airplanes traveling at supersonic speeds is necessarily small because of the low thickness ratios of the wings. (Wing volumes are treated in appendix B.)

Values of specific fuel consumption for the same power plants are also shown in figure 4(a). Units of pounds per horsepower-hour are used because of the familiarity of this unit for the conventional engine. When the cooling and propeller losses of the conventional engine are considered, the economy shown at a Mach number of 1.5 equals that of a conventional-engine propeller system at design speed and military power, at a Mach number of 2 equals the economy of the engine propeller systems in cruising, and at a Mach number of 3 or 4 is better than that of the most efficient engine propeller system.

Figure 4(b) shows the thrust and economy of power plants designed to operate at sea level with a fuel-air ratio of 0.033. The designs have entrance pipes for a length-diameter ratio of 10. Favorable thrust and economy are shown. For example, at a Mach number of 2.0 the computed thrust is 3000 pounds per square foot of combustion-chamber area and the specific fuel consumption is 0.65 pound per thrust-horsepower-hour. At a Mach number of 3.2 the thrust is 3750 pounds per square foot and the specific fuel consumption is 0.46 pound per thrust-horsepower-hour.

Operation of a Power Unit with Fixed Areas at Various Flight Speeds

The power-plant operation so far considered has been at a design operating speed. Some factors affecting

the operation of a given unit at other than design speed will be considered. For a system of fixed dimensions the mass flow of air entering the duct at stream velocity is proportional to the forward speed. The condition that the product of the density and speed of the gases at the throat of the nozzle is proportional to the forward speed must therefore be met. Because of the increased compression of the air at operating speeds above design speed, the throat is more than large enough for operation at design fuel-air ratio with the shock wave at the entrance. Pressure and temperature combinations giving the required conditions at the nozzle throat are obtained by either a readjustment of the internal flow through a movement of the shock wave or a change in the fuel-air ratio.

Movement of shock wave.- A movement of the shock wave in the duct is forced by a change in downstream pressure whether the duct is an expanding or a constant-diameter pipe. Experimental verification of these phenomena is presented in references 4 and 5. In order to illustrate the nature of these phenomena, figure 5(a) shows the calculated equilibrium conditions between shock-wave position in a constant-diameter pipe and the pressure at the end of the pipe. This computation was carried out for a friction factor of 0.003, an entrance Mach number of 2.0, and a pipe length of 25.55 diameters, which is the choking length of the pipe for the assumed conditions. As the position of the shock wave moves downstream, the increased amount of energy lost in friction accounts for the drop in pressure at the end of the pipe. Figure 5(b) shows the calculated equilibrium between pressure at the end of an expanding pipe and the position of the shock wave. The entrance Mach number is 1.5, the expansion angle measured between the walls of the pipe is 3.0°, $l/d_1 = 13.2$, and the friction factor is 0.003. Small movement of the shock wave in a tapered pipe corresponds to considerable pressure regulation. A larger travel of the shock wave is needed in a straight pipe. In a ram-jet duct with a cylindrical entrance pipe there is no reason why the shock wave cannot move through the pipe into the subsonic diffuser.

Figure 6 shows the change in thrust of power plants with increase in speed at constant fuel-air ratio for two types of entrance. At the lowest Mach number

shown for each entrance, the shock wave is in the extreme forward position and moves back with an increase in forward Mach number. This type of regulation is advantageous because it is purely automatic. If the speed is decreased below that at which the shock wave is at the throat of the supersonic diffuser or the entrance to the straight pipe, the shock wave moves out in front and the mass flow and power output are reduced. Another result of the movement of the normal shock in front of the entrance is an increase in the external pressure drag.

Control by change in fuel-air ratio.- In order to obtain increased thrust at speeds above design speed or for flight at reduced speed, control is effected by regulation of the fuel-air ratio. Figure 7 shows the results obtainable above and below design speed by varying the fuel-air ratio to keep the shock wave at the entrance.

The curves are computed for a unit with entrance-pipe for $l/d = 10$. Entrance and throat area are optimum for a fuel-air ratio of 0.033 and a Mach number of 2.0. The required range of fuel-air ratio is from 0.018 to 0.056 for a range of operating Mach number from 1.5 to 2.5. The curve of fuel-air ratio applies to all the thrust curves shown. The thrust curves are drawn for three ratios of nozzle-exit area to combustion-chamber area: 0.79, 0.89, and 1.0. These areas expand the exhaust gases to atmospheric pressure at stream Mach numbers of 1.5, 1.75, and 2, respectively. At higher Mach numbers the pressure at the nozzle exit is above atmospheric. The reduced thrust with the smaller nozzle-exit areas at a given Mach number is due to incomplete expansion of the combustion gases in the nozzle.

A comparison of the thrust curves of figures 6(a) and 7 for a ratio of exit area to combustion-chamber area of unity shows that the increase in thrust as the speed is increased from a stream Mach number of 2.0 to 2.5 is 12 percent with a constant fuel-air ratio of 0.033 and 77 percent with change in fuel-air ratio. The specific fuel consumption also drops with change in fuel-air ratio (not shown) from 0.70 to 0.63 pound per horsepower-hour.

Effect of Changing Design Fuel-Air Ratio

A decrease in the fuel-air ratio for a given operational speed and altitude creates hotter exhaust gases that occupy a larger volume per pound of gas. The ratios of nozzle area to entrance area are therefore increased to accommodate the increased volume of flow. A change in the design fuel-air ratio for any given design speed and altitude necessitates a change in the dimensions of the power plant.

Figures 8(a) and 8(b) show power-plant characteristics at sea level for two design values of fuel-air ratio. The stream Mach number is 1.5. The nozzle-exit areas A_7 are the proper size to expand the exhaust gases to atmospheric pressure. The design thrust per square foot of combustion-chamber area at a fuel-air ratio of 0.033 is 1950 pounds. If the mixture is given all the fuel that can be burned, fuel-air ratio of 0.067, F/A_4 is 2390 pounds per square foot. The primary reason why the thrust did not increase more rapidly is the reduction in mass flow (v_4 is reduced from 300 to 230 fps) to make the nozzle-exit area equal to the combustion-chamber area. At $v_4 = 248$ feet per second the velocity at the exit of the combustion chamber reaches the speed of sound, or choking takes place. This velocity is marked by a vertical line on figure 8(b). No higher velocity is possible at this fuel-air ratio. Because of the high flame temperatures with a fuel-air ratio of 0.067, choking takes place at a lower value of v_4 than for leaner mixtures. A nozzle designed for this condition would have no throat but would merely flare outward. The thrust per square foot of this power plant is 2440 pounds.

A ram jet designed for a fuel-air ratio of 0.033 at 35,500 feet has entrance and nozzle-throat areas of 0.343 and 0.908 square foot per square foot of combustion-chamber area. From a series of figures such as 8(a) and 8(b) it can be determined that for this design to operate at sea level with the shock wave at the entrance a fuel-air ratio of 0.048 is required. The extra thrust so derived may be used for acceleration or climb.

AIRPLANE PERFORMANCE

The purpose of a performance-parameter study is to relate the knowledge in the particular field and determine from the relationships of this knowledge the influence of each parameter on performance possibilities in the light of existing data. No experimental data exist on the drag of bodies and wings at supersonic speed other than for the simplest shapes. Simple body and wing shapes, such as the cylinder, the cone and the wedge, were therefore chosen as the basis of computation. The accuracy of the lift and drag results computed from equations available for these simple shapes is sufficient for establishing trends. Knowledge in the field of supersonic flow, however, is today in a state of rapid growth. As theoretical and experimental drag data for more complex shapes become available, these shapes may be shown to be superior to the simple shapes herein considered; therefore the results given in the present paper tend to be conservative.

In making a performance-parameter study many variables must be fixed at mean or accepted values in order to investigate the main parameters involved. For example, all external surfaces are assumed to be perfectly smooth and without protuberances of any kind. If it becomes necessary to add various items that raise the external drag above that of a smooth body, the results herein presented will be unconservative.

The following study of the performance of supersonic airplanes powered with ram-compression engines is presented as an engineering approximation of the possibilities of such airplanes. The effects of weight, wing area, frontal area, and altitude on the possible speed and range performance of two families of airplanes are shown. As experience makes more exact knowledge available, these estimates of performance possibilities and trends will have to be reevaluated.

Description of Airplane Characteristics

The speed and range performances are computed for airplanes housing a single power plant in a fuselage of the same diameter as the power plant. Computations are

carried out for a wide range of gross weight, power-plant size, and wing area.

Performance is computed for the basic design condition of the power plants at a fuel-air ratio of 0.033 The fuel-air ratio is arbitrarily chosen at a value between the lower limit for complete combustion, 0.067, and a value of 0.0167, which is common in turbojet units because of temperature limitations in the turbine. A value of 0.033 was chosen; this value allows a margin for enriching the mixture to obtain excess power for climb and for flexibility of operation. The other essential characteristics are:

(1) The nose is conical and has a slope of 1/10.

(2) The body is cylindrical.

(3) The over-all length-diameter ratio is either 10 or 15.

(4) The wing has a thickness ratio of 5 percent and a double-circular-arc section except where diamond-section airfoils are introduced to show the effect of a change in section. The section thickness is to be measured in a plane parallel to the air stream. A study of reference 3 shows that the wing-drag equations used herein (appendix D) apply with sufficient accuracy if the shock wave is attached to the leading edge. Aside from the restrictions stated, the plan form is not specified. Induced tip losses are assumed to be negligible. If necessary, this condition can be met by making the angle between the tip line and the stream direction greater than the Mach angle (reference 3). All lift is assumed to be carried on the wing.

(5) The tail area is 25 percent of the wing area.

Speed

Figures 9(a) and 9(b) show the speed of two families of ram-jet units with length-diameter ratios of 10 and 15 at an altitude of 60,000 feet. The speeds are plotted with coordinates of weight per unit power-plant area W/A and wing loading W/S_w, where W is the gross weight, A is the power-plant and also the fuselage frontal area,

and S_w is the wing area. The wing area used does not include the area projected through the fuselage. The curves are for inlet and nozzle areas designed for the speeds shown and the nozzle designs are uncompromised for other speeds. Weight per unit power-plant area is a quantity parallel to power loading for a conventional engine because the thrust and power of a series of geometrically similar ram-jet units are proportional to frontal area. The fact that power is proportional to frontal area makes the speed charts applicable regardless of the size of the units. No important scale effects enter the problem as with the conventional airplane engine, for which power per unit frontal area of the engine is much greater in the larger units.

If the angle of attack of a wing in flight at supersonic speed is too great, an excessive blocking of the air stream occurs. The shock wave then is detached from the leading edge and forms a bow wave, and the drag increases. At a Mach number of 1.5 the highest obtainable lift coefficient for circular-arc sections with a thickness ratio of 5 percent is approximately 0.4. The performance curves for this Mach number are accordingly terminated at a wing loading corresponding to this lift coefficient. The limiting values are higher at higher Mach numbers and are off the charts.

The use of the speed chart will be illustrated by examples.

Example 1.- For a flight Mach number of 2.0 what is the most favorable wing loading and maximum total weight that can be carried by a ram-jet airplane with a power-plant area of 1 square foot at an altitude of 60,000 feet? Solution: From figure 9(a) the most favorable wing loading is 85 pounds per square foot and the total weight may be 1100 pounds if the over-all length is 10 diameters. If the over-all length is 15 diameters, figure 9(b) shows the same wing loading to be optimum and the weight to be 895 pounds.

Example 2.- Same as example 1 (wing loading of 85 lb/sq ft) except that the power-plant area is 10 square feet. Solution: The maximum weight for $l/d = 10$ is 11,000 pounds and for $l/d = 15$ is 8950 pounds.

Example 3.- What could the weight of the airplanes of example 1 (wing loading of 85 lb/sq ft) be at (1) 35,000 feet? (2) at sea level? Solution: (1) From figures 9(c) and 9(d), 1990 and 1630 pounds could be supported at 35,500 feet, about an 80-percent increase in carrying capacity. (2) From figure 9(e), 1900 pounds could be supported at sea level.

Example 4.- What could the weight of the airplane be at 35,500 feet if the wing loading were optimum for this altitude? Solution: From figures 9(c) and 9(d) at a flight Mach number of 2.0 and a wing loading of 270 pounds per square foot, the weight capacities are 3550 and 2880 pounds.

Range

Ranges obtainable by the airplanes for $l/d = 10$ represented in figures 9(a) and 9(c) are given in figures 10(a) and 10(b) for the same conditions of operation; that is, for the same altitude, speeds, and combinations of W/A and W/S_w. These ranges are based on the assumption that the fuel weight is 50 percent of the gross weight. The range, however, is proportional to the percentage of fuel carried and the ranges for any other amount of fuel carried may be obtained by proportion.

Example 5.- Find the range of the ram-jet airplane of example 1 (wing loading of 85 lb/sq ft) if the fuel load is 50 percent of the weight and $l/d = 10$. Solution: From figure 10(a) the range at 60,000 feet is 1225 miles.

Example 6.- Find the range of the ram-jet airplane of example 1 at 35,500 feet altitude. Solution: From figure 10(b) the range is 690 miles.

Example 7.- What is the range at an altitude of 35,500 feet if the optimum wing loading is used? Solution: From figure 10(b), at a wing loading of 270 pounds per square foot the range is 1225 miles, a value identical with that obtainable at 60,000 feet.

Example 8.- What is the range of a sea-level design similar to the airplane of example 1 if 50 percent of the

weight is fuel load? Solution: Figure 10(c) shows that the range at a wing loading of 85 pounds per square foot has dropped to 190 miles. Extremely high wing loading is needed for a more favorable range.

Effect of Wing Section on Speed

The total wing drag at supersonic speed is substantially the sum of the pressure drag due to wing section, the pressure drag due to lift, and the skin-friction drag. If the drag due to wing section is reduced, the drag due to lift or weight can be increased a like amount for a given speed. For thin sections the drag of a symmetrical wedge section is three-fourths the drag of a double-circular-arc section, and the section drag is proportional to the square of the section thickness ratio. Figure 11(a) shows a gain in carrying capacity of 8 percent for a change from the circular-arc to the wedge section and a gain of 51 percent for a change to zero thickness ratio. Figure 11(b) gives the same percentage increases in range if fuel load remains 50 percent of the gross weight.

Effect of Size on Performance

It has already been pointed out that speed and range are functions of the parameters W/A and W/S_W; however, the possible values of W/A depend on the size and proportions of the airplane. The value of W is dependent on the fuselage length or length-diameter ratio and also on the fuselage area A. Consequently the ratio of W to A is also dependent on A. Because of the relatively small wings of a supersonic airplane, W depends on the wing area to a smaller extent than on the fuselage size. The weight depends on, first, the structural weights and, second, the available space for cargo and the cargo density. In order to obtain some idea of the variation of W/A and W/S_W with A, structural weights were roughly estimated and a cargo of a density equal to that of fuel, or 45 pounds per cubic foot, was assumed to occupy all available space in both wing and fuselage. No allowance was made for metal-wall thicknesses in computing cargo space. The manner of estimating structural weights and volumes is described in appendix B. The resulting values of

fuselage area, which should be considered merely comparative because of the assumptions involved, are shown by the dashed lines of figure 12 for length-diameter ratios of 10 and 15. Values of W/A increase rapidly with increases in A.

Ranges are computed for the idealized case in which no allowance is made for the weight of controls or fixed equipment and the total cargo is fuel. Figure 12(a) shows that the range increases markedly with an increase in the size parameter A. The airplane with the larger over-all length-diameter ratio is smaller for the same range. For example, the curve for a range of 400 miles intersects the curve for a frontal area of 5 square feet on figure 12(a) and the curve for a frontal area of 2 square feet on figure 12(b). The limitation of cargo space for fuel on a supersonic airplane is responsible for the variation of range with size and length-diameter ratio.

Figure 13, which is plotted from the same computation as figure 12, shows how the range varies with gross weight and wing loading. The values obtained are only comparative. Figure 13(a) shows that a very large gross weight corresponds to the larger ranges for a length-diameter ratio of 10. The minimum weight is 160,000 pounds for the 1200-mile range. Figure 13(b) shows that the same range is obtainable at a gross weight of 63,000 pounds if the length-diameter ratio is 15. It is concluded that the gross weights need not be nearly so great to have good range for the larger length-diameter ratio.

CONCLUDING REMARKS

Calculations for the supersonic continuous-flow ram-compression power plants demonstrate favorable thrust and economy characteristics. For example, with a cylindrical entrance pipe in which the normal-shock loss occurs, a fuel-air ratio of 0.033, a flight Mach number of 2.0, and standard sea-level air density, the computed thrust is 3000 pounds per square foot of cross-sectional area and the specific fuel consumption is 0.65 pound per thrust-horsepower-hour. Computations show that it is possible to operate a fixed design over a range of

supersonic speeds and that the thrust can be regulated by changing the amount of fuel injected.

Calculations made on simple pilotless airplanes between flight Mach numbers of 1.5 and 4.0 demonstrate favorable performance possibilities. For example, for a body with a conical nose, a cylindrical body and a wing and a tail of circular-arc sections and 5-percent thickness ratio, level-flight speeds up to a Mach number of 4 and a range of 1200 miles were calculated.

Langley Memorial Aeronautical Laboratory
National Advisory Committee for Aeronautics
Langley Field, Va.

APPENDIX A

SUBSONIC CONTINUOUS-FLOW RAM-COMPRESSION POWER PLANTS

The subsonic power plant differs from the supersonic power plant in the shape of the entrance region and the exhaust nozzle. Air entering a subsonic ram-compression power plant is partly compressed externally. The leading edge of the duct, or entrance lip, should be rounded to prevent high external drag. Also, the exhaust velocity is less than the local speed of sound in the exhaust gases at discharge. If the duct were frictionless and no heat were added, the total pressure (stagnation pressure) at exit would equal the total pressure at inlet. Under these circumstances, when the pressure of the exhaust gases is reduced to atmospheric pressure, the local Mach number of the exhaust stream is equal to the Mach number of the entering stream, or the flight Mach number. Both friction and heat cause a reduction in total pressure. The local Mach number of the exhaust gases when expanded to atmospheric pressure must then be less than the flight Mach number. The subsonic power plant therefore requires a simple converging nozzle rather than the converging-diverging nozzle of the supersonic power plant. The same assumptions and methods of computing performance are used for subsonic power plants as for supersonic power plants except that the incoming air does not pass through a shock wave.

Figures 14(a) and 14(b) show subsonic-power-plant data similar to the supersonic data of figure 3. Maximum thrust at a Mach number of 0.4 is 96 pounds per square foot of frontal area. At a Mach number of 0.8 the maximum thrust is 440 pounds per square foot, or the thrust varies about as the square of the speed. The thrust curve is very flat, so that v_4 may be selected from considerations other than thrust, such as low combustion-chamber velocity, to simplify the burner-installation problem. The fuel rate is proportional to v_4, so that the power plant is least economical at high values of v_4.

Nozzle-exit area (expressed as a fraction of the combustion-chamber area) is the only significant area in the subsonic ram jet. (The nozzle has no throat.) From the standpoint of control of the internal flow, it makes no important difference what part of the compression takes place externally and what part, internally. The size of the entrance is therefore not critical. At a given forward speed the value of v_4 is determined mainly by the exit area. Figure 14(a) shows that, at a Mach number of 0.4 and an exit area A_7 of 0.80, v_4 is 110 feet per second and thrust is at its peak. At a Mach number of 0.8 (fig. 14(b)) the same exit again places the thrust near its peak. From this observation it is apparent that a given exit area gives nearly the same power-economy compromise regardless of stream Mach number. In other words, a subsonic ram-jet power plant will operate consistently over a wide speed range. To a first degree of approximation, the internal velocities are proportional to the stream Mach number, as is normal for a duct system of fixed dimensions.

Figure 14(c) shows, for a fuel-air ratio of 0.053, the maximum thrust and corresponding specific fuel consumption at various subsonic Mach numbers. The upper thrust curve shows the thrust available with an open-nose cowling and the lower one shows for an extreme case the penalty for running the air through a duct at high speed $\left(\frac{v_2}{v_1} = 0.3\right)$. The duct has a length giving an over-all l/d of 10. The specific fuel consumption for the subsonic ram jet is extremely poor; the specific fuel consumption has a value of about 4 pounds of fuel per horsepower-hour at a Mach number of 0.8 and increases without limit as the speed decreases.

APPENDIX B

CONDITIONS USED IN ANALYSIS

The conditions used in the analysis are listed in detail below and their applications are demonstrated in appendix D:

(1) One-dimensional-flow theory is assumed to hold with sufficient accuracy.

(2) The friction pressure drop in the entrance pipe (if one is used) is computed with a friction factor $f = 0.003$ in the expression $\Delta p_f = 4f \frac{l_{2,3}}{d_2} q_{2,3}$ where $l_{2,3}/d_2$ is the entrance-pipe length-diameter ratio and $q_{2,3}$ is the average dynamic pressure in the pipe. The flow is compressible and the momentum pressure drop is computed. A friction factor f of 0.003 is used for all external surfaces in addition to pressure drags.

(3) The instantaneous values of the ratio of specific heats γ used for air and for the products of combustion are given in figure 15(a). The corresponding average values between 0° F absolute and the temperature in question $\bar{\gamma}$ are given in figure 15(b). The values of the gas constant used for the products of combustion are given in figure 15(c). These values are computed from specific-heat equations and constants obtained from reference 6.

(4) The expanding (subsonic) diffuser used with the pipe entrance is assumed to have a total-pressure recovery equal to 90 percent of the reduction in dynamic pressure through the diffuser.

(5) The fuel is added at the entrance of the combustion chamber. The momentum required to bring the fuel up to combustion-chamber velocity is charged as a momentum pressure loss.

(6) The friction pressure loss in the combustion chamber is taken as 10 percent of the average of the initial and final dynamic pressures in the combustion chamber. The lower heating value of the fuel is 19,000 British thermal units per pound.

(7) The heat lost through the combustion-chamber walls is treated as a reduction in combustion efficiency. The values of combustion efficiency assumed for various fuel-air ratios are given in figure 16.

(8) The exhaust nozzle is assumed to have a velocity coefficient of 0.97 when operating at design pressure ratio or as an underexpanding nozzle. No computations were made for overexpanding nozzles.

(9) Performance data for a supersonic diffuser capable of operating at Mach numbers at and above 1.673 were obtained from reference 4. This diffuser is used as the basis of performance calculations of power plants with design Mach numbers up to 2.0. This diffuser has a contraction ratio (ratio of entrance to throat area) of 1.137. The included angle between the walls of the contracting cone is 13°, and the included angle between the walls of the expanding cone is 3°. The test values of total-pressure-recovery ratio under the ideal operating condition in which the normal shock wave is located very near the throat is given in figure 17. This operating condition is referred to herein as a "design" condition. Other positions of the normal shock wave result in a reduced pressure-recovery ratio.

(10) For ram-jet motors having an entrance pipe and operating at design speed, it is assumed that a normal shock occurs in the entrance and extends completely across the pipe. The usual equations for a plane shock disk are used to determine the velocity, pressure, and density ratios across the wave. These ratios, shown in figure 18, were obtained from reference 7.

(11) The length of the constant-diameter entrance pipe is determined by subtracting the length of the nozzle, combustion chamber, and subsonic diffuser from the over-all length. For this purpose, the combustion-chamber length is taken as 2 diameters, and the nozzle and diffuser are assumed to have cone angles giving them an average slope of 1/10; that is, the nozzle and diffuser lengths are five times the difference in their respective inlet and outlet diameters.

(12) For computing speed

(a) The wings are assumed to have double-circular-arc sections of 5-percent thickness ratio in the free-stream direction, except as otherwise noted.

(b) Ackeret's theory of pressure drag is applied.

(c) The tail surfaces have an area equal to 25 percent of the wing area and have the same sections.

(d) The conical nose has a half-angle of 5.73°, or 0.1 radian. The equation (from reference 2) used to estimate the pressure drag of the nose is that applying to the conical nose of a very pointed bullet

$$C_D = \alpha^2 \log_e \frac{4}{\alpha^2\sqrt{(v/c)^2 - 1}}$$

where

C_D drag coefficient based on frontal area

α half-angle of cone, radians

v/c flight Mach number

The drag equation for a pointed cone was used in the computations because no equation for the drag of an open-end conical nose was available at the time the computations were made. Actual nose drags would be higher than those calculated by the foregoing equation because the flow at the air entrance becomes two-dimensional.

(13) For computing ranges the fuel weight in most instances is taken as 50 percent of the gross weight. In some instances the proportion of fuel weight is estimated by first estimating the structural weights and volume available for fuel storage. For this purpose the wing is chosen with an aspect ratio of 4, a design load factor of 4, a thickness ratio of 5 percent, and a taper ratio of 2.5. The wing weights obtained are shown in figure 19. The wing volumes for an aspect ratio of 4 and taper ratio of 2.5 are shown in figure 20(a). The volumes are those generated by the wing sections; no allowance has been made for metal thickness. In calculating the aspect ratio, only the area and span extending outside the fuselage are used. Figures 20(b) and 20(c) give volumes of wings with aspect ratios of 2.0 and 1.0

and infinite taper ratio (pointed tips). Tail weight is taken as 15 percent of the wing weight. Fuselage proportions used are appropriate for a design Mach number of 2.0. The fuselage is assumed to be built of duralumin, but the combustion chamber and nozzle are of steel. The fuselage-wall thickness is given in figure 21 as a function of the diameter.

APPENDIX C

LIST OF SYMBOLS

a	coefficient of X^2 in quadratic equation $ax^2 + bx + c = 0$
A	projected frontal area of power plant or fuselage, sq ft
A_2	area of air-duct entrance, sq ft
A_f	projected frontal area of cone, sq ft $(A - A_2)$
b	coefficient of x in quadratic equation
c	speed of sound, fps; also constant term in quadratic equation
C	ratio of friction pressure loss in combustion chamber to average dynamic pressure
C_D	drag coefficient
C_{D_n}	pressure drag coefficient of nose
C_{D_w}	pressure drag coefficient of wing
C_L	lift coefficient
C_v	nozzle velocity coefficient
d	diameter of cylindrical fuselage, ft
d_2	diameter of air-duct entrance, ft
f	friction factor
F	ram-jet thrust, lb
g	acceleration of gravity (32.17 ft/sec^2)

H	stagnation pressure, lb/sq ft
H.V.	lower heating value of fuel, Btu/lb
J	mechanical equivalent of heat (778 ft-lb/Btu)
l	over-all length, ft
$l_{2,3}$	length of entrence pipe, ft
l_n	length of conical nose, ft
p	static pressure, lb/sq ft
Δp_f	friction pressure drop, lb/sq ft
q	dynamic pressure, lb/sq ft $\left(\frac{1}{2}\rho v^2\right)$
q_c	impact pressure, lb/sq ft (H - p)
R	range, miles
R_a	gas constant for air (53.3 ft-lb/($^\circ$F)(lb))
R_c	gas constant for products of combustion, ft-lb/($^\circ$F)(lb)
S_f	area of fuselage surface, sq ft
S_w	wing area, sq ft
t	temperature, $^\circ$F
T	temperature, $^\circ$F abs.
v	air or gas speed, fps
V	speed of ram-jet airplane, fps
w_f	weight of fuel, lb
W	gross weight of ram-jet airplane, lb
W_a	weight rate of air flow, lb/sec

W_f weight rate of fuel flow, lb/sec

α half-angle of conical nose

β half-angle between upper and lower wing surfaces at leading or trailing edge

γ ratio of specific heat at constant pressure to specific heat at constant volume

$\bar{\gamma}$ average value of γ between 0° F abs. and temperature T

η_c combustion efficiency

η_d subsonic-diffuser efficiency

ρ mass density, slugs/cu ft

Subscripts denoting stations along power-plant duct:

1 free stream

2 entrance

3 end of cylindrical entrance pipe; entrance to diffuser

4 end of diffuser; entrance to combustion chamber

5 end of combustion chamber; entrance to nozzle

6 nozzle throat

7 end of nozzle

APPENDIX D

METHODS OF COMPUTATION

The method of computing thrust, maximum temperature, and nozzle throat and exit area is described below and an example is calculated in table I. The solution for these quantities, in general, involves the computation of the velocity, pressure, density, and temperature at each of the significant stations. For example the velocity, pressure, density, and temperature are known at station 1 in free air and are computed in turn at stations 2, 3, 4, 5, and 6 (shown in fig. 1). The first case considered is a ram jet with a pipe entrance and a plane shock just inside the entrance, the position of the shock wave for minimum internal loss. Figure 18, obtained from reference 7, shows Mach number plotted against v_2/v_1, the ratio of velocity after the shock to the velocity before the shock. The velocity before the shock is the speed of the ram-jet airplane or the product of its flight Mach number and the speed of sound

$$v_1 = \text{Mach number} \times c_1$$

Also plotted against v_2/v_1 in figure 18 are the ratios of pressure before and after the shock p_2/p_1 and of density before and after the shock ρ_2/ρ_1. Therefore, with initial or atmospheric conditions given, the state of the air after the shock wave in the tube is determined completely. The temperature is obtained by the gas law

$$T_2 = \frac{p_2}{\rho_2 g R_a} \tag{1}$$

The flow through the straight pipe may be solved graphically or by means of the approximation that the friction pressure drop is proportional to the product of the friction factor, length-diameter ratio of the pipe, and the mean dynamic pressure

$$\Delta p_f = 4f \frac{l_{2,3}}{d_2} \frac{q_2 + q_3}{2} \tag{2}$$

where

$$q = \frac{\rho v^2}{2}$$

The subscript 2 refers to a point near the entrance behind the shock wave and 3 refers to the exit. The laws of energy, momentum, and mass then yield a solution for v_3

$$v_3 = \frac{-b_3 - \sqrt{b_3^2 - 4c_3}}{2} \tag{3}$$

where

$$b_3 = \frac{2\bar{\gamma}_3}{\bar{\gamma}_3\left(1 + 2f\frac{l}{d}\right) + 1}\left[\frac{p_2}{\rho_2 v_2} + \left(1 - f\frac{l}{d}\right)v_2\right] \tag{3a}$$

$$c_3 = \frac{\bar{\gamma}_3 - 1}{\bar{\gamma}_3\left(1 + 2f\frac{l}{d}\right) + 1}\left(\frac{2\bar{\gamma}_2}{\bar{\gamma}_2 - 1}\frac{p_2}{\rho_2} + v_2^2\right) \tag{3b}$$

and $\bar{\gamma}$ is the average ratio of specific heats for air between an arbitrary temperature datum and the temperature at the station denoted by the subscript (fig. 15(b)). When $4c_3$ is equal to b_3^2, the velocity at station 3 equals the speed of sound, or choking occurs. A value of $4c_3$ larger than b_3^2 signifies that an impossible flow condition has been assumed. A shorter entrance pipe is one remedy for this situation. The density at station 3 may be obtained from the continuity relation

$$\rho_3 = \frac{\rho_2 v_2}{v_3} \tag{4}$$

The pressure at station 3 may be obtained from the equation of momentum

$$p_3 = p_2 - \rho_2 v_2(v_3 - v_2) - \Delta p_f \tag{5}$$

The temperature is obtained by the general gas law

$$T_3 = \frac{p_3}{\rho_3 g R_a} \tag{6}$$

where R_a is the gas constant for air.

Next the flow through the diffuser must be determined. If the subscripts 3 and 4 denote the entrance and exit of the diffuser, respectively, the equation expressing the total-pressure recovery as a percentage of the reduction in dynamic pressure is

$$\eta_d = 1 - \frac{H_3 - H_4}{q_{c_3} - q_{c_4}} \tag{7}$$

where η_d is taken as 0.90 in the calculations. The stagnation pressure at station 3 is given by the expression

$$H_3 = p_3 \left[1 + \frac{\gamma_3 - 1}{2} \left(\frac{v_3}{c_3} \right)^2 \right]^{\frac{\gamma_3}{\gamma_3 - 1}} \tag{8}$$

and

$$q_3 = H_3 - p_3$$

If H_4 and q_{c_4} are written in the incompressible form because of the low velocity at station 4, the pressure at this station becomes

$$p_4 = H_3 - \eta_d \frac{\rho_4 v_4^2}{2} - (1 - \eta_d)(H_3 - p_3) \tag{9}$$

The combustion-chamber area is always taken as unity. The continuity relation gives

$$\rho_4 = \frac{\rho_3 A_3 v_3}{v_4} \tag{10}$$

The equation of conservation of energy is

$$\frac{2\bar{\gamma}_4}{\bar{\gamma}_4 - 1}\frac{p_4}{\rho_4} + v_4^2 = \frac{2\bar{\gamma}_3}{\bar{\gamma}_3 - 1}\frac{p_3}{\rho_3} + v_3^2 \tag{11}$$

If the expressions for p_4 and ρ_4 from equations (9) and (10) are substituted in equation (11), the value of v_4 is given by the quadratic formula

$$v_4 = \frac{-b_4 - \sqrt{b_4^2 - 4a_4c_4}}{2a_4} \tag{12}$$

where

$$a_4 = \eta_d \frac{\bar{\gamma}_4}{\bar{\gamma}_4 - 1} - 1 \tag{12a}$$

$$b_4 = -\frac{2\bar{\gamma}_4}{\bar{\gamma}_4 - 1}\frac{H_3 - (1 - \eta_d)(H_3 - p_3)}{\rho_3 v_3 A_3} \tag{12b}$$

$$c_4 = \frac{2\bar{\gamma}_3}{\bar{\gamma}_3 - 1}\frac{p_3}{\rho_3} + v_3^2 \tag{12c}$$

The velocity, density, pressure, and temperature at station 4 are determined by equations (12), (10), (9), and the general gas law

$$T_4 = \frac{p_4}{\rho_4 g R_a} \tag{13}$$

Next the flow through the unit-area combustion chamber must be considered. Let W_a be air flow and W_f be fuel flow, both in pounds per second. The

equation of continuity is

$$\rho_5 v_5 = \rho_4 v_4 + \frac{W_f}{g}$$

or

$$\rho_5 = \rho_4 \frac{v_4}{v_5} \frac{W_a + W_f}{W_a} \tag{14}$$

The momentum equation is

$$p_5 + \left(\rho_4 v_4 + \frac{W_f}{g}\right) v_5 + \frac{C}{2}(q_4 + q_5) - p_4 - \rho_4 v_4^2 = 0$$

where $\frac{C}{2}(q_4 + q_5)$ is the friction pressure loss. Solving for p_5 gives

$$p_5 = p_4 + \rho_4 v_4^2 \left(1 - \frac{C}{4}\right) - \rho_4 v_4 v_5 \left(1 + \frac{C}{4}\right) \frac{W_a + W_f}{W_a} \tag{15}$$

The value of C that has been used is 0.1. The equation of conservation of energy is

$$\left[\left(\frac{\bar{\gamma}_5}{\bar{\gamma}_5 - 1}\right)\frac{p_5}{g\rho_5} + \frac{v_5^2}{2g}\right](W_a + W_f) = \left[\left(\frac{\bar{\gamma}_4}{\bar{\gamma}_4 - 1}\right)\frac{p_4}{g\rho_4} + \frac{v_4^2}{2g}\right](W_a + W_f) + J(H.V.)\eta_c W_f$$

where

J mechanical equivalent of heat (778 ft-lb/Btu)

H.V. assumed lower heating value of the fuel (19,000 Btu/lb)

η_c combustion efficiency (fig. 16)

$\bar{\gamma}$ average for products of combustion.

Substituting ρ_5 and p_5 from equations (14) and (15) into the energy equation gives the solution for the

velocity at exit from the combustion chamber as a quadratic equation with $a_5 = 1$

$$v_5 = \frac{-b_5 - \sqrt{b_5^2 - 4c_5}}{2} \tag{16}$$

where

$$b_5 = -\frac{2\bar{\gamma}_5}{\bar{\gamma}_5\left(1 + \frac{C}{2}\right) + 1} \frac{W_a}{W_a + W_f}\left[\frac{p_4}{\rho_4 v_4} + v_4\left(1 - \frac{C}{4}\right)\right] \tag{16a}$$

$$c_5 = \frac{\bar{\gamma}_5 - 1}{\bar{\gamma}_5\left(1 + \frac{C}{2}\right) + 1}\left[\frac{2\bar{\gamma}_4}{\bar{\gamma}_4 - 1}\frac{p_4}{\rho_4} + v_4^2 + \frac{5 \times 10^4 (H.V.)\eta_c}{\left(W_a + W_f\right)/W_f}\right] \tag{16b}$$

and $\bar{\gamma}$ is average for products of combustion (fig. 15(b)).

A graphical solution for v_5 is given in figure 22 for the values of the combustion parameters used in this report. The gas law is again employed for the temperature

$$T_5 = \frac{p_5}{\rho_5 g R_o} \tag{17}$$

The equation used to obtain the critical pressure at the throat is

$$p_6 = p_5\left[\frac{2}{\gamma + 1} + \frac{\gamma - 1}{\gamma(\gamma + 1)}\frac{\rho_5 v_5^2}{p_5}\right]^{\frac{\gamma}{\gamma - 1}} \tag{18}$$

For simplicity, γ in equations (18) and (19) may be taken for the temperature at the end of combustion, (fig. 15(a)). The other values at the throat are obtained by the following equations:

$$T_6 = T_5\left(\frac{p_6}{p_5}\right)^{\frac{\gamma - 1}{\gamma}}$$

$$= T_5\left[\frac{2}{\gamma + 1} + \frac{\gamma - 1}{\gamma(\gamma + 1)}\frac{\rho_5 v_5^2}{p_5}\right] \tag{19}$$

$$\rho_6 = \frac{p_6}{gR_c T_6} \tag{20}$$

$$v_6 = \sqrt{\gamma_6 g R_c T_6} \tag{21}$$

where γ_6 is instantaneous for products of combustion (fig. 15(a)). The continuity relation between stations 5 and 6 is

$$\frac{A_6}{A_5} = \frac{\rho_5 v_5}{\rho_6 v_6} \tag{22}$$

The conditions at station 7, the nozzle exit, are obtained in a similar manner. The temperature at station 7 is first guessed and the instantaneous value of γ for the average temperature is used. The following equations are used:

$$T_7 = T_5\left(\frac{p_7}{p_5}\right)^{\frac{\gamma_{5,7}^{-1}}{\gamma_{5,7}}} \tag{23}$$

$$v_7 = C_v\sqrt{2gR_c\left(\frac{\bar{\gamma}_5 T_5}{\bar{\gamma}_5 - 1} - \frac{\bar{\gamma}_7 T_7}{\bar{\gamma}_7 - 1}\right) + v_5^2} \tag{24}$$

where C_v is a velocity coefficient allowing for friction in the nozzle. The value $C_v = 0.97$ was used for

under-expanding and design-pressure-ratio nozzles. The density at station 7 is

$$\rho_7 = \frac{p_7}{gR_o T_7} \tag{25}$$

and the area is given by

$$\frac{A_7}{A_5} = \frac{\rho_5 v_5}{\rho_7 v_7} \tag{26}$$

The expression for thrust consists of three terms; the first gives the thrust from the acceleration of the air mass, the second gives the thrust from the acceleration of the fuel mass, and the third becomes effective if the exhaust pressure is above atmospheric. The thrust per square foot of frontal area is

$$\frac{F}{A_4} = \rho_4 v_4 (v_7 - v_1) + \frac{\rho_4 v_4}{W_a/W_f} v_7 + (p_7 - p_1)\frac{A_7}{A_4} \tag{27}$$

Supersonic Diffuser

A converging-diverging supersonic diffuser may be used in place of the inlet pipe and subsonic diffuser. Available data are in the form of a total-pressure-recovery ratio for the case in which the dynamic pressure after diffusion is negligible so that the total pressure is equal to the static pressure. In the present case the dynamic pressure after diffusion (station 4) is small but not negligible. The total pressure H_4 is given with sufficient accuracy by

$$H_4 = p_4 + \frac{1}{2}\rho_4 v_4^2$$

or

$$H_1\left(\frac{H_4}{H_1}\right) = p_4 + \frac{1}{2}\rho_4 v_4^2$$

The test values of $\frac{H_4}{H_1}$ available (fig. 17) should hold with good accuracy in this equation as long as $\frac{1}{2}\rho_4 v_4^2$ is not large. Substituting

$$\rho_4 = \frac{p_4}{gR_a T_4} \tag{28}$$

and solving for p_4 gives

$$p_4 = \frac{H_1\left(\frac{H_4}{H_1}\right)}{1 + \frac{v_4^2}{2gR_a T_4}} \tag{29}$$

The temperature is obtained from the energy relation

$$T_4 = T_1 + \frac{v_1^2}{2g}\frac{\bar{\gamma}_1 - 1}{\bar{\gamma}_1 R_a} - \frac{v_4^2}{2g}\frac{\bar{\gamma}_4 - 1}{\bar{\gamma}_4 R_a} \tag{30}$$

By continuity the supersonic entrance area A_2 is given by

$$\frac{A_2}{A_4} = \frac{\rho_4 v_4}{\rho_1 v_1} \tag{31}$$

The velocity v_4 is chosen or a series of values are investigated. The equations are applied in this order: (30), (29), (28), (31). Equations (28) to (31) can easily be transformed to yield v_4 when A_2 is given.

The value of $\frac{H_4}{H_1}$ is given for the shock wave just behind the section of smallest diameter (throat). This shock-wave position gives the highest diffuser efficiency possible. The efficiency obtainable depends on the contraction ratio, which is the entrance area divided by

the diffuser-throat area. Figure 17 (from fig. 8 of reference 4) gives values of $\frac{H_4}{H_1}$ for a contraction ratio of 1.137. There is a lower limit to the Mach number, at which the flow can be started with a given contraction ratio. The curve is ended at the limiting Mach number.

Speed

The wing drag is calculated for double-circular-arc airfoils by Ackeret's theory. Using β to represent the half-angle between the upper and lower surfaces at the leading or trailing edge gives as the formula for the pressure-drag coefficient of the wing

$$C_{D_w} = \frac{4}{3} \frac{\beta^2}{\sqrt{(V/c)^2 - 1}} + C_L^2 \frac{\sqrt{(V/c)^2 - 1}}{4} \qquad (32)$$

and

$$C_L = \frac{W}{\frac{\rho}{2} S_w V^2}$$

An approximate formula used for pressure-drag coefficient of the conical nose based on wing area is

$$C_{D_n} = \alpha^2 \frac{A_f}{S_w} \log_e \frac{4}{\alpha^2 \left[(V/c)^2 - 1\right]} \qquad (33)$$

where

α half-angle of cone

S_w wing area

A_f projected frontal area of cone $(A - A_2)$

A frontal area of cylinder

A_2 entrance area

An expression for the surface area of the cylindrical body and conical nose is

$$S_f = \pi d\left(l - l_n\right) + \pi\frac{d + d_2}{2} l_n$$

where

l over-all length

l_n length of nose

d diameter of cylinder

d_2 entrance diameter

Putting

$$l_n = 5(d - d_2)$$

gives

$$S_f = A\left[4\frac{l}{d} - 10\left(1 - \sqrt{\frac{A_2}{A}}\right)^2\right]$$

The friction-drag coefficient is taken as 0.0060 for the wing, and the fuselage-surface friction-drag coefficient based on wing area is $0.0030\frac{S_f}{S_w}$. Tail-surface shape and friction drag are considered to be 25 percent of those for the wing, so that the corresponding terms for the wing are multiplied by 1.25 to allow for tail drag. Equating thrust to drag for a unit with A as frontal area in square feet and utilizing the foregoing expressions for drag coefficient gives

$$\frac{F}{A_4} = \frac{\rho}{2} S_w V^2 \left\{ 1.25 \frac{4}{3} \frac{\beta^2}{\sqrt{(V/c)^2 - 1}} + (1.25)(0.0060) \right.$$

$$\left. + \left(\frac{W/S_w}{\frac{\rho}{2} V^2} \right)^2 \frac{\sqrt{(V/c)^2 - 1}}{4} + \alpha^2 \frac{A_f}{S_w} \log_e \frac{4}{\alpha^2 \left[(V/c)^2 - 1 \right]} \right.$$

$$\left. + 0.003 \frac{S_f}{S_w} \right\} \qquad (34)$$

The required ratio A/S_w may now be calculated for a given flight Mach number V/c and wing loading W/S_w.

Range

The basic equation for range is the expression for miles per pound of fuel

$$\frac{dR}{dW} = \frac{\text{Miles per hour}}{\text{Pounds of air per hour} \times \text{Fuel-air ratio}} \qquad (35)$$

In supersonic flight the inlet velocity equals flight speed V_1 and the inlet density is atmospheric density ρ_1. With an entrance area A_2, the weight rate of air flow in pounds per hour is

$$3600 g \rho_1 V_1 A_2$$

Substituting this expression in equation (35) gives

$$\frac{dR}{dW} = \frac{V_1 \frac{60}{88}}{\frac{3600 g \rho_1 V_1 A_2}{W_a / W_f}}$$

and the flight speed cancels, so that

$$\frac{dR}{dW} = \frac{5.887 \times 10^{-6}\left(\frac{W_a}{W_f}\right)}{\rho_1 A_2}$$

If fuel-air ratio and altitude are constant and w_f is used to represent the weight of fuel, the range in miles is

$$R = \frac{5.887 \times 10^{-6}\left(\frac{W_a}{W_f}\right)w_f}{\rho_1 A_2} \qquad (36)$$

REFERENCES

1. Taylor, G. I.: Applications to Aeronautics of Ackeret's Theory of Aerofoils Moving at Speeds Greater Than That of Sound. R. & M. No. 1467, British A.R.C., 1932.

2. Sanger, Eugen: Recent Results in Rocket Flight Technique. NACA TM No. 1012, 1942.

3. Busemann, A.: Aerodynamic Lift at Supersonic Speeds. 2844, Ae. Techl. 1201, British A.R.C., Feb. 3, 1937.

4. Kantrowitz, Arthur, and Donaldson, Coleman duP.: Preliminary Investigation of Supersonic Diffusers. NACA ACR No. L5D20, 1945.

5. Frossel, W.: Flow in Smooth Straight Pipes at Velocities above and below Sound Velocity. NACA TM No. 844, 1938.

6. Kiefer, Paul J., and Stuart, Milton C.: Principles of Engineering Thermodynamics. John Wiley & Sons, Inc., 1930, p. 167, equations (a).

7. Bairstow, Leonard: Applied Aerodynamics. Second ed., Longmans, Green and Co., 1939, p. 582.

TABLE I.- ILLUSTRATIVE EXAMPLE

Given: Mach number = 2.5
Altitude = 35,500 ft
Combustion-chamber area = 1 sq ft
Entrance area = 0.35687 sq ft
Length-diameter ratio of entrance pipe = 8.675

From fig. 18, $\frac{v_2}{v_1} = 0.300$ or

$\frac{\rho_2}{\rho_1} = 3.333$

$\frac{p_2}{p_1} = 7.125$

$\rho_1 = 0.0007212$ slug/cu ft
$p_1 = 485.9$ lb/sq ft
$v_1 = 2425.43$ fps
$T_1 = 392.6$ °F abs.
Fuel-Air ratio = 0.033
$v_2 = 727.6$ fps
$\rho_2 = 0.002404$ slug/cu ft
$p_2 = 3462$ lb/sq ft

Quantity	Equation	Equation number	Substitution	Solution
T_2	$\frac{p_2}{\rho_2 g R_a}$	(1)	$\frac{3462}{(0.002404)(32.17)(53.3)}$	839.9 °F abs.
b_3	$-\frac{2\bar{\gamma}_3}{\bar{\gamma}_3\left(1 + 2f\frac{l}{d}\right) + 1}\left[\frac{p_2}{\rho_2 v_2} + \left(1 - f\frac{l}{d}\right)v_2\right]$	(3a)	$-\frac{(2)(1.398)}{1.398\left[1 + (2)(0.003)(8.675)\right] + 1}\left\{\frac{3462}{(0.002404)(727.6)} + \left[1 - (0.003)(8.675)\right](727.6)\right\}$	-3041.6
c_3	$\frac{\bar{\gamma}_3 - 1}{\bar{\gamma}_3\left(1 + 2f\frac{l}{d}\right) + 1}\left(\frac{2\bar{\gamma}_2}{\bar{\gamma}_2 - 1}\frac{p_2}{\rho_2} + v_2^2\right)$	(3b)	$\frac{1.398 - 1}{1.398\left[1 + 2(0.003)(8.675)\right] + 1}\left[\frac{2(1.398)}{1.398 - 1} \times \frac{3462}{0.002404} + (727.6)^2\right]$	1,714,600
v_3	$\frac{-b_3 - \sqrt{b_3^2 - 4c_3}}{2}$	(3)	$\frac{-(-3041.6) - \sqrt{(-3041.6)^2 - 4(1,714,600)}}{2}$	747.4 fps
ρ_3	$\frac{\rho_2 v_2}{v_3}$	(4)	$\frac{(0.002404)(727.6)}{747.4}$	0.002340 slug/cu ft
Δp_f	$2f\frac{l_{2,3}}{d_2}(q_2 + q_3)$	(2)	$2(0.003)(8.675)\left[\frac{(0.002404)(727.6)^2}{2} + \frac{(0.002340)(747.4)^2}{2}\right]$	67.2 lb/sq ft
p_3	$p_2 - \rho_2 v_2(v_3 - v_2) - \Delta p_f$	(5)	$3462 - (0.002404)(727.6)(747.4 - 727.6) - 67.2$	3360 lb/sq ft
T_3	$\frac{p_3}{\rho_3 g R_a}$	(6)	$\frac{3360}{(0.002340)(32.17)(53.3)}$	837.4 °F abs.
H_3	$p_3\left[1 + \left(\frac{\gamma_3 - 1}{2}\right)\left(\frac{v_3}{c_3}\right)^2\right]^{\frac{\gamma_3}{\gamma_3 - 1}}$	(8)	$3360\left[1 + \left(\frac{1.392 - 1}{2}\right)\left(\frac{747.4}{1417}\right)^2\right]^{\frac{1.392}{1.392 - 1}}$	4057 lb/sq ft
a_4	$\eta_d\left(\frac{\bar{\gamma}_4}{\bar{\gamma}_4 - 1}\right) - 1$	(12a)	$0.9\left(\frac{1.398}{1.398 - 1}\right) - 1$	2.164
b_4	$-\frac{2\bar{\gamma}_4}{\bar{\gamma}_4 - 1}\frac{H_3 - (1 - \eta_d)(H_3 - p_3)}{\rho_3 v_3 A_3}$	(12b)	$\frac{2(1.398)}{(1.398 - 1)}\frac{4057 - (1 - 0.9)(4057 - 3360)}{(0.002340)(747.4)(0.3569)}$	-44,876
c_4	$\frac{2\bar{\gamma}_3}{\bar{\gamma}_3 - 1}\frac{p_3}{\rho_3} + v_3^2$	(12c)	$\frac{2(1.398)}{1.398 - 1}\left(\frac{3360}{0.002340}\right) + (747.4)^2$	10,643,000
v_4	$\frac{-b_4 - \sqrt{b_4^2 - 4a_4c_4}}{2a_4}$	(12)	$\frac{-(-44876) - \sqrt{(-44876)^2 - 4(2.164)(10,643,000)}}{2(2.164)}$	239.9 fps
ρ_4	$\frac{\rho_3 A_3 v_3}{v_4}$	(10)	$\frac{(0.002340)(0.3569)(747.4)}{239.9}$	0.002602 slug/cu ft

TABLE I.- ILLUSTRATIVE EXAMPLE - Concluded

Quantity	Equation	Equation number	Substitution	Solution
p_4	$H_3 - \eta_d \frac{\rho_4 v_4^2}{2} - (1 - \eta_d)(H_3 - p_3)$	(9)	$4057 - \frac{0.9(0.002602)(239.9)^2}{2} - (1 - 0.9)(4057 - 3360)$	3920 lb/sq ft
T_4	$\frac{p_4}{\rho_4 g R_a}$	(13)	$\frac{3920}{(0.002602)(32.17)(53.3)}$	878.6 °F abs.
b_5	$-\frac{2\bar{\gamma}_5}{\bar{\gamma}_5\left(1 + \frac{c}{2}\right) + 1} \frac{W_a}{W_a + W_f}\left[\frac{p_4}{\rho_4 v_4} + v_4\left(1 - \frac{c}{4}\right)\right]$	(16a)	$-\frac{2(1.351)}{1.351\left(1 + \frac{0.1}{2}\right) + 1} \frac{30}{30 + 1}\left[\frac{3920}{(0.002602)(239.9} + 239.9\left(1 - \frac{0.1}{4}\right)\right]$	-7042
c_5	$\frac{\bar{\gamma}_5 - 1}{\bar{\gamma}_5\left(1 + \frac{c}{2}\right) + 1}\left[\frac{2\bar{\gamma}_4}{\bar{\gamma}_4 - 1}\frac{p_4}{\rho_4} + v_4^2 + \frac{5 \times 10^4 (H.V.)\eta_c}{(W_a + W_f)/W_f}\right]$	(16b)	$\frac{1.351 - 1}{1.351\left(1 + \frac{0.1}{2}\right) + 1}\left[\frac{2(1.383)}{1.383 - 1}\frac{3920}{0.002602} + (239.9)^2 + \frac{(50,000)(13,000)(0.91)}{(30 + 1)/1}\right]$	5,634,500
v_5	$\frac{-b_5 - \sqrt{b_5^2 - 4c_5}}{2}$	(16)	$\frac{-(-7042) - \sqrt{(-7042)^2 - 4(5,634,500)}}{2}$	920.5 fps
ρ_5	$\rho_4 \frac{v_4}{v_5}\frac{W_a + W_f}{W_a}$	(14)	$(0.002602)\left(\frac{239.9}{920.5}\right)\left(\frac{30 + 1}{30}\right)$	0.0007007 slug/cu ft
p_5	$p_4 + \rho_4 v_4^2\left(1 - \frac{c}{4}\right) - \rho_4 v_4 v_5\left(1 + \frac{c}{4}\right)\frac{W_a + W_f}{W_a}$	(15)	$3920 + (0.002602)(239.9)^2\left(1 - \frac{0.1}{4}\right) - (0.002602)(239.9)(920.5)\left(1 + \frac{0.1}{4}\right)\left(\frac{30 + 1}{30}\right)$	3457 lb/sq ft
T_5	$\frac{p_5}{\rho_5 g R_c}$	(17)	$\frac{3457}{(0.0007007)(32.17)(53.73)}$	2854 °F abs.
p_6	$p_5\left[\frac{2}{\gamma + 1} + \frac{\gamma - 1}{\gamma(\gamma + 1)}\frac{\rho_5 v_5^2}{p_5}\right]^{\frac{\gamma}{\gamma - 1}}$	(18)	$3457\left[\frac{2}{1.305 + 1} + \frac{1.305 - 1}{(1.305)(1.305 + 1)}\frac{(0.0007007)(920.5)^2}{3457}\right]^{\frac{1.305}{1.305 - 1}}$	2051 lb/sq ft
T_6	$T_5\left[\frac{2}{\gamma + 1} + \frac{\gamma - 1}{\gamma(\gamma + 1)}\frac{\rho_5 v_5^2}{p_5}\right]$	(19)	$2854\left[\frac{2}{1.305 + 1} + \frac{1.305 - 1}{(1.305)(1.305 + 1)}\frac{(0.0007007)(920.5)^2}{3457}\right]$	2526 °F abs.
ρ_6	$\frac{p_6}{g R_c T_6}$	(20)	$\frac{2051}{(32.17)(53.73)(2526)}$	0.0004697 slug/cu ft
v_6	$\sqrt{\gamma_6 g R_c T_6}$	(21)	$\sqrt{(1.317)(32.17)(53.73)(2526)}$	2398 fps
A_6/A_5	$\frac{\rho_5 v_5}{\rho_6 v_6}$	(22)	$\frac{(0.0007007)(920.5)}{(0.0004697)(2398)}$	0.5726
T_7	$T_5\left[\frac{p_7}{p_5}\right]^{\frac{\gamma_{5,7} - 1}{\gamma_{5,7}}}$	(23)	$2854\left(\frac{485.9}{3457}\right)^{\frac{1.324 - 1}{1.324}}$	1766 °F abs.
v_7	$C_v\sqrt{2 g R_c\left(\frac{\bar{\gamma}_5 T_5}{\bar{\gamma}_5 - 1} - \frac{\bar{\gamma}_7 T_7}{\bar{\gamma}_7 - 1}\right)} + v_5^2$	(24)	$0.97\sqrt{2(32.17)(53.73)\left[\frac{(1.351)(2854)}{1.351 - 1} - \frac{(1.370)(1766)}{1.370 - 1}\right]} + (920.5)^2$	3906 fps
ρ_7	$\frac{p_7}{g R_c T_7}$	(25)	$\frac{485.9}{(32.17)(53.73)(1766)}$	0.0001592 slug/cu ft
A_7/A_5	$\frac{\rho_5 v_5}{\rho_7 v_7}$	(26)	$\frac{(0.0007007)(920.5)}{(0.0001592)(3908)}$	1.037
F/A_4	$\rho_4 v_4(v_7 - v_1) + \frac{\rho_4 v_4}{W_a/W_f} v_7 + (p_7 - p_1)\frac{A_7}{A_4}$	(27)	$(0.002602)(239.9)(3906 - 2425) + \frac{(0.002602)(239.9)(3906)}{30/1} + 0$	1006 lb/sq ft

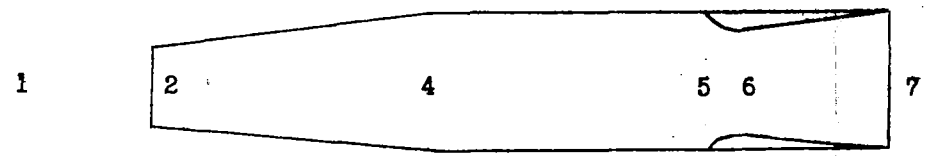

(a) Unit with diverging conical entrance.

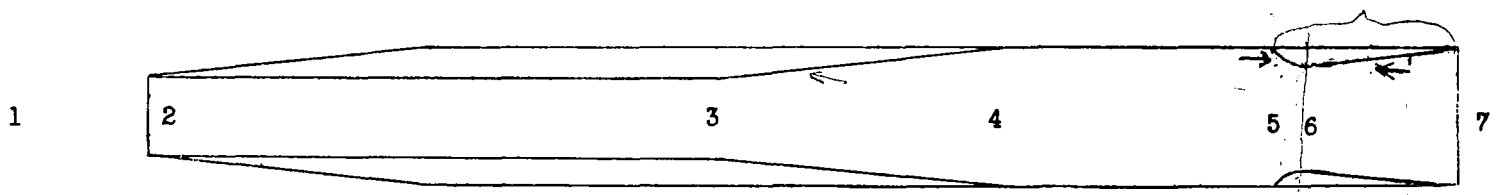

(b) Unit with cylindrical entrance.

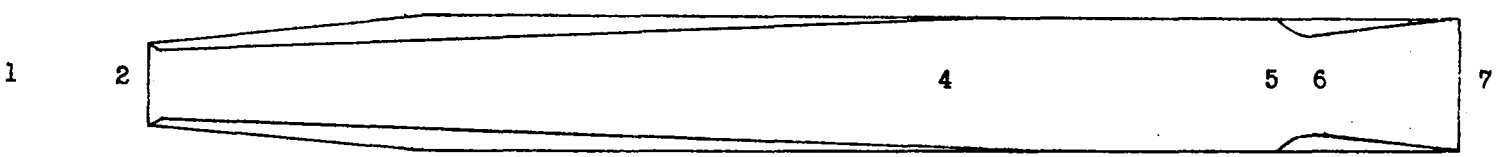

(c) Unit with supersonic-diffuser entrance.

NATIONAL ADVISORY COMMITTEE FOR AERONAUTICS

Figure 1.- Schematic drawing of supersonic ram-jet units.

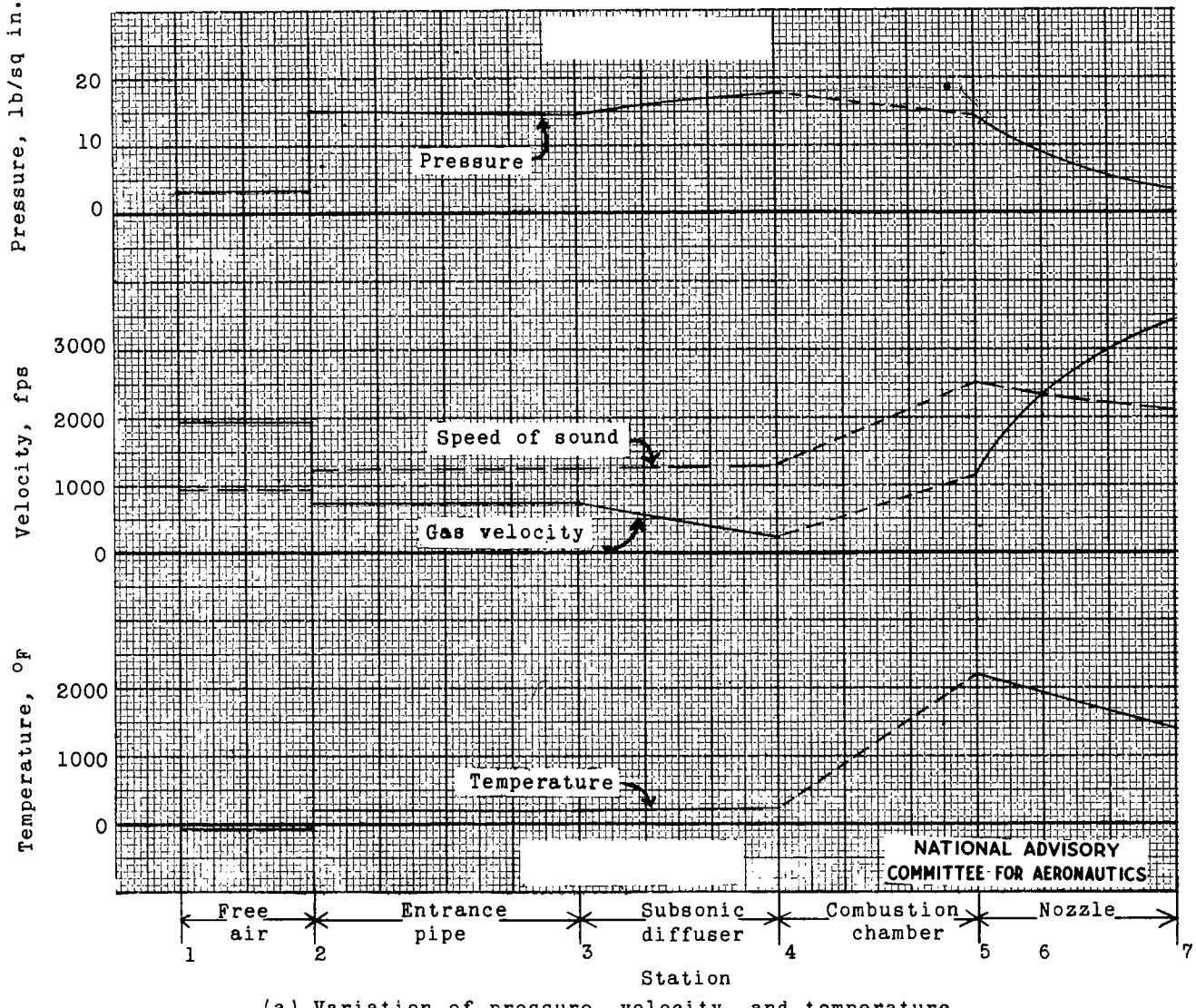

(a) Variation of pressure, velocity, and temperature.

Figure 2.- Power-plant cycle. Pipe entrance; stream Mach number, 2.0; altitude, 35,500 feet.

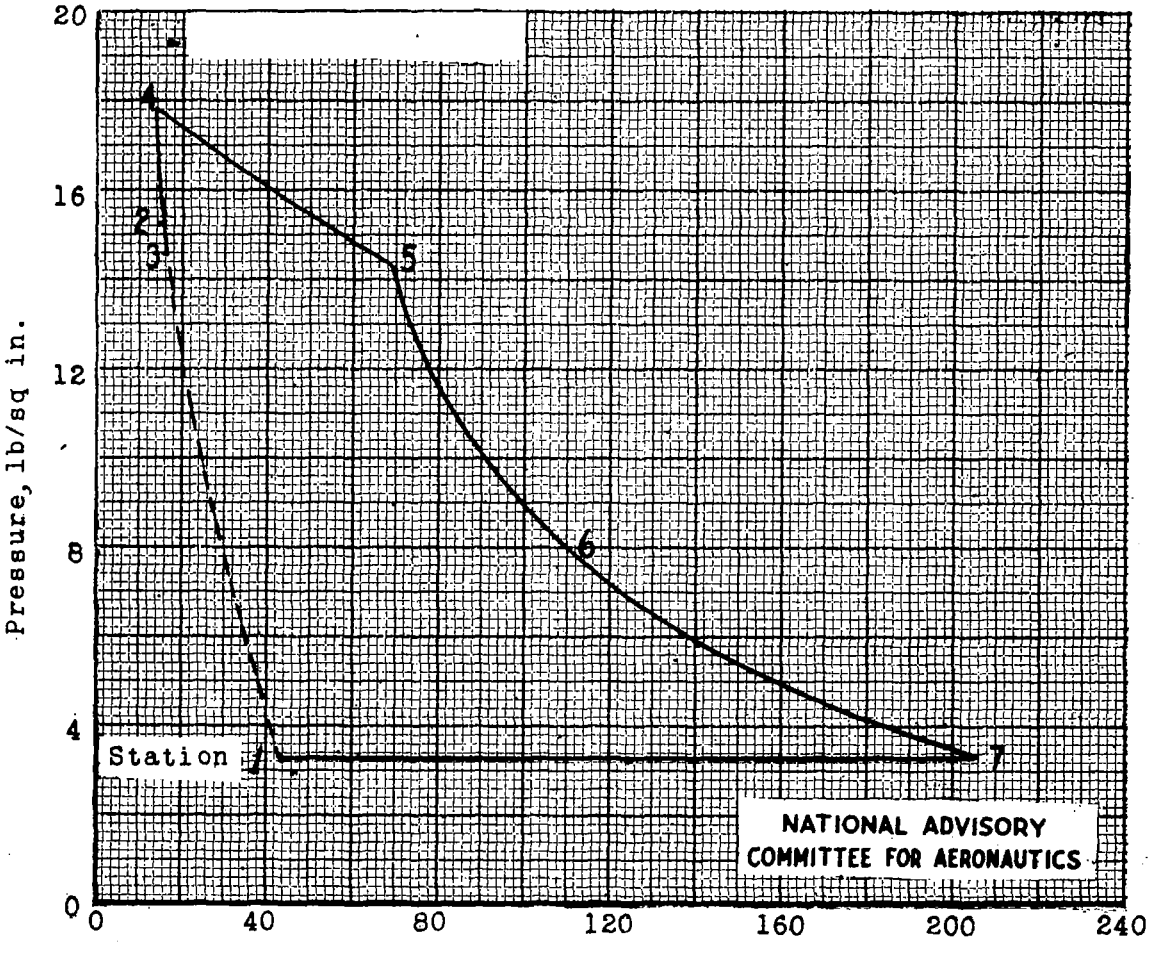

(b) Pressure-volume diagram.

Figure 2.- Concluded.

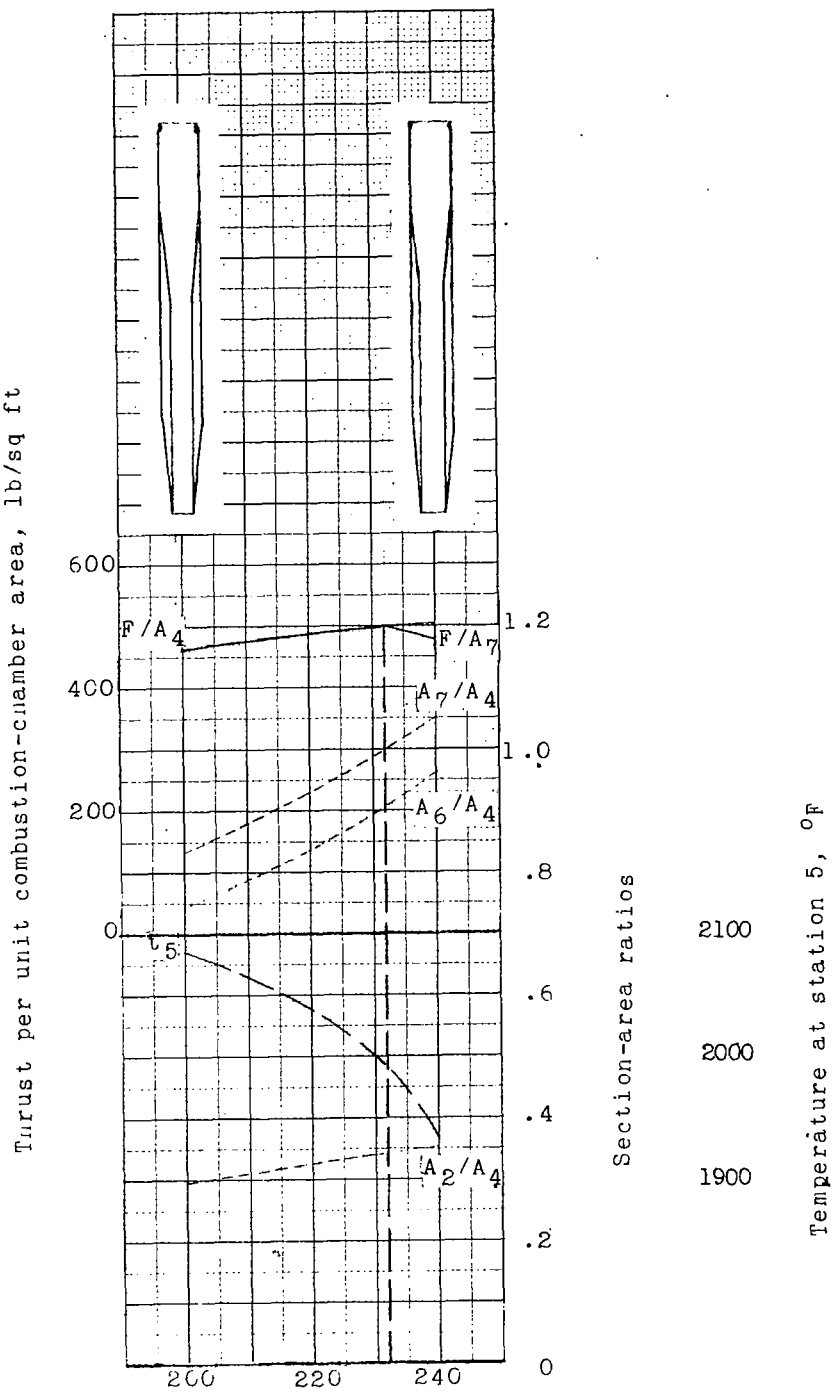

(a) Pipe entrance; stream Mach number, 1.5.

Figure 3. - Power-plant data. Altitude, 35,500 feet; fuel-air ratio, 0.033

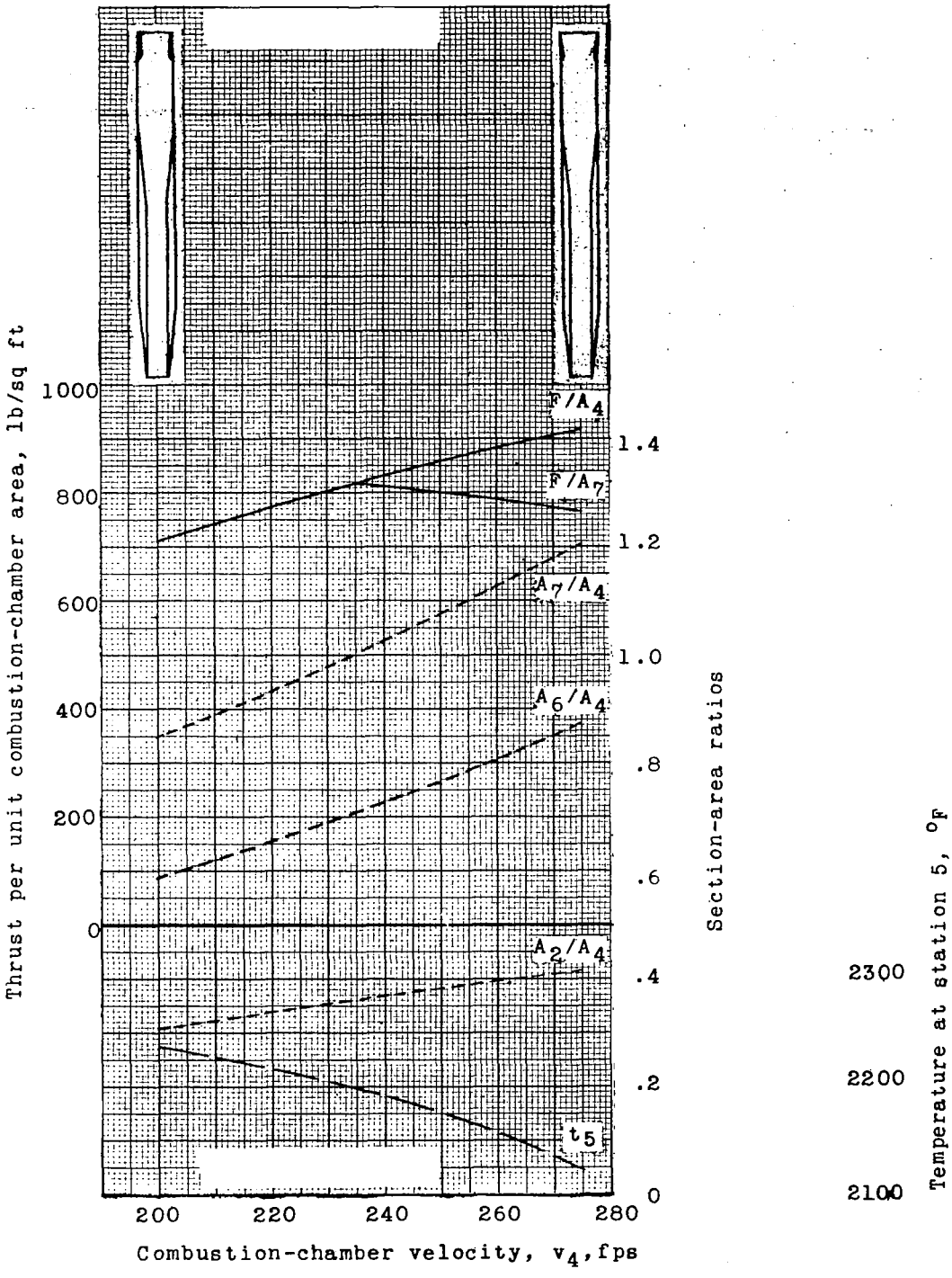

(b) Pipe entrance; stream Mach number, 2.0.

Figure 3.- Continued.

NATIONAL ADVISORY
COMMITTEE FOR AERONAUTICS

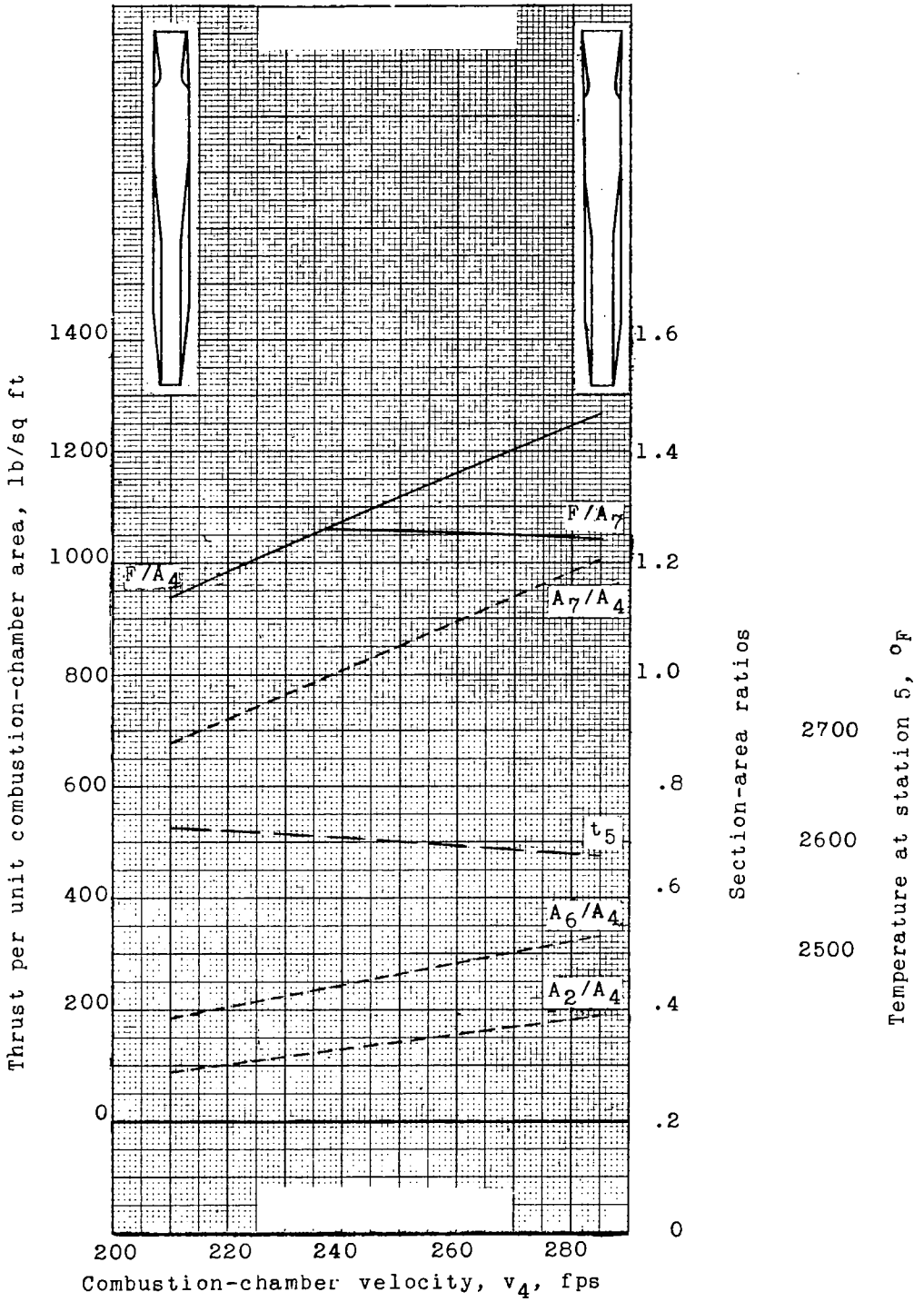

(c) Pipe entrance; stream Mach number, 3.0.

Figure 3.- Continued.

NATIONAL ADVISORY COMMITTEE FOR AERONAUTICS

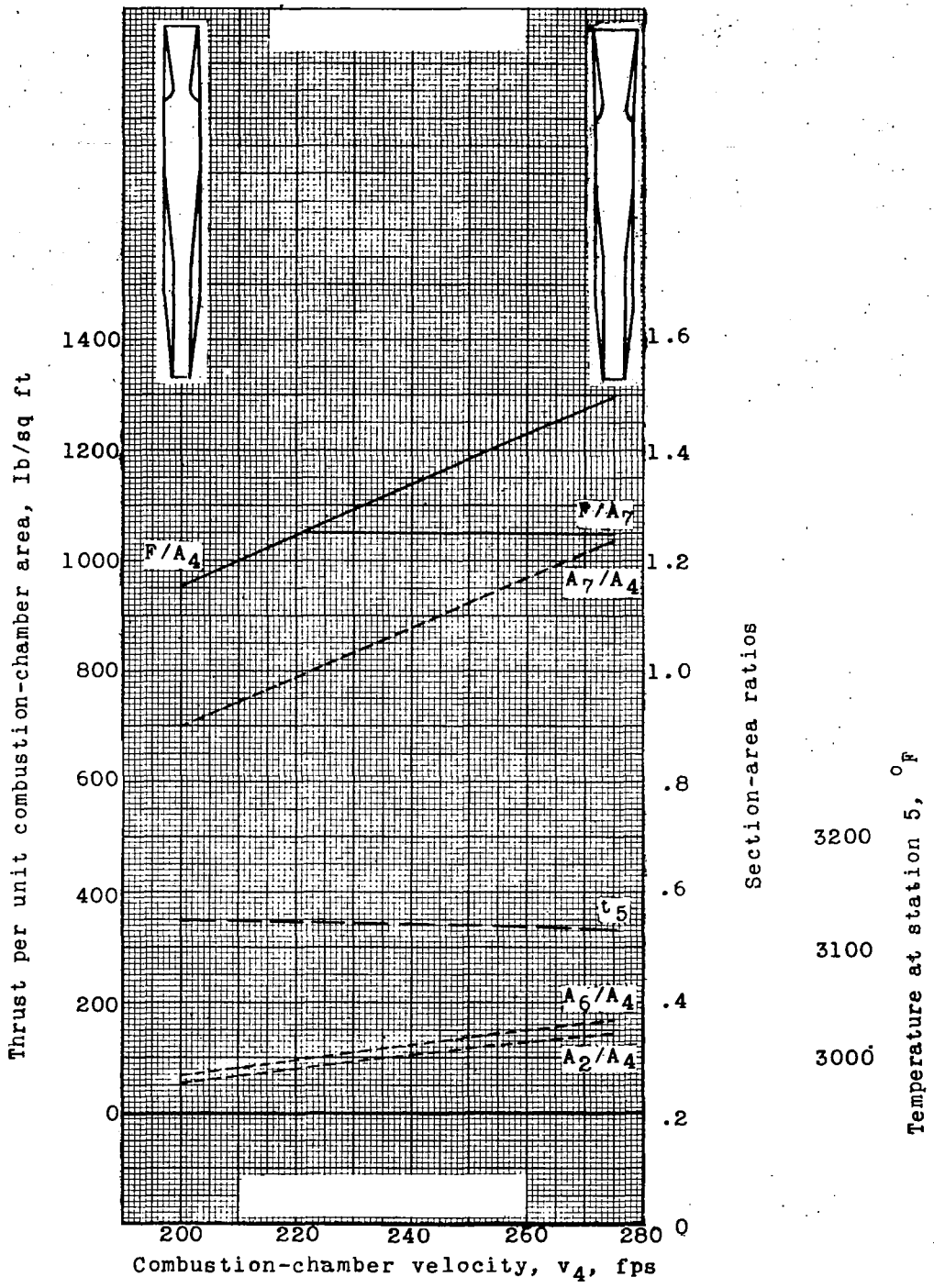

(d) Pipe entrance; stream Mach number, 4.0.

Figure 3.- Continued.

NATIONAL ADVISORY
COMMITTEE FOR AERONAUTICS

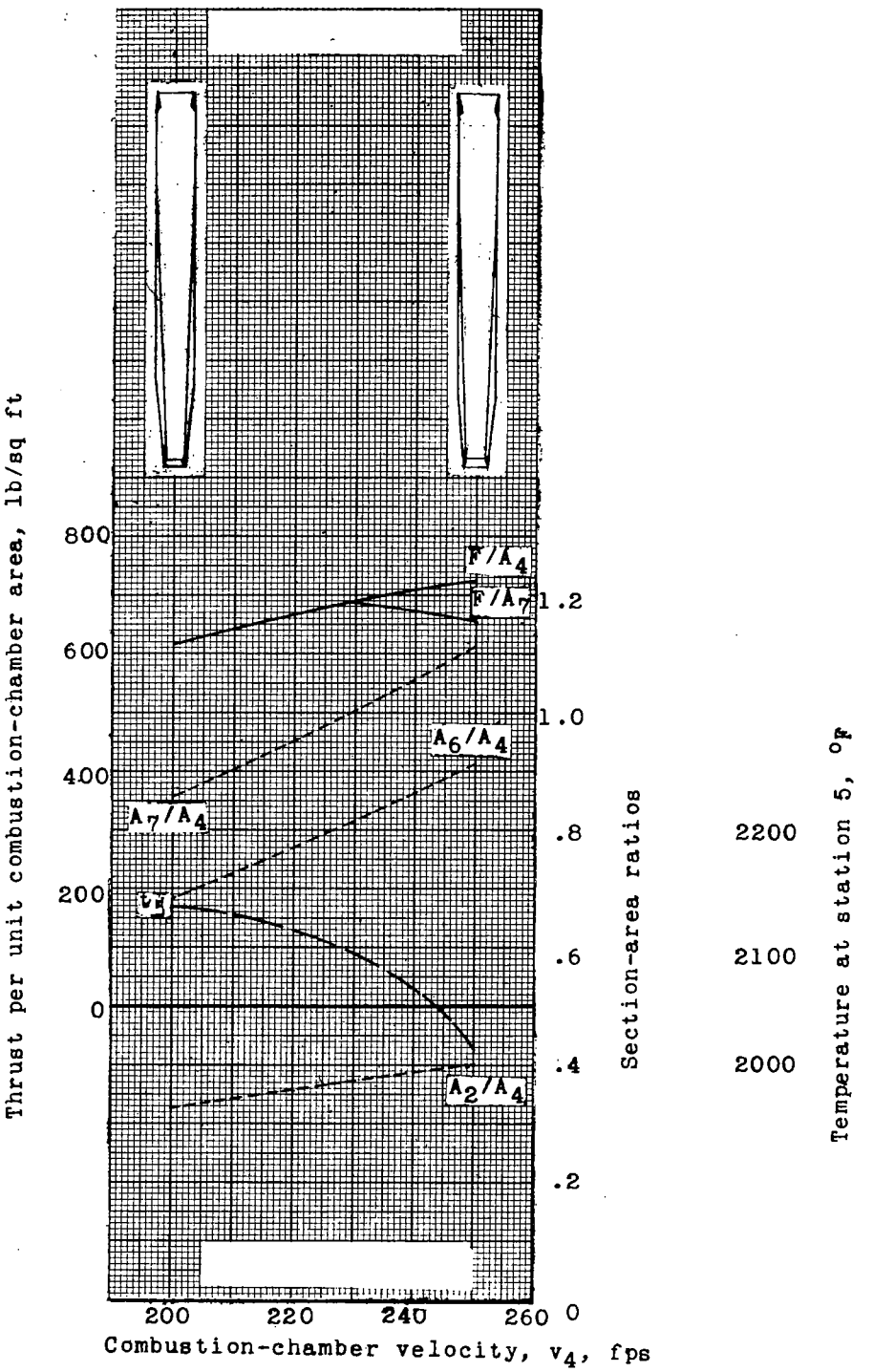

(e) Supersonic-diffuser entrance with contraction ratio of 1.137; stream Mach number, 1.673.

Figure 3.- Continued.

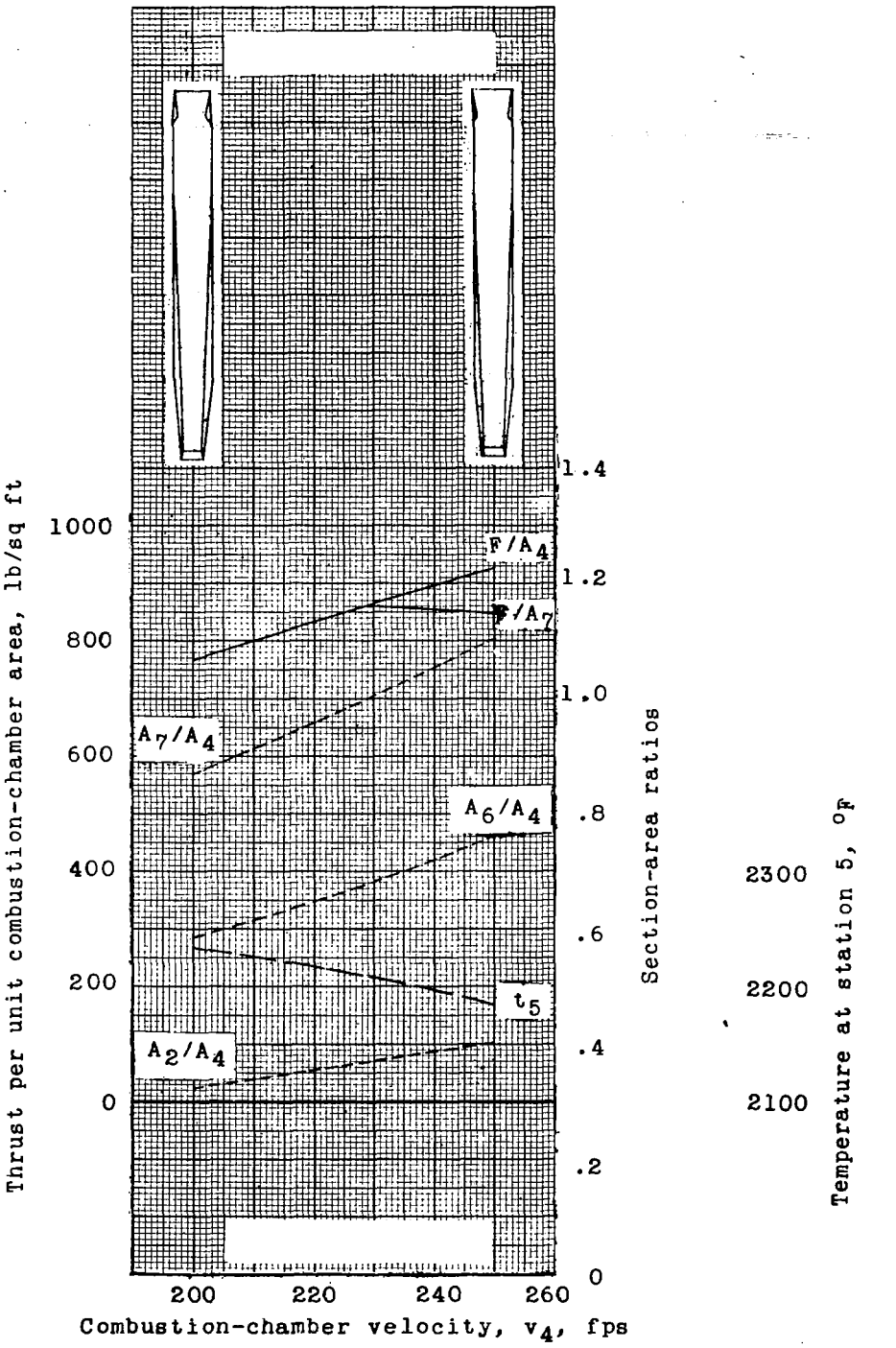

(f) Supersonic-diffuser entrance with contraction ratio of 1.137; stream Mach number, 2.0.

Figure 3.- Continued.

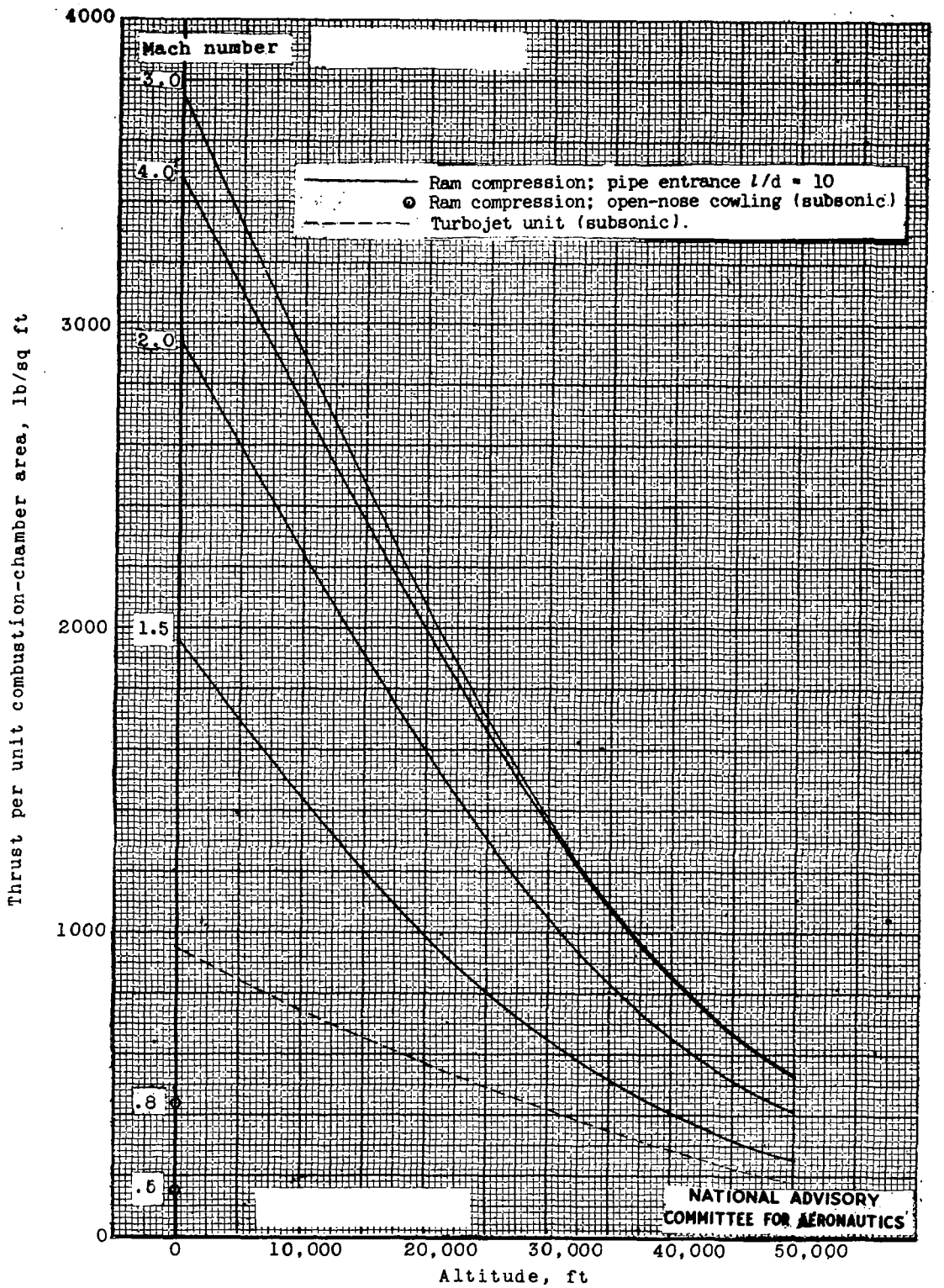

(g) Comparison of thrust of ram-compression power plants with thrust of typical turbojet units.

Figure 3.- Continued.

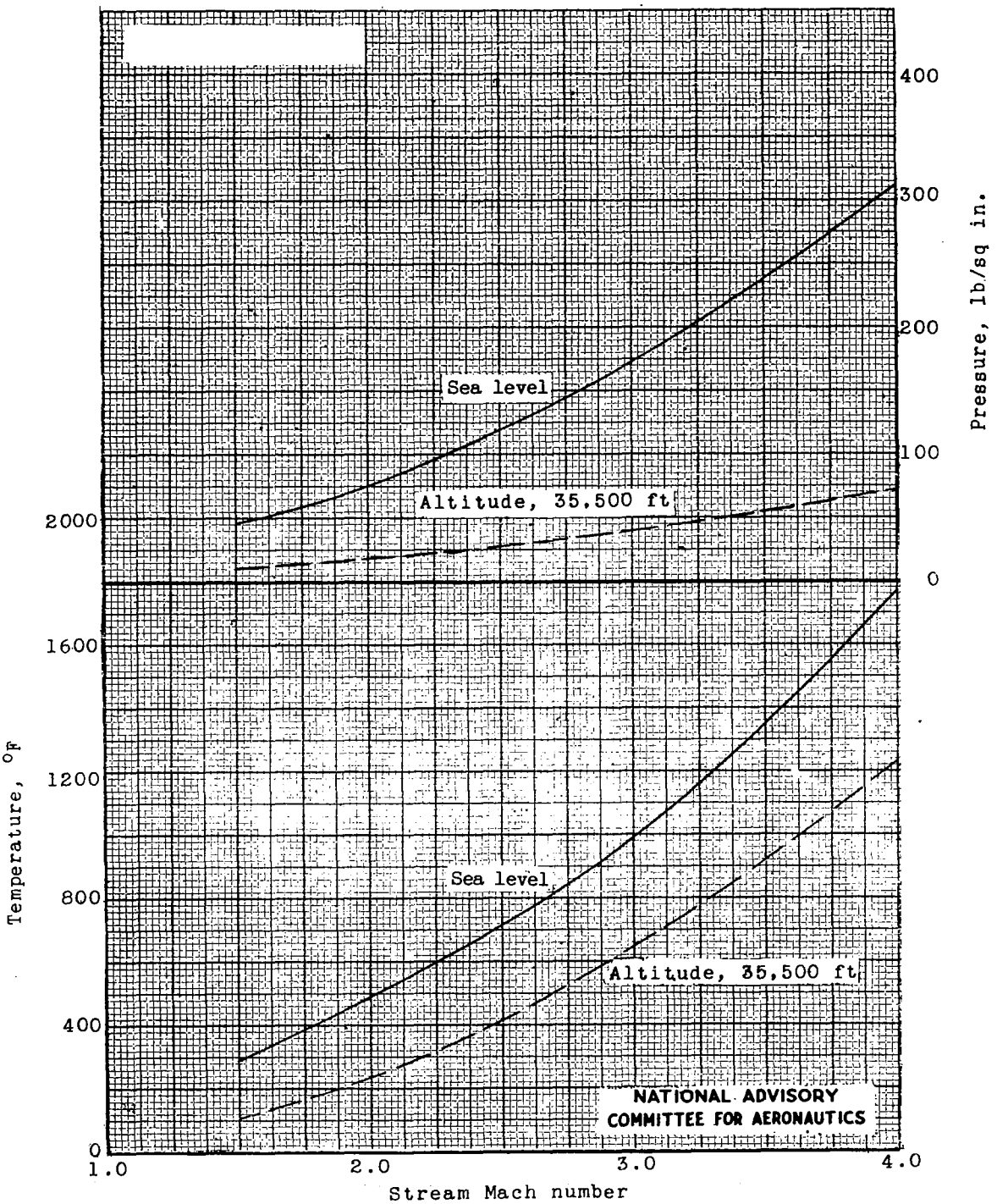

(h) Pressure and temperature of air entering combustion chamber.

Figure 3.- Concluded.

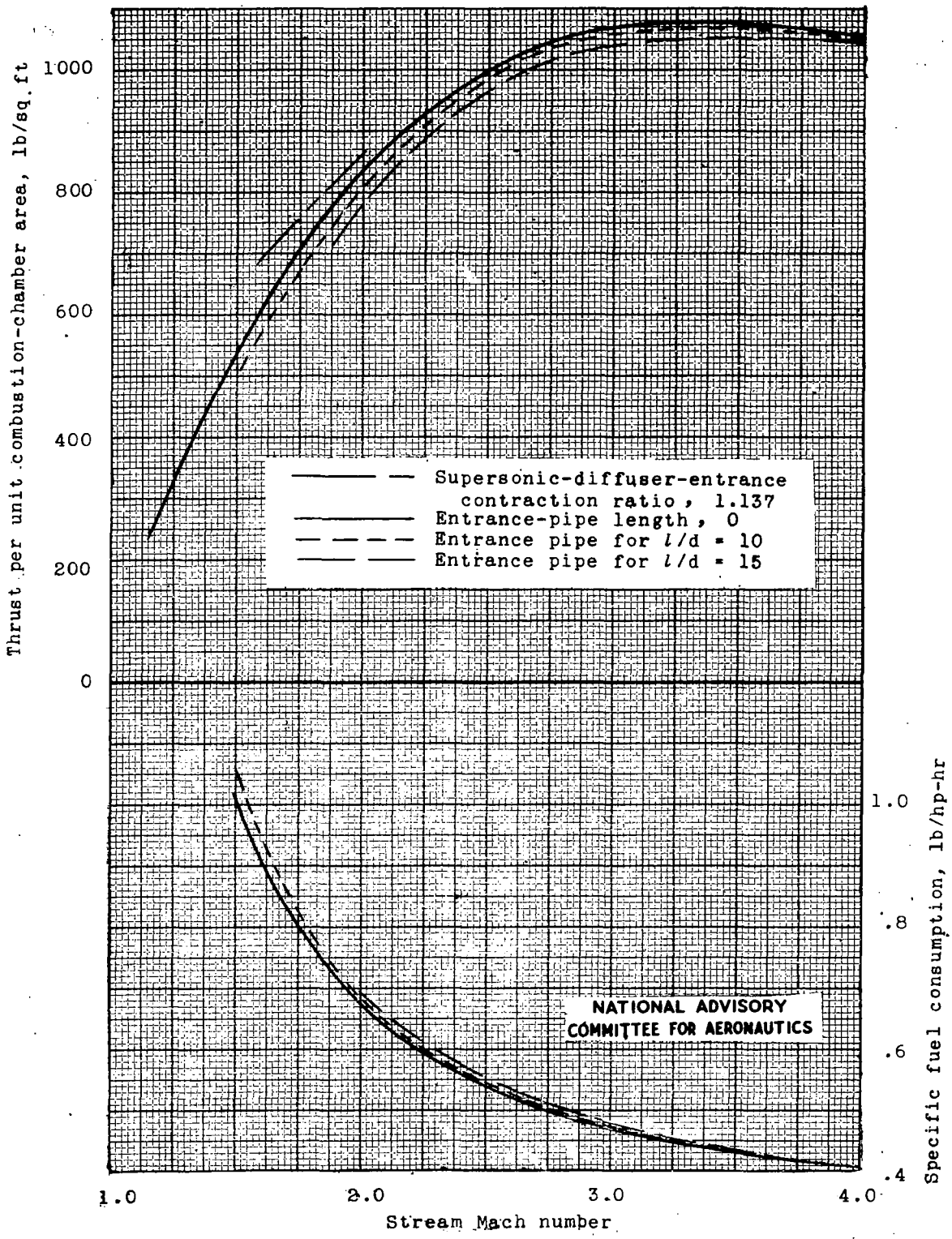

(a) Altitude, 35,500 feet; fuel-air ratio, 0.033.

Figure 4. - Thrust and economy of supersonic power plants.

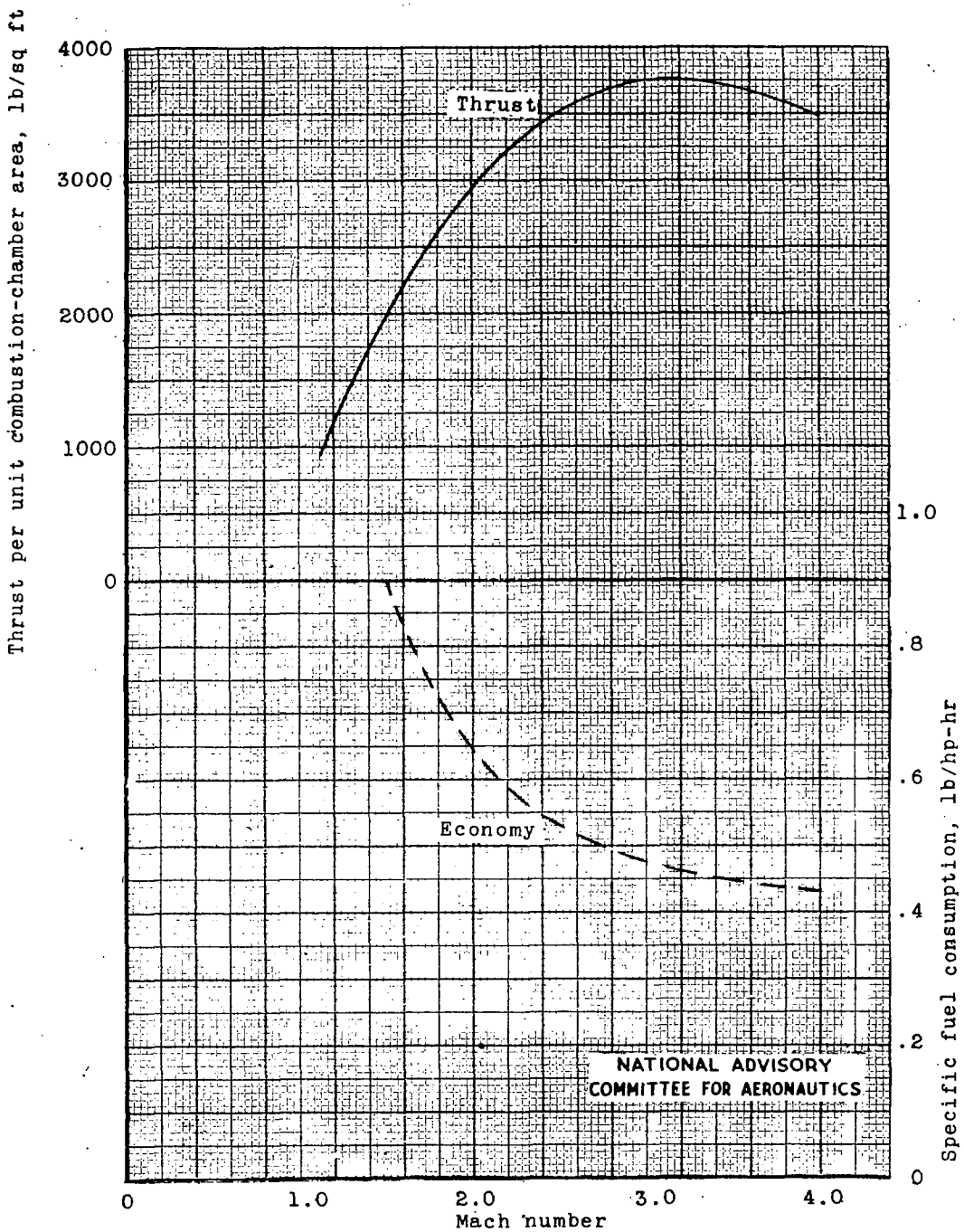

(b) Sea level; fuel-air ratio, 0.033; entrance pipe for $\ell/d = 10$.

Figure 4.- Concluded.

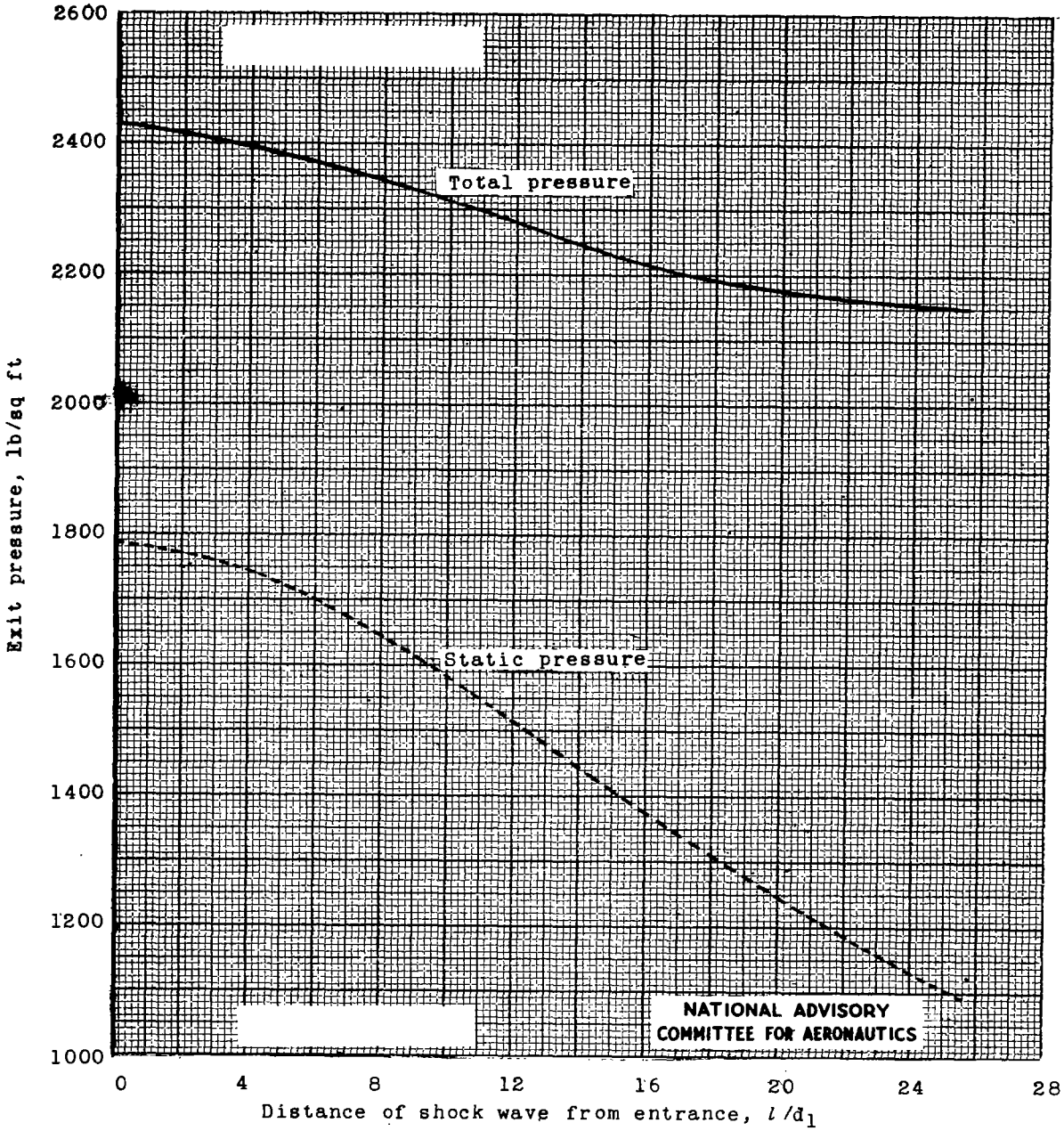

(a) Cylindrical pipe; l/d = 25.55; entrance Mach number, 2.0.

Figure 5.-Change in pressure at the end of a duct with travel of shock wave. Friction factor, 0.003.

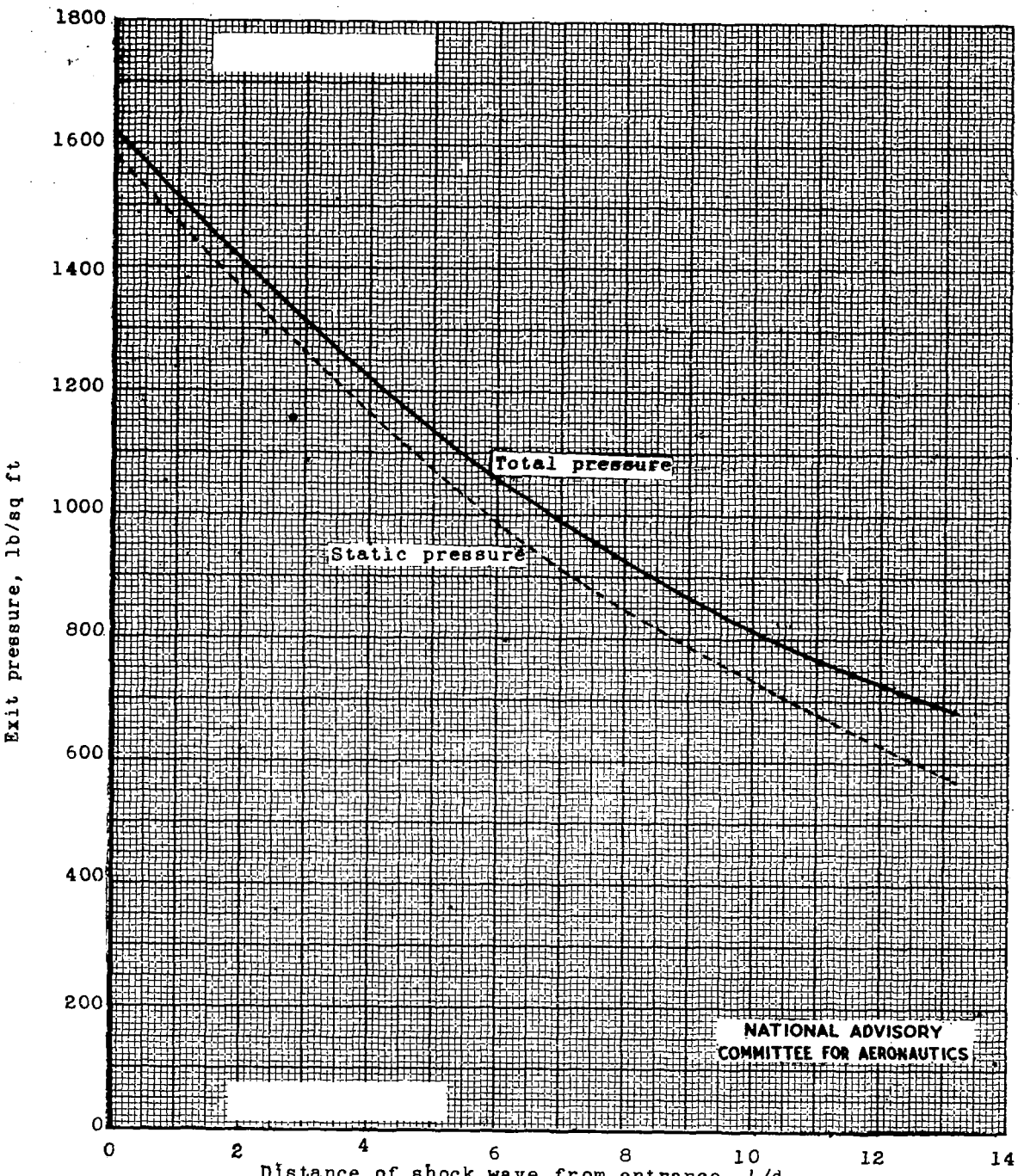

(b) Conical diffuser; l/d_1=13.2; entrance Mach number, 1.5; expansion angle, 3°.

Figure 5.- Concluded.

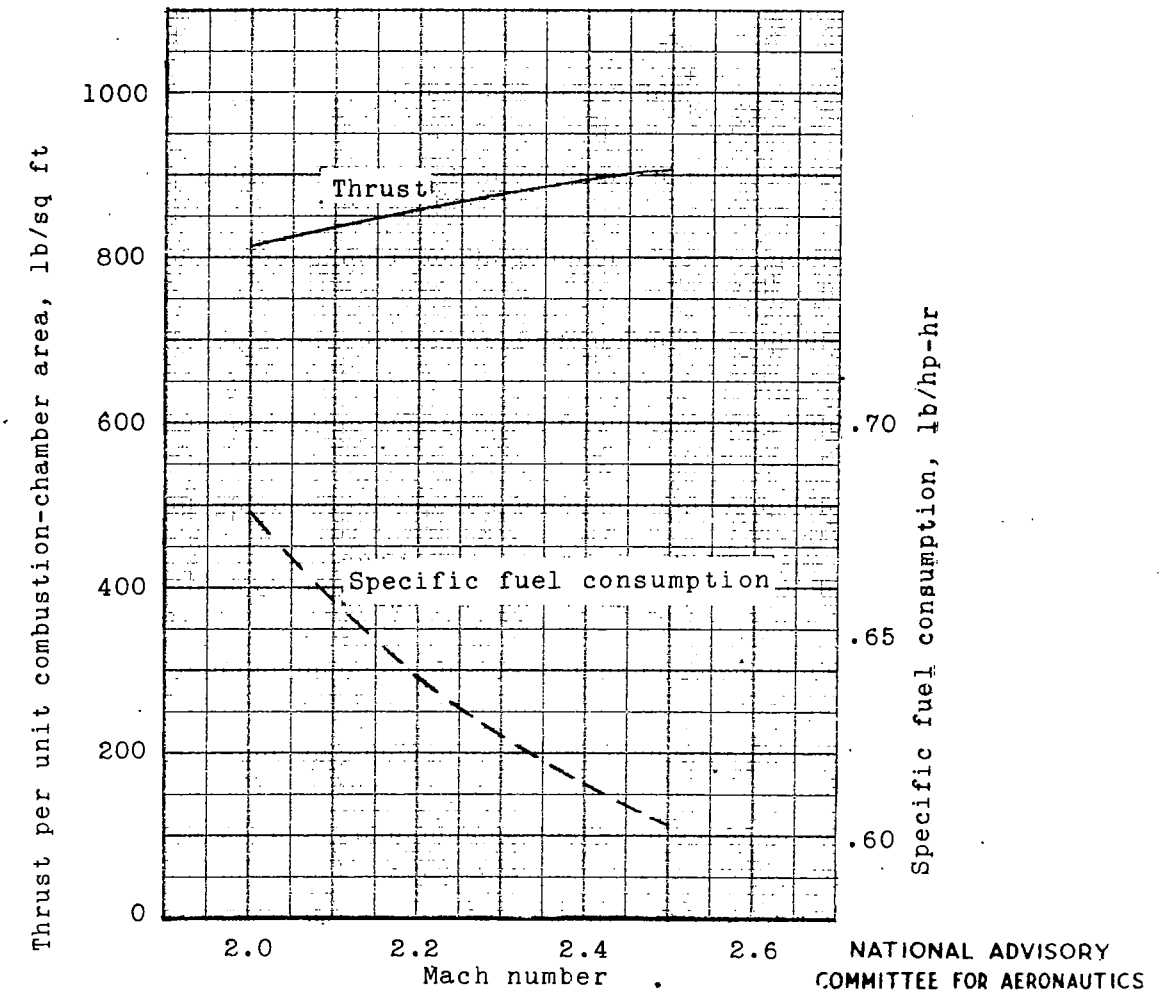

(a) Pipe entrance; design Mach number, 2.0.

Figure 6. - Change of thrust with stream Mach number. Dimensions fixed; altitude, 35,500 feet; fuel-air ratio, 0.033.

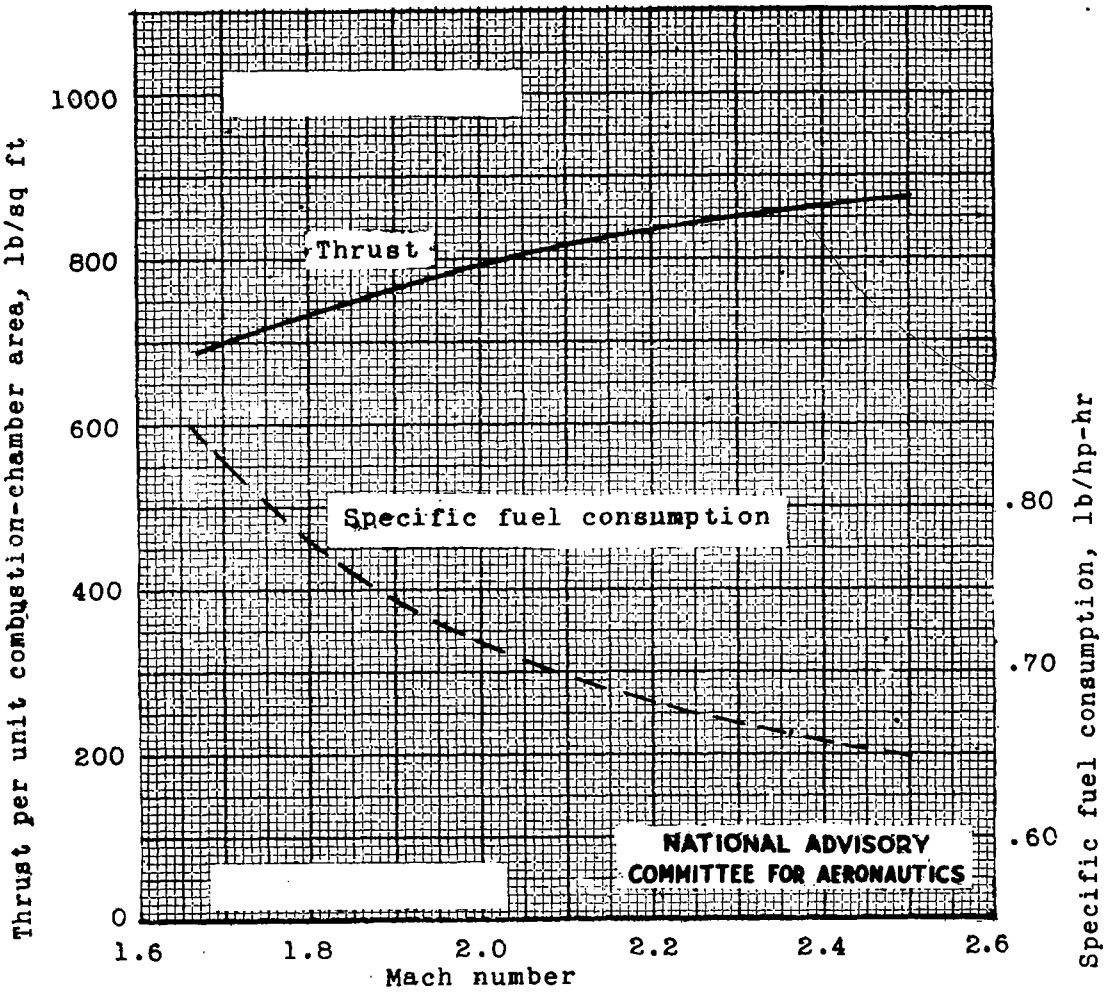

(b) Supersonic-diffuser entrance; design Mach number, 1.673.

Figure 6.- Concluded.

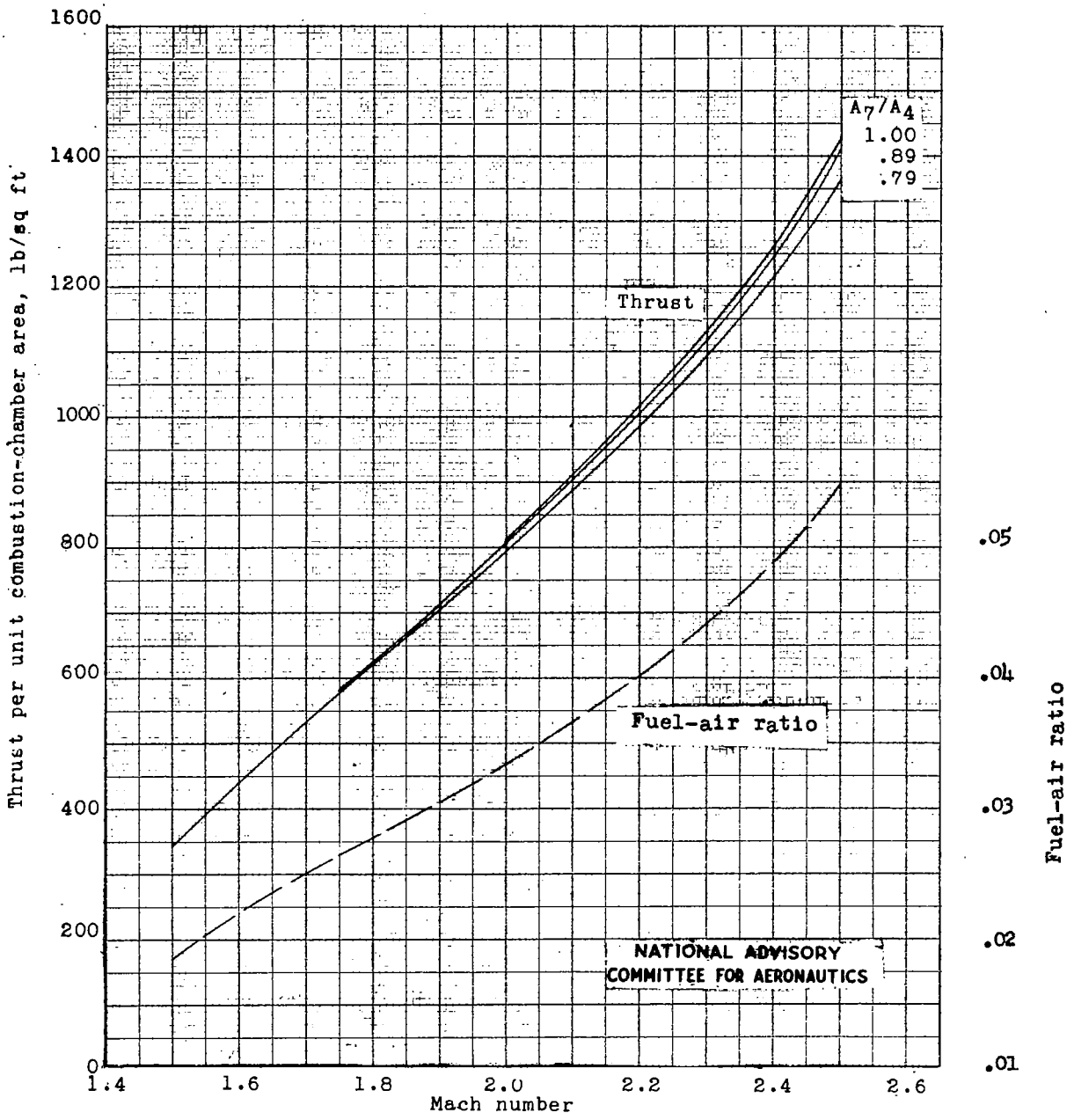

Figure 7. - Change of thrust with Mach number. Dimensions fixed; altitude, 35,500 feet; fuel-air ratio varied; pipe entrance for l/d = 10.

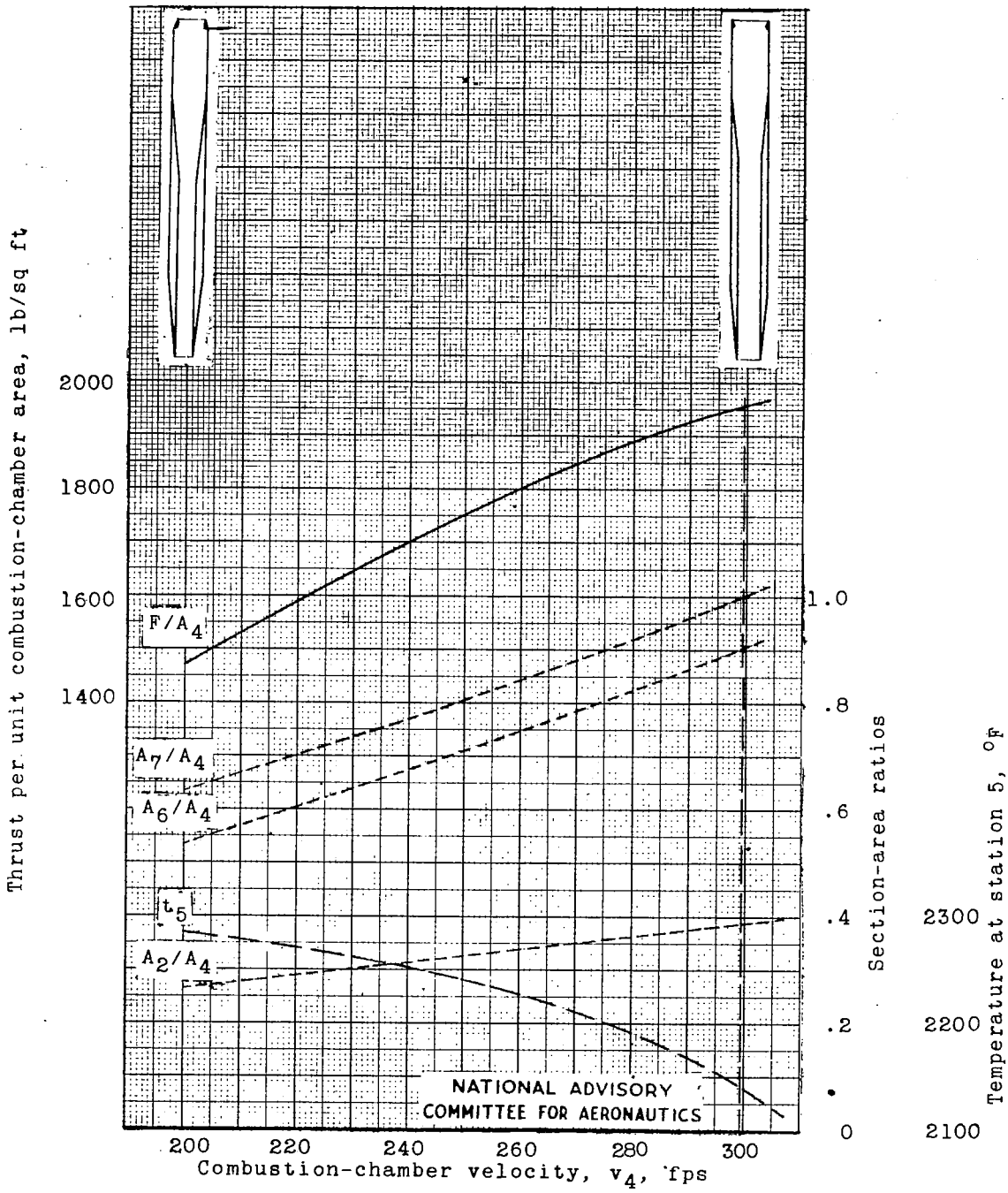

(a) Fuel-air ratio, 0.033.

Figure 8. - Power-plant characteristics for several values of fuel-air ratio. Pipe entrance for $\ell/d = 10$; sea level; stream Mach number, 1.5.

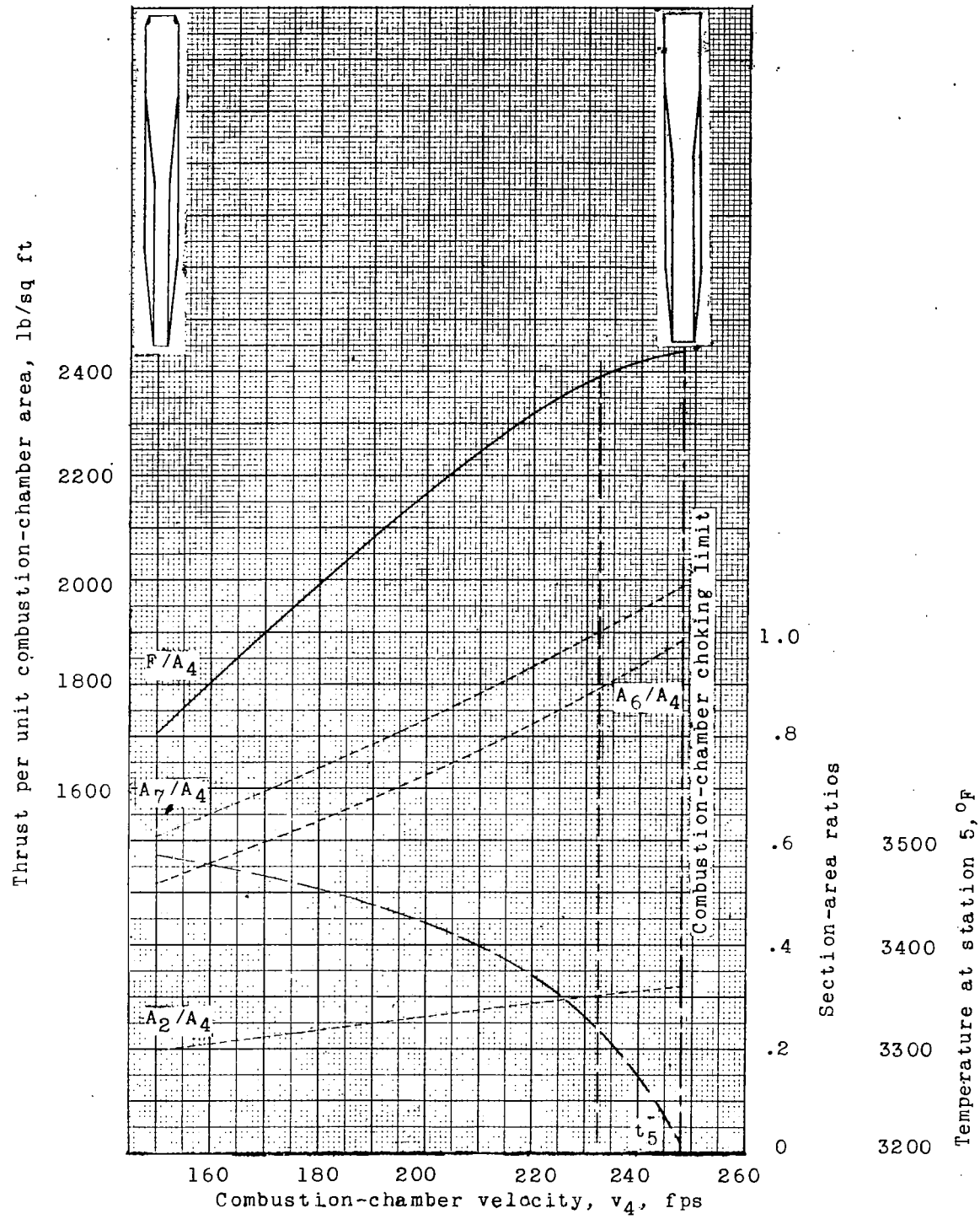

(b) Fuel-air ratio, 0.067.

Figure 8. - Continued.

NATIONAL ADVISORY COMMITTEE FOR AERONAUTICS

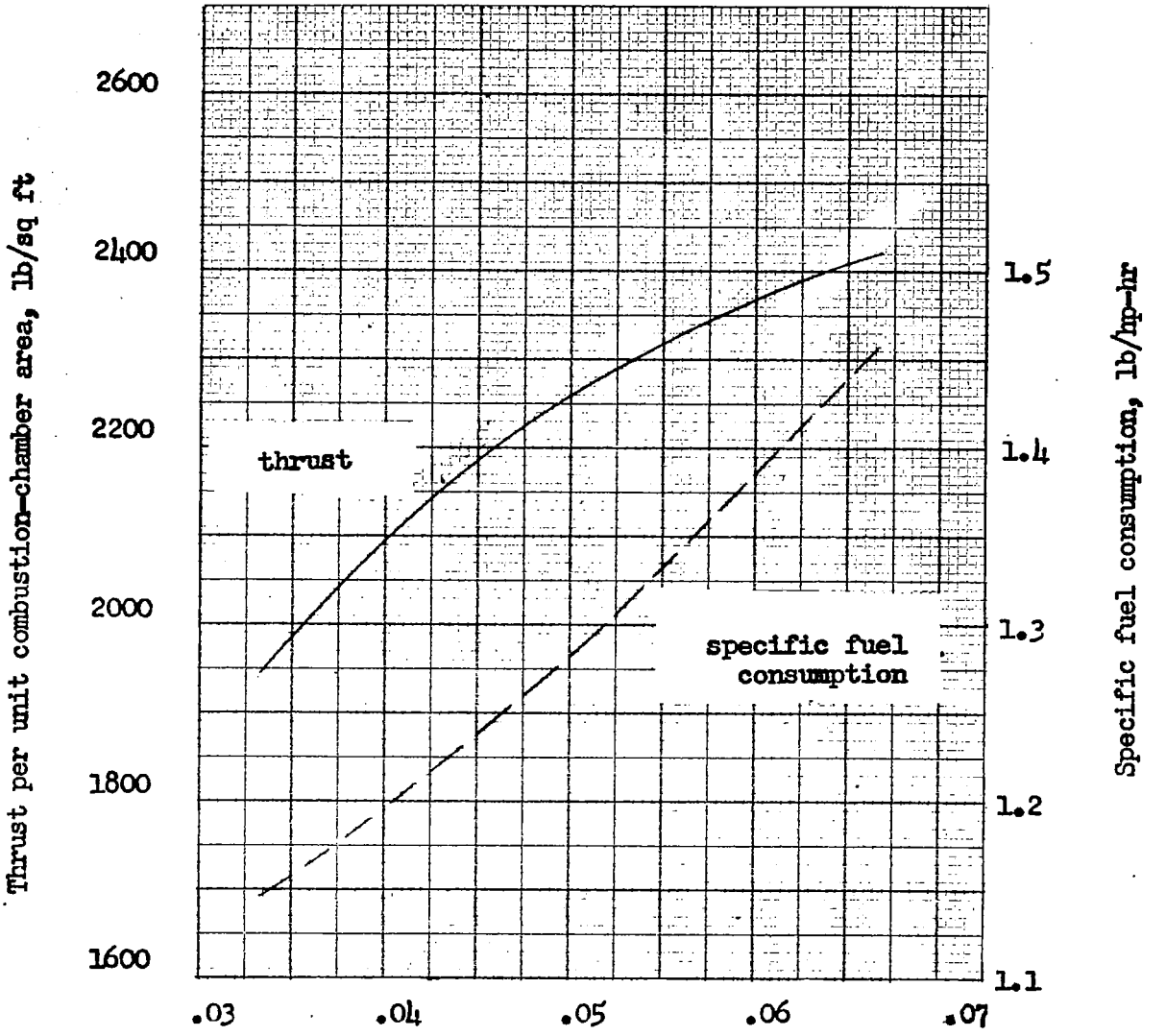

(c) Thrust and economy cross plots.
Figure 8. - Concluded.

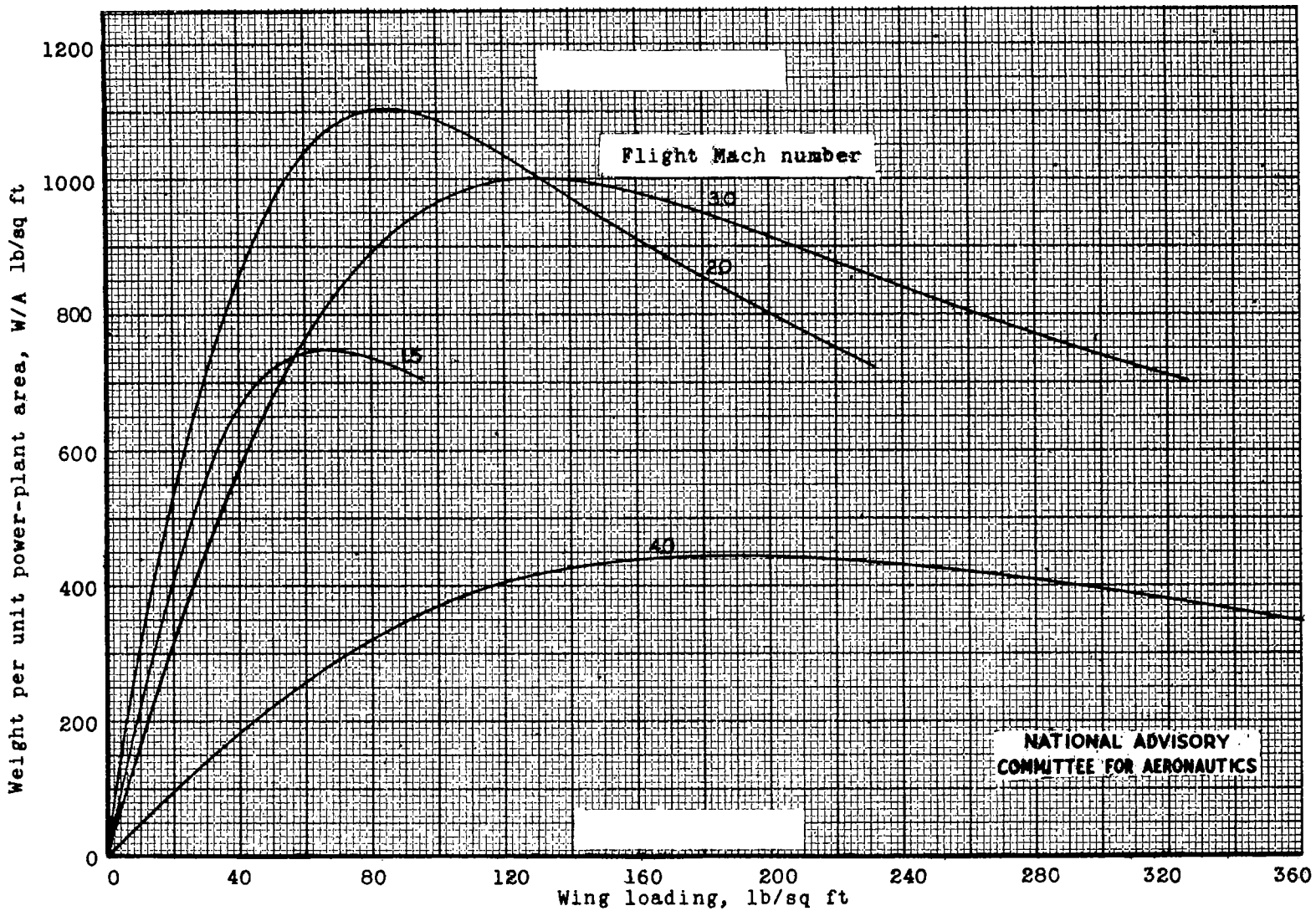

(a) Altitude, 60,000 feet; l/d = 10.

Figure 9.- Speed performance chart.

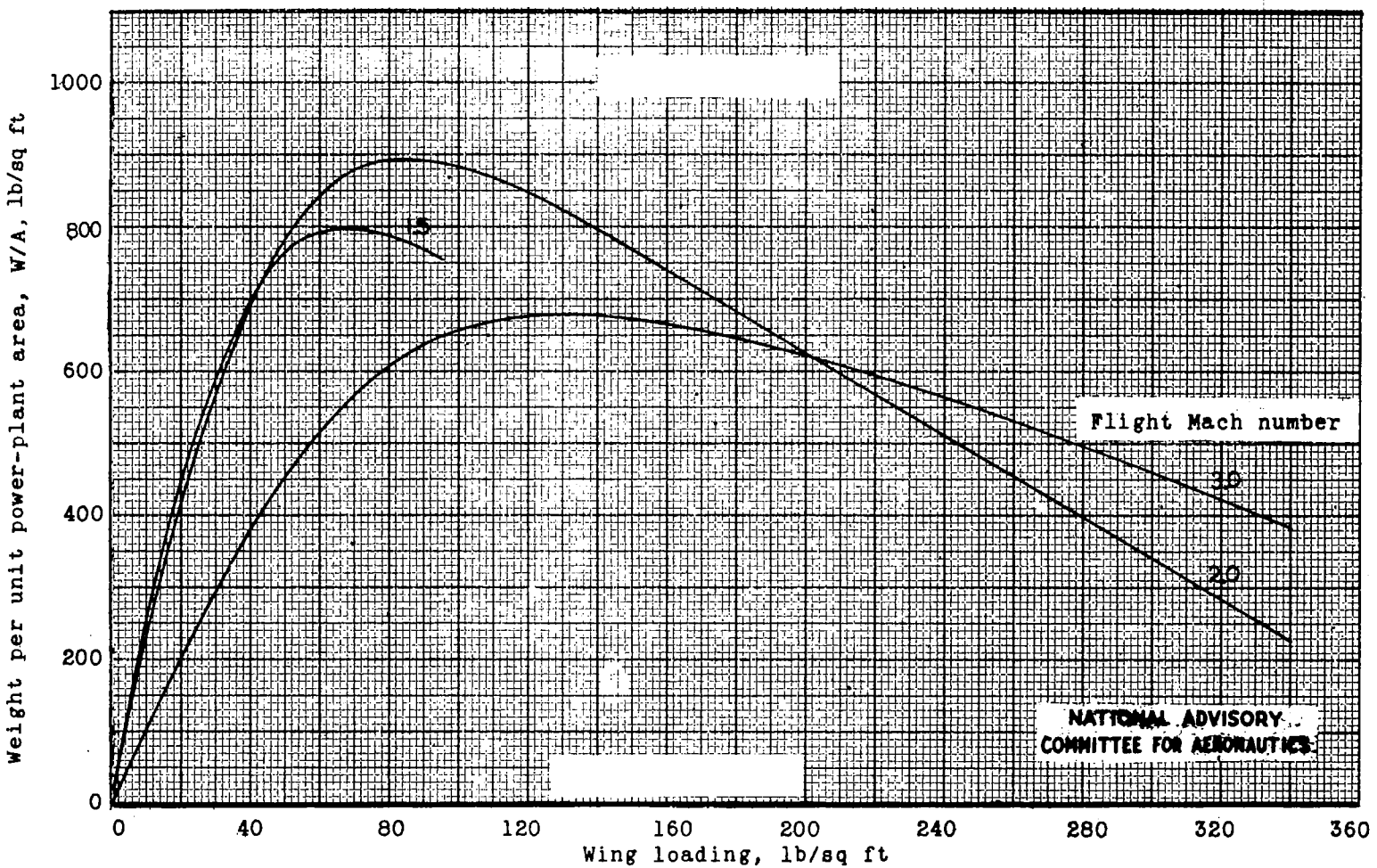

(b) Altitude, 60,000 feet; l/d = 15.

Figure 9.- Continued.

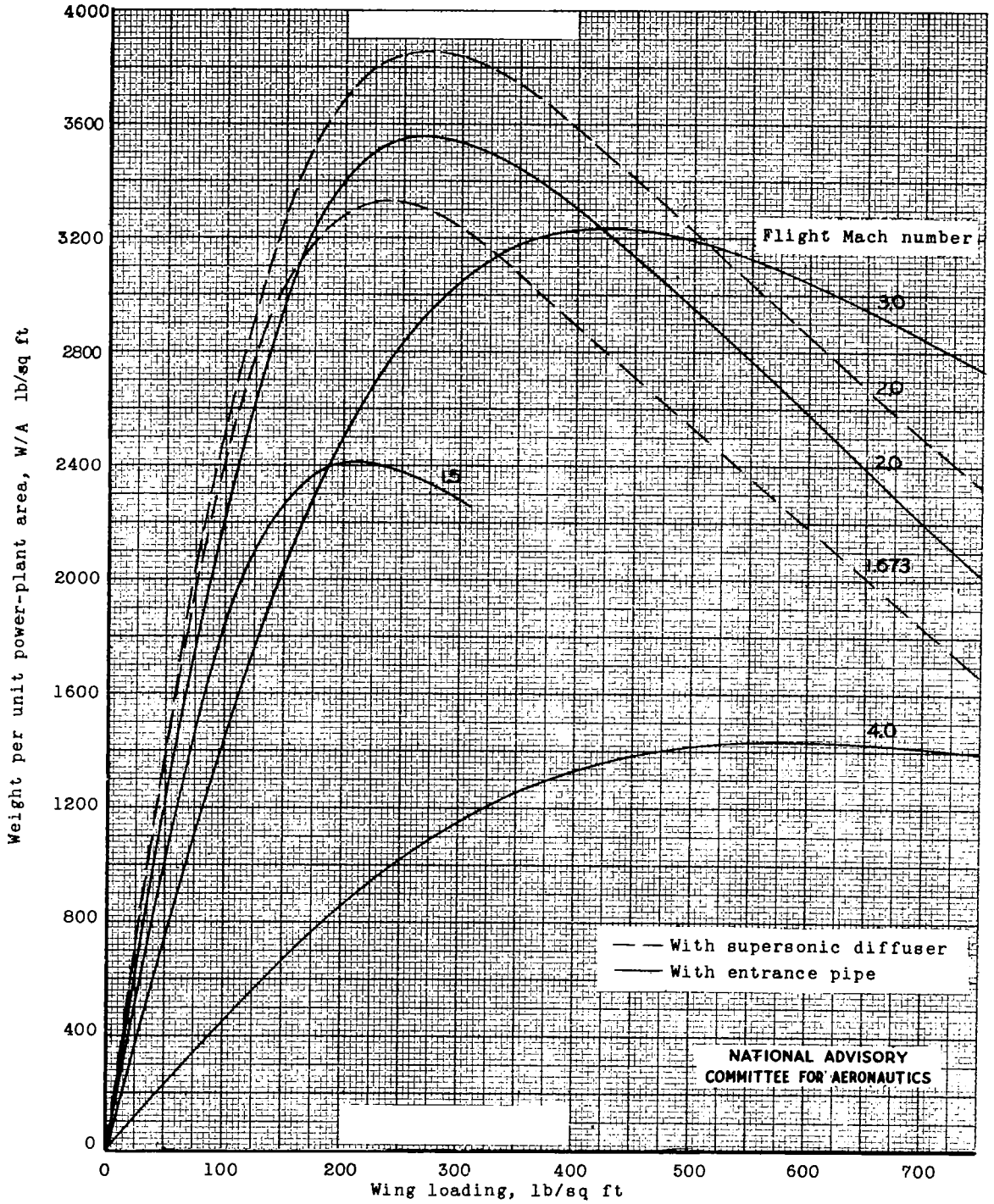

(c) Altitude, 35,500 feet; l/d = 10.

Figure 9.- Continued.

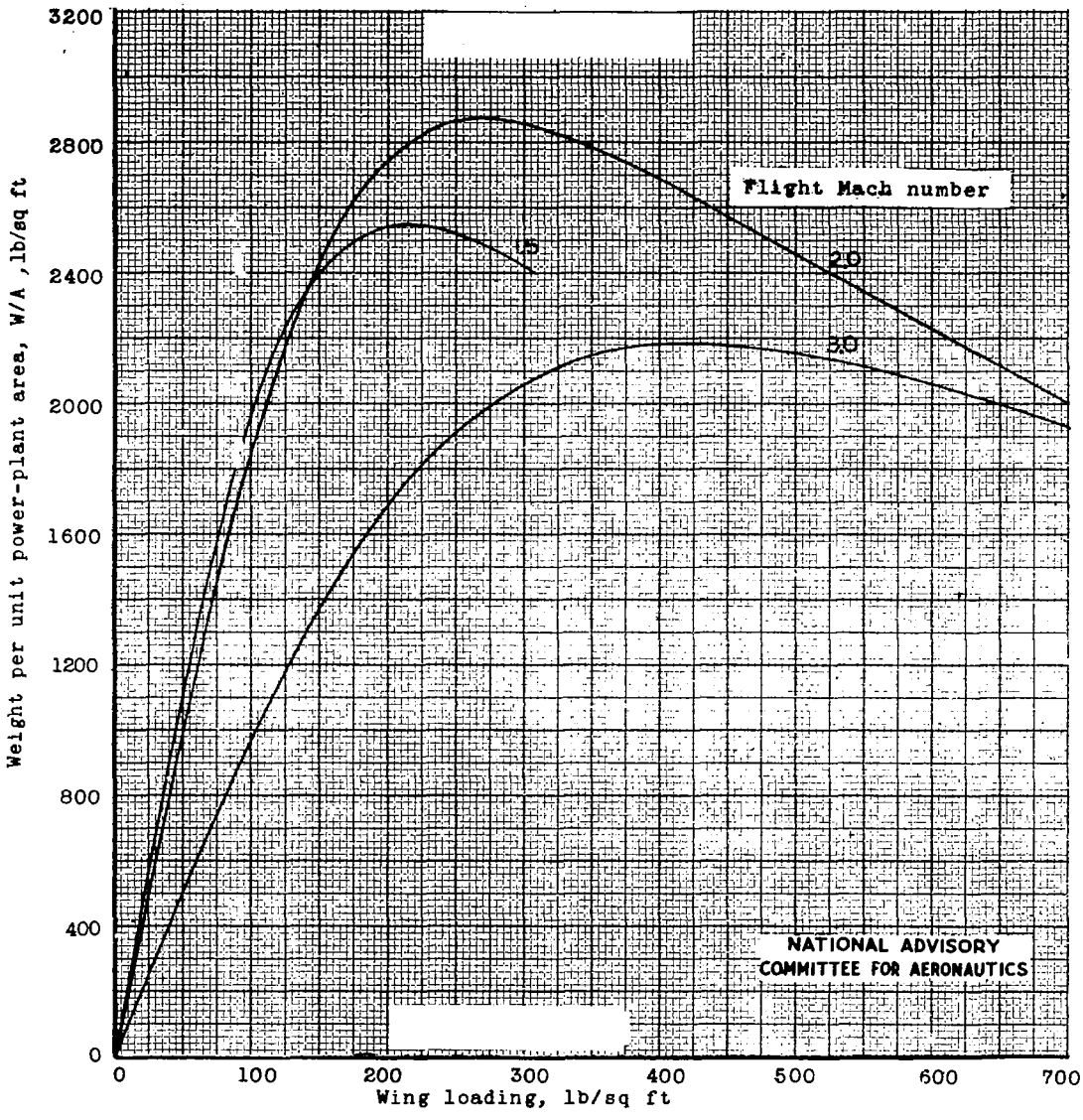

(d) Altitude, 35,500 feet; $l/d = 15$.

Figure 9.- Continued.

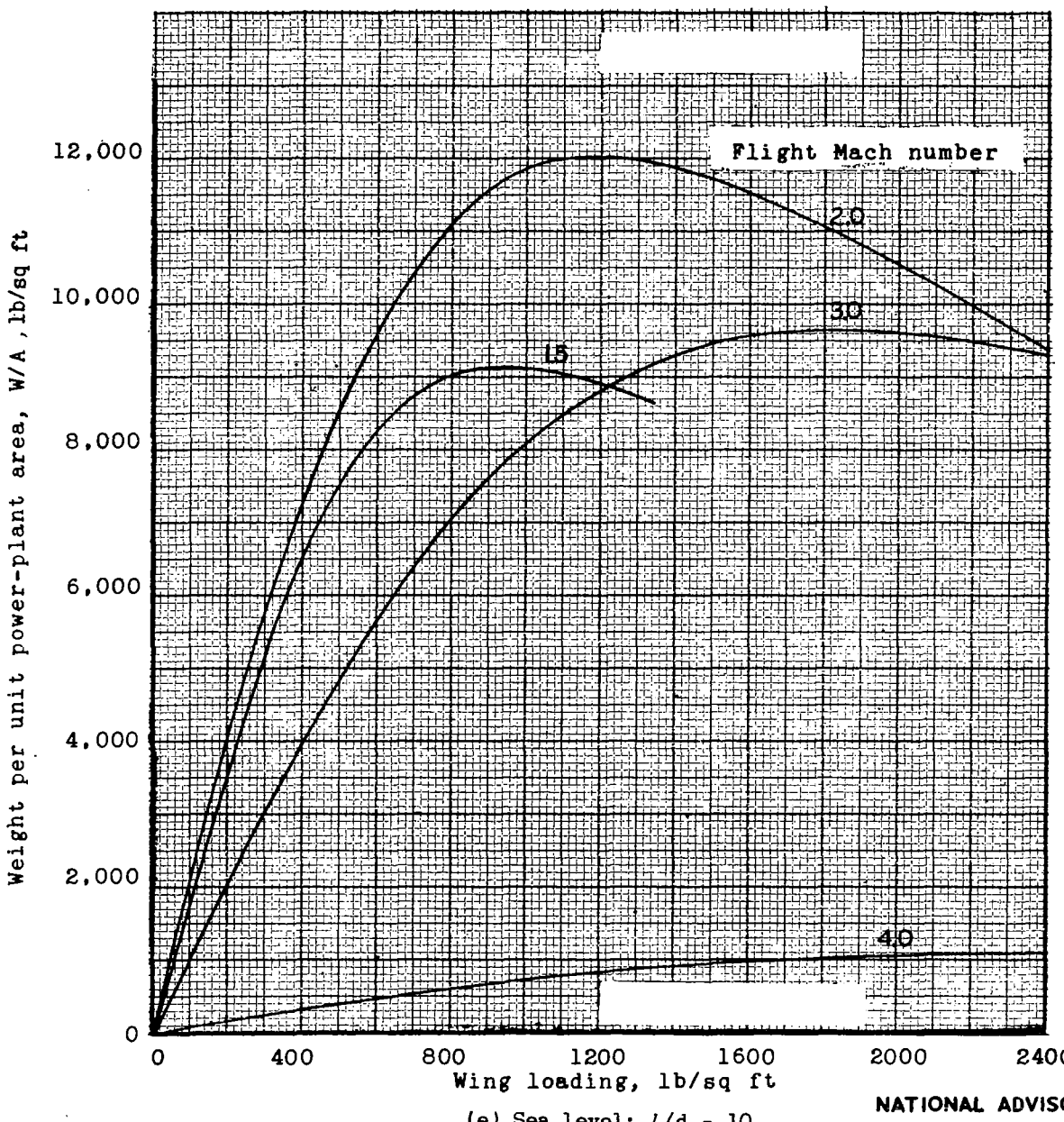

(e) Sea level; $l/d = 10$.

Figure 9.- Concluded.

NATIONAL ADVISORY COMMITTEE FOR AERONAUTICS

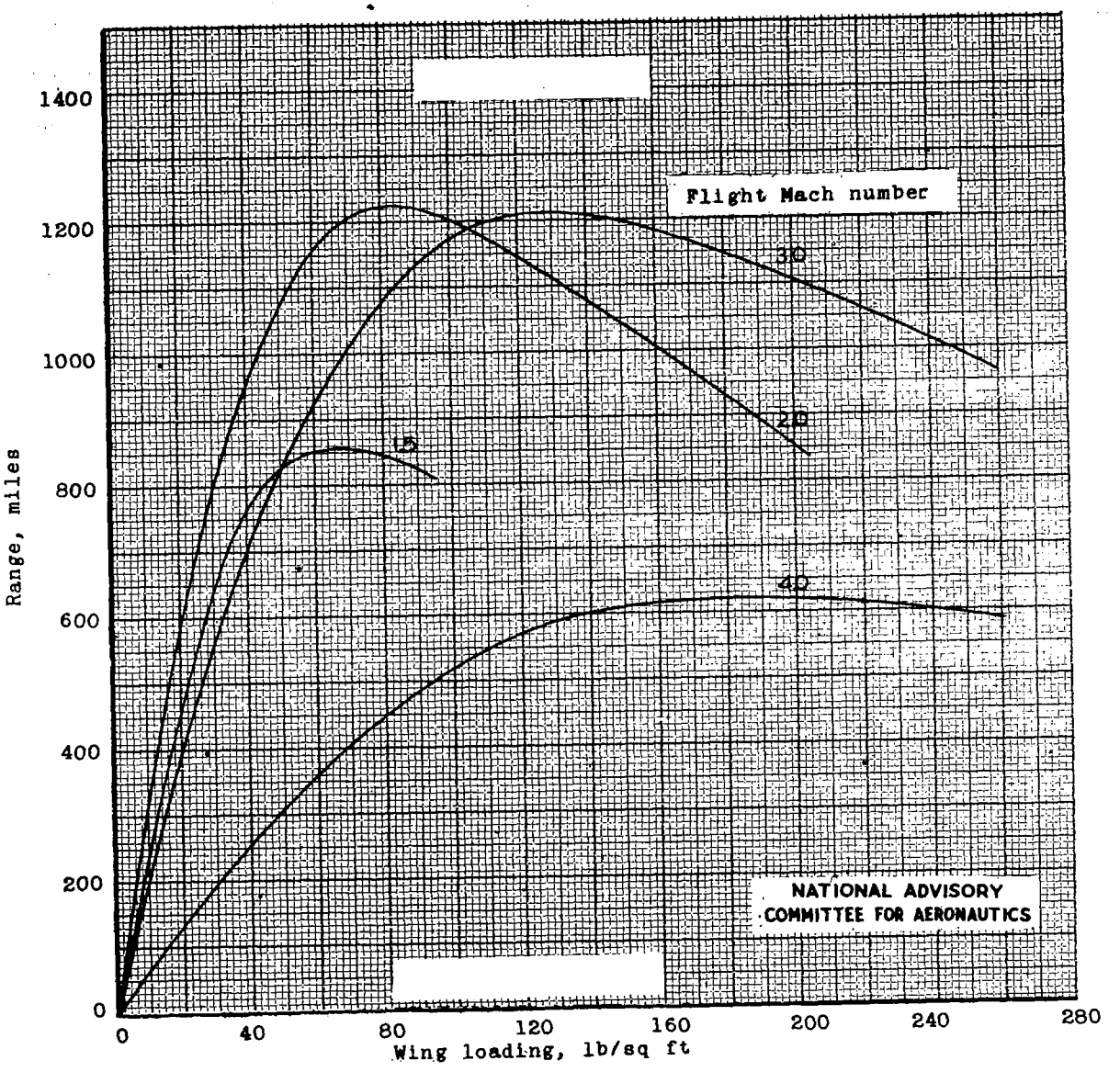

(a) Altitude, 60,000 feet; l/d = 10.

Figure 10.- Range performance with fuel load 50 percent of gross weight.

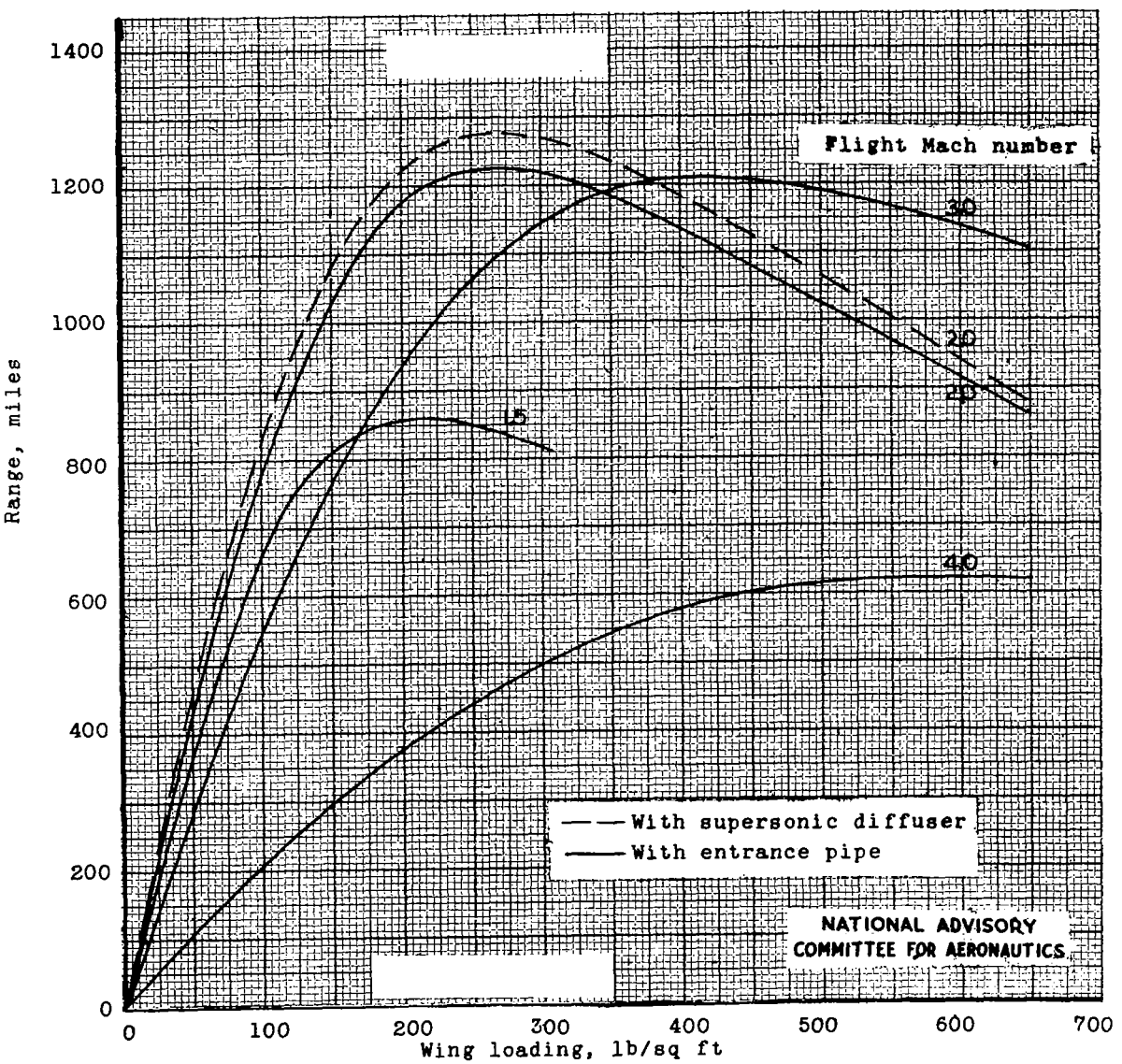

(b) Altitude, 35,500 feet; l/d = 10.

Figure 10.- Continued.

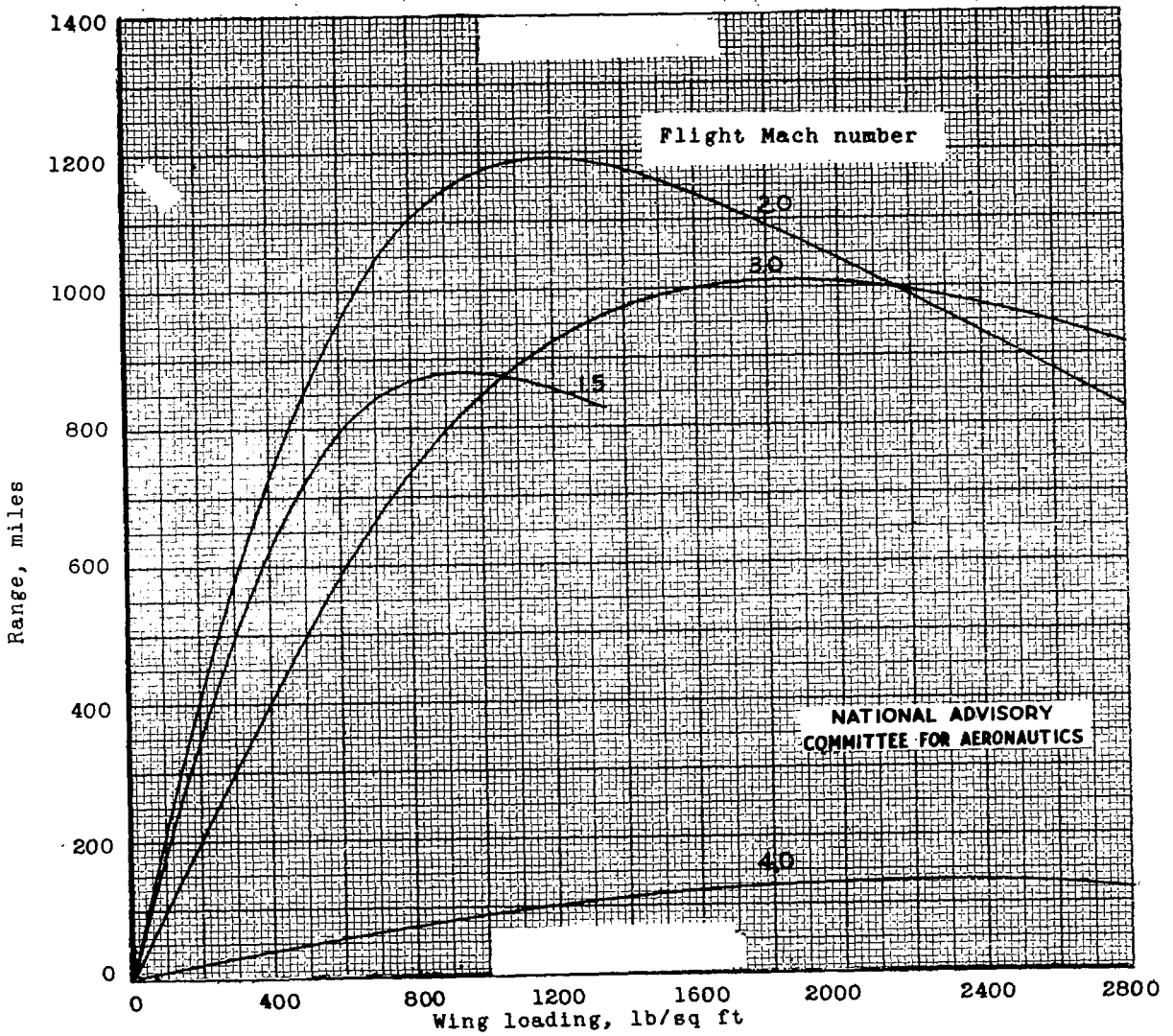

(c) Sea level; l/d = 10.

Figure 10.- Concluded.

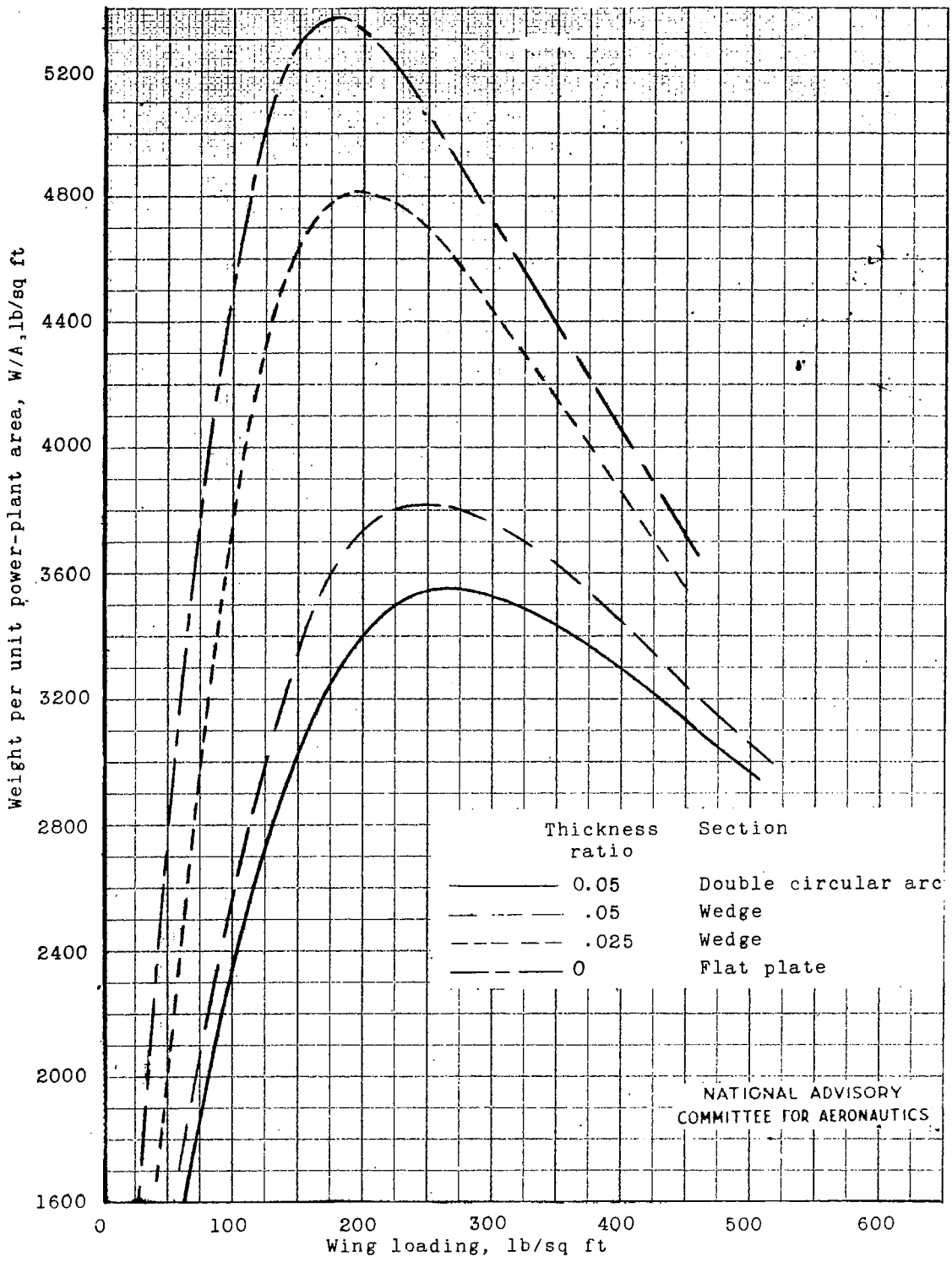

(a) Effect on speed.

Figure 11. - Effect of wing section on speed and range. Altitude, 35,500 feet; fuel-air ratio, 0.033; l/d = 10; flight Mach number, 2.0.

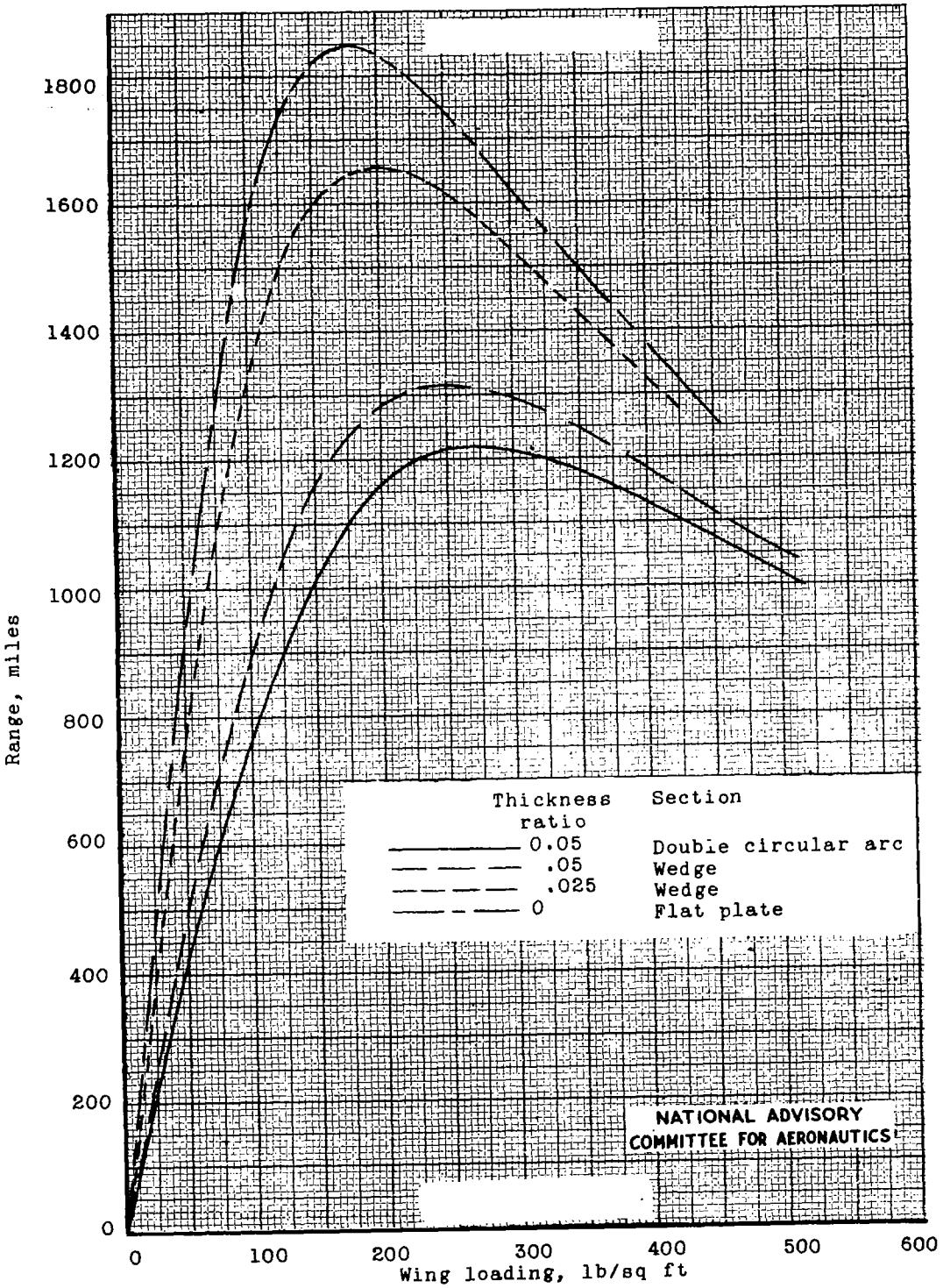

(b) Effect on range. Fuel load 50 percent of gross weight.

Figure 11.- Concluded.

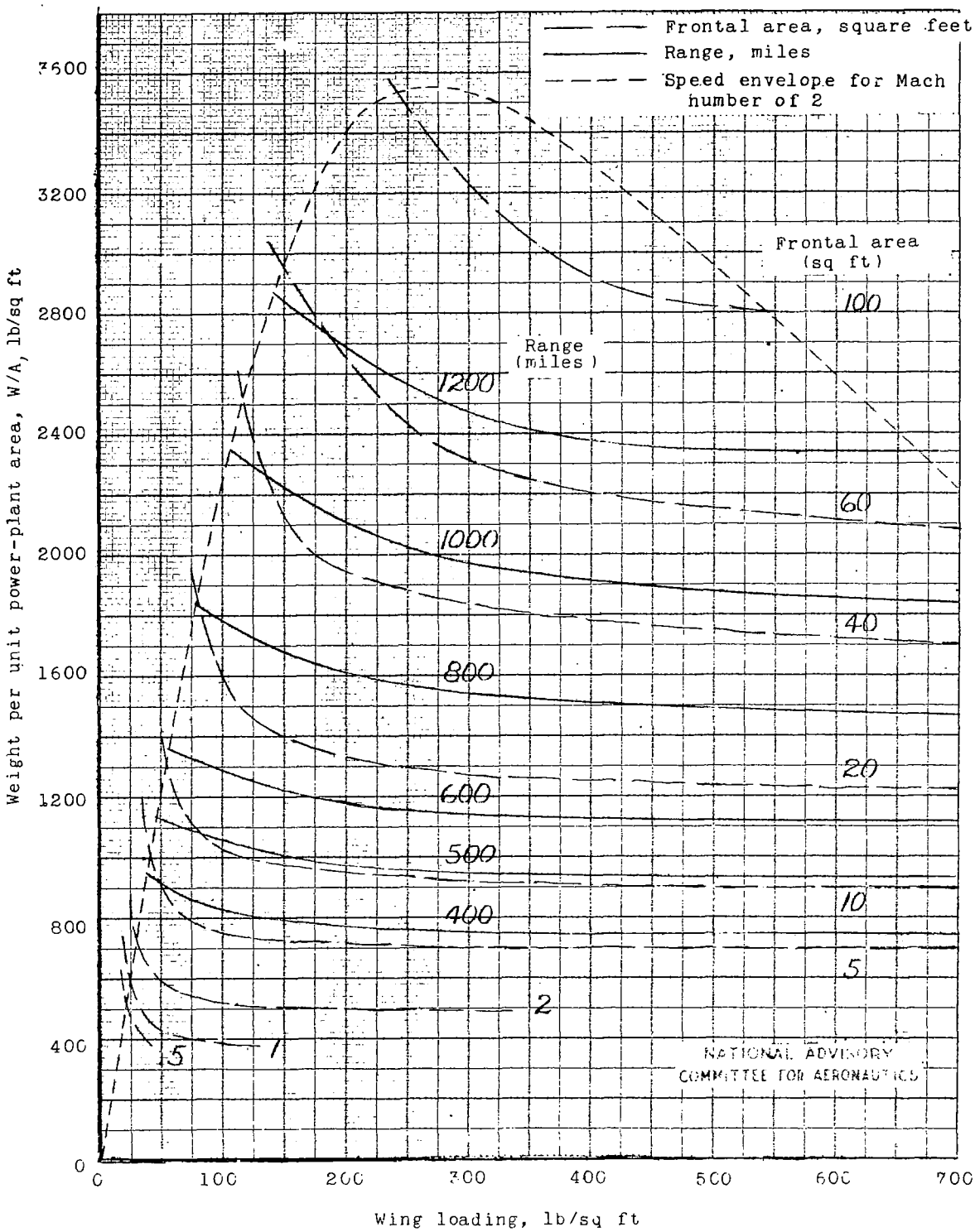

(a) $l/d=10$.

Figure 12. - Range obtained by using estimated fuel weight. Altitude, 35,500 feet; fuel-air ratio, 0.033

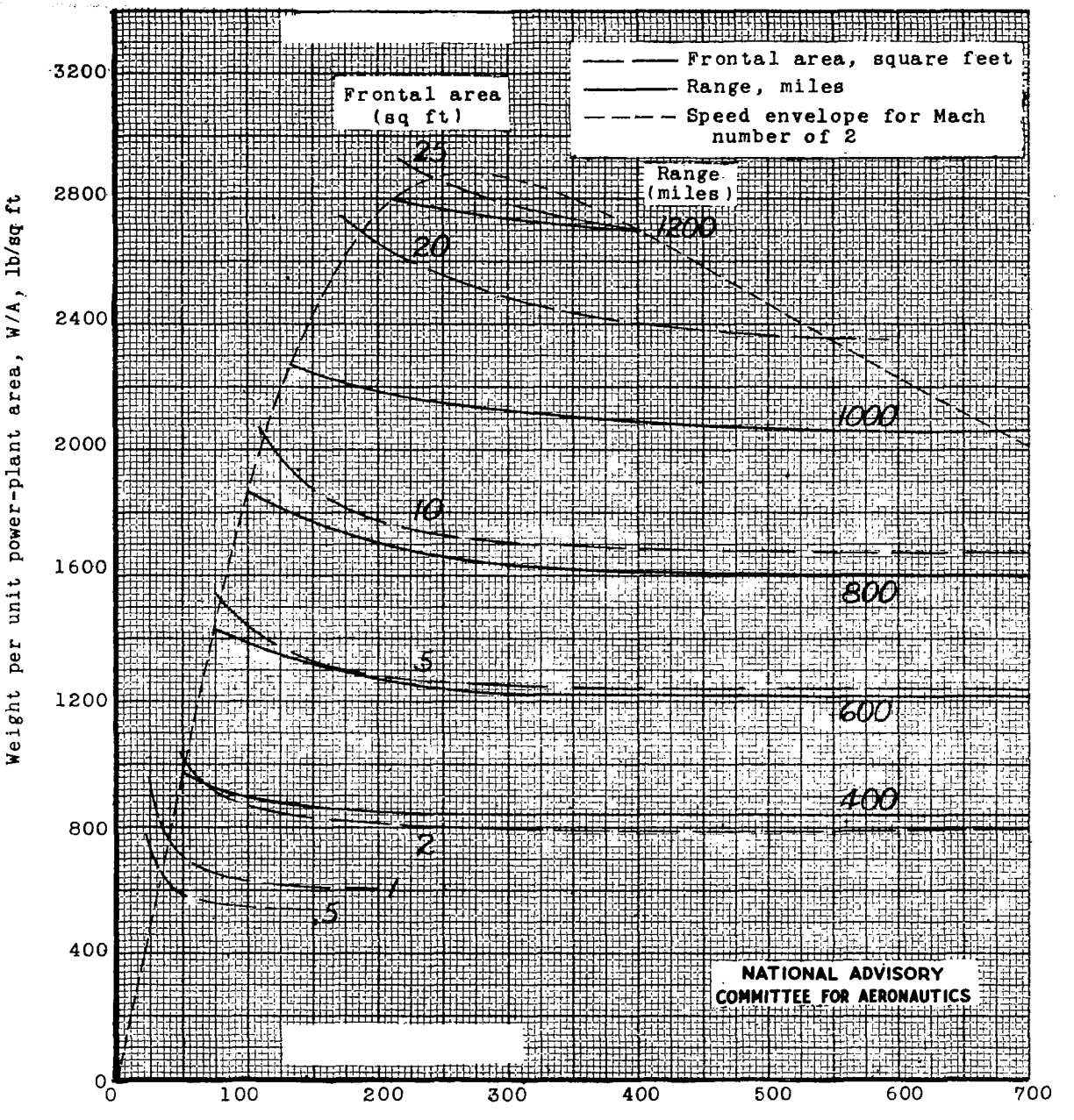

(b) $l/d=15$.

Figure 12.- Concluded.

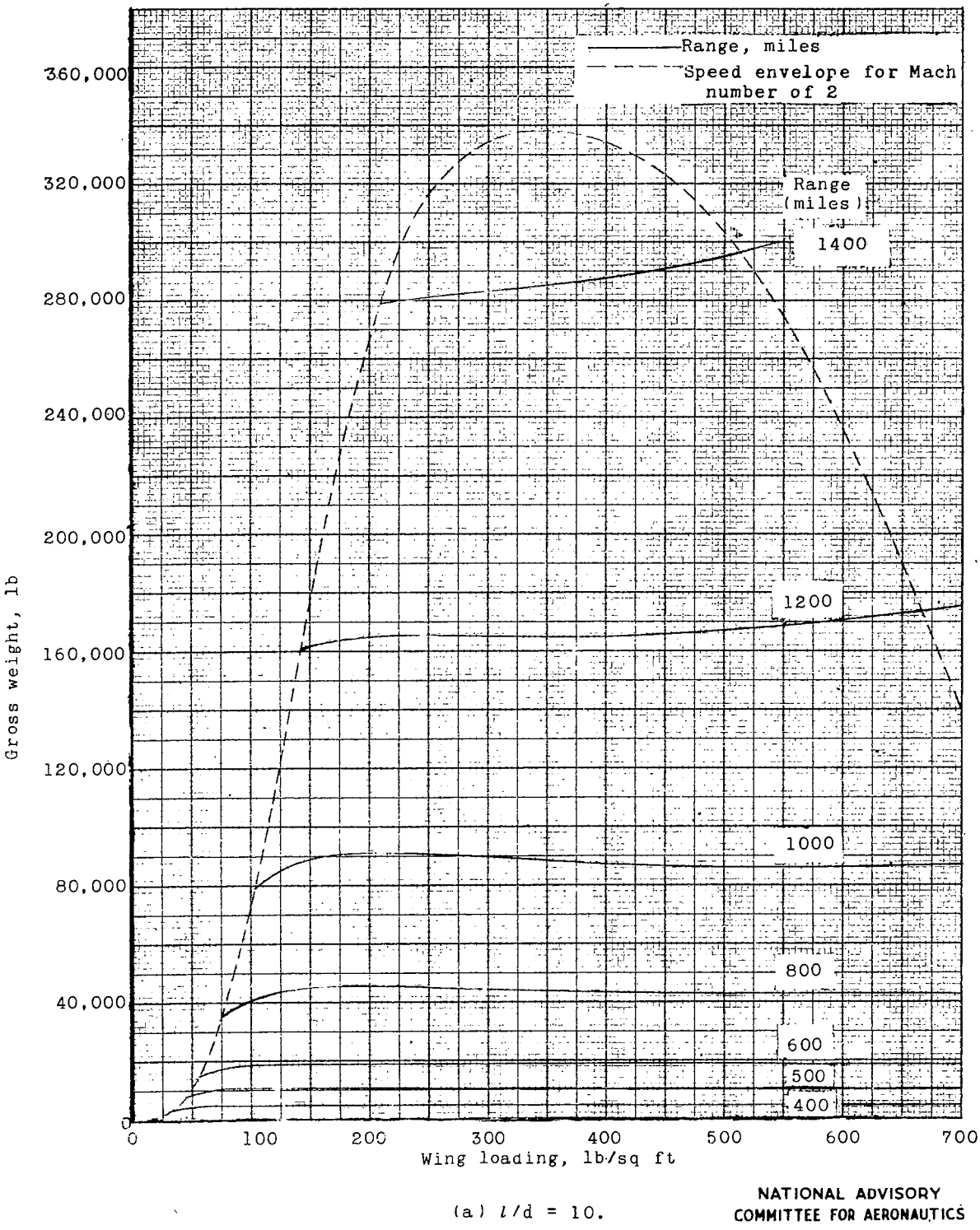

Figure 13.- Range as a function of gross weight and wing loading. Estimated fuel weight; altitude, 35,500 feet; fuel-air ratio, 0.033.

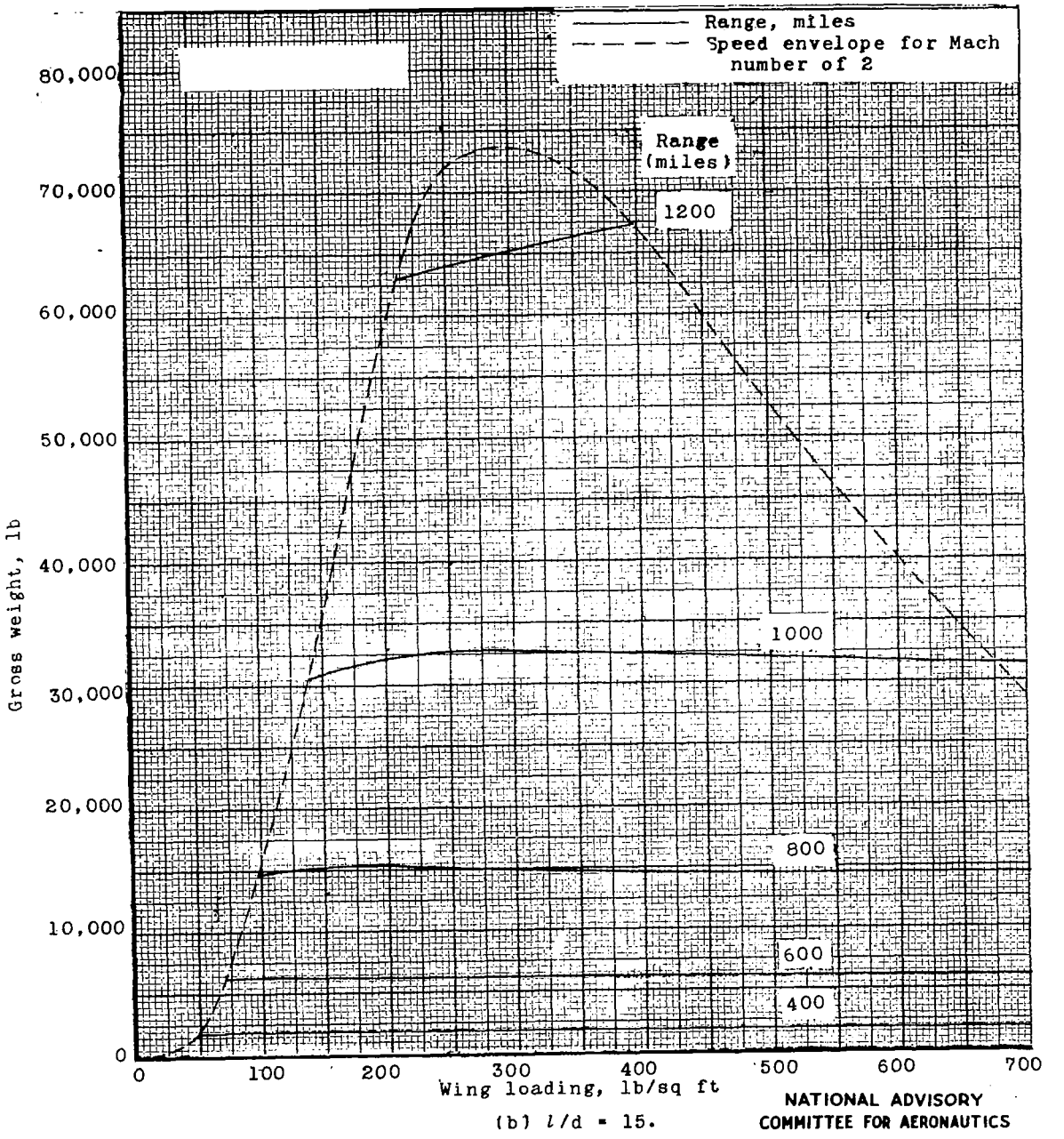

(b) $l/d = 15$.

Figure 13.- Concluded.

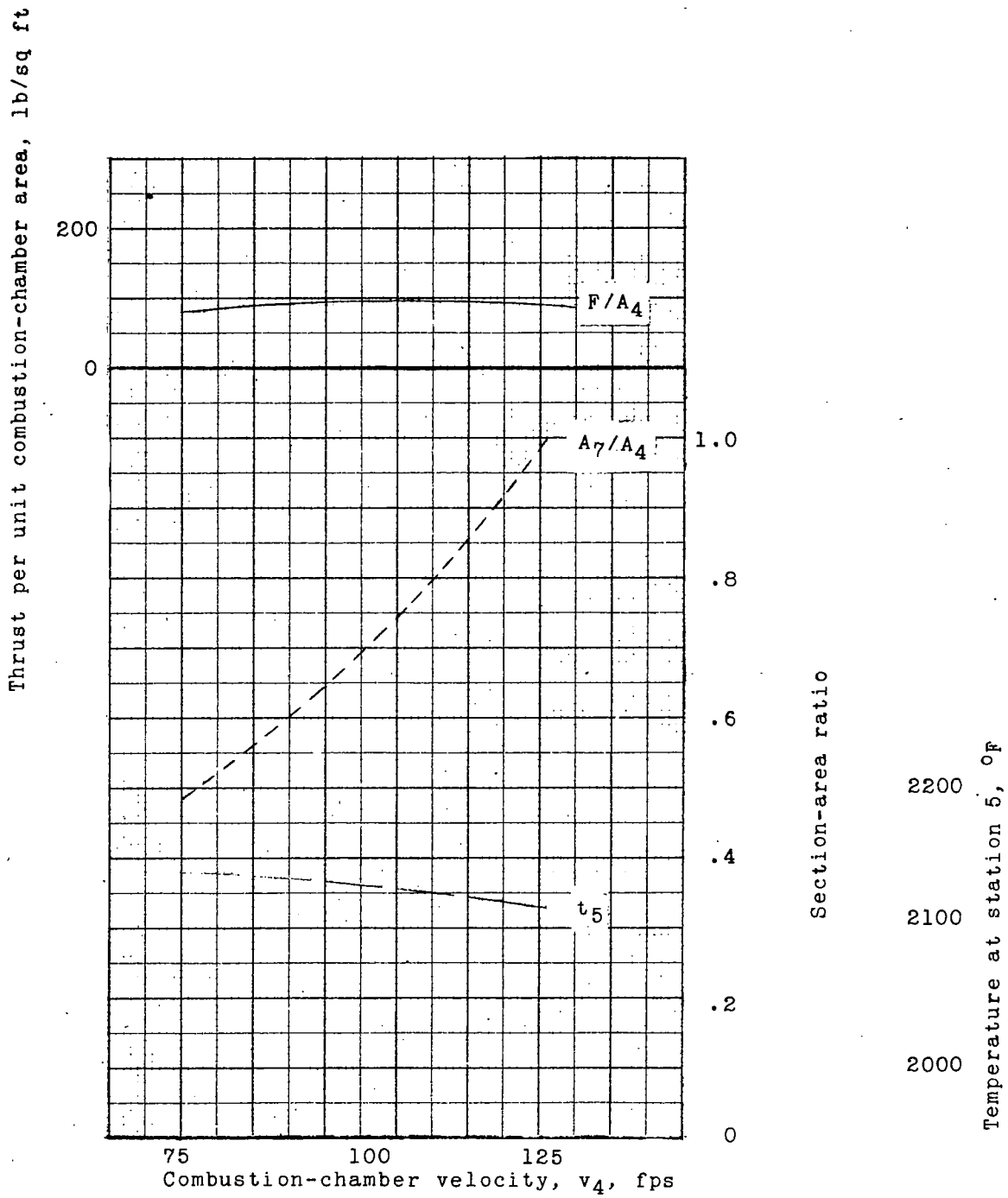

(a) Mach number, 0.4; open-nose cowling.

Figure 14. - Data for subsonic power plant. Sea level; fuel-air ratio, 0.033.

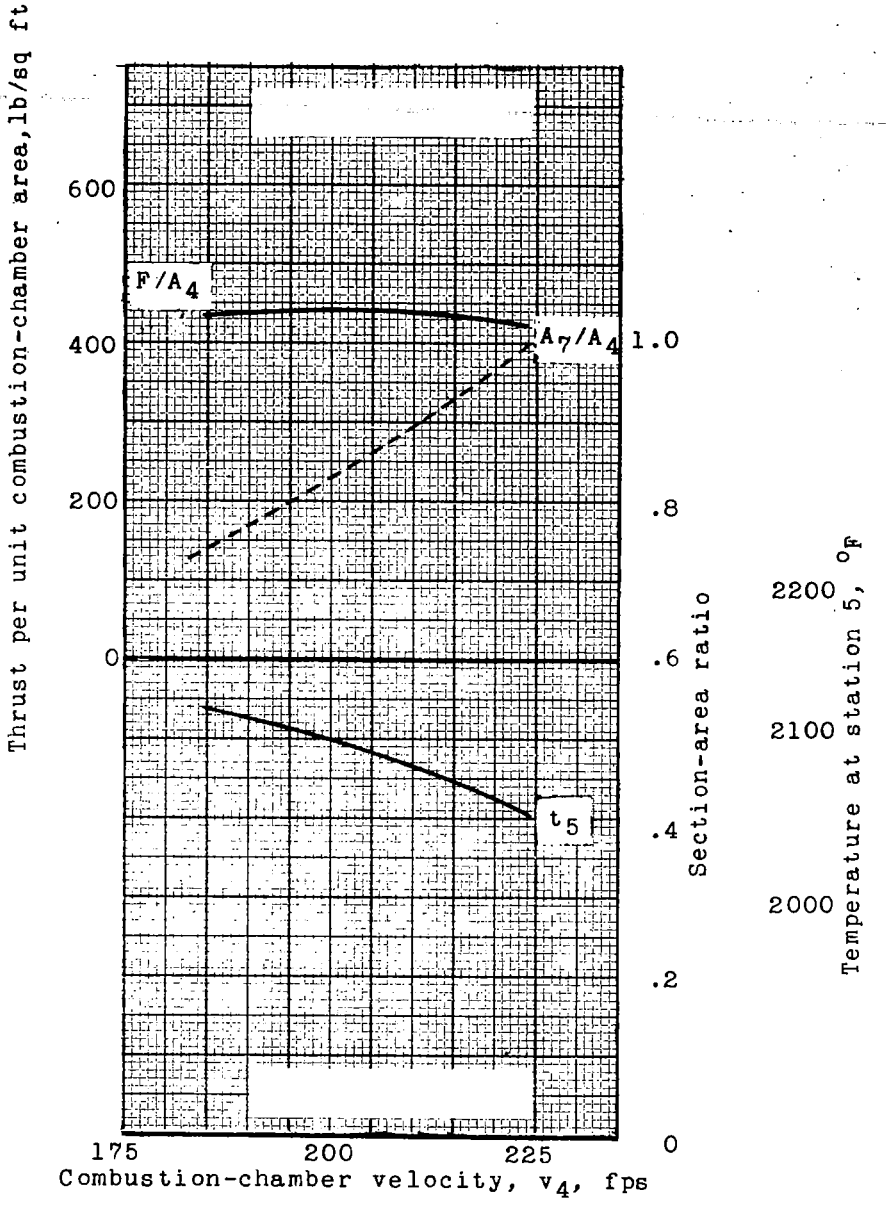

(b) Mach number, 0.8; open-nose cowling.

Figure 14.- Continued.

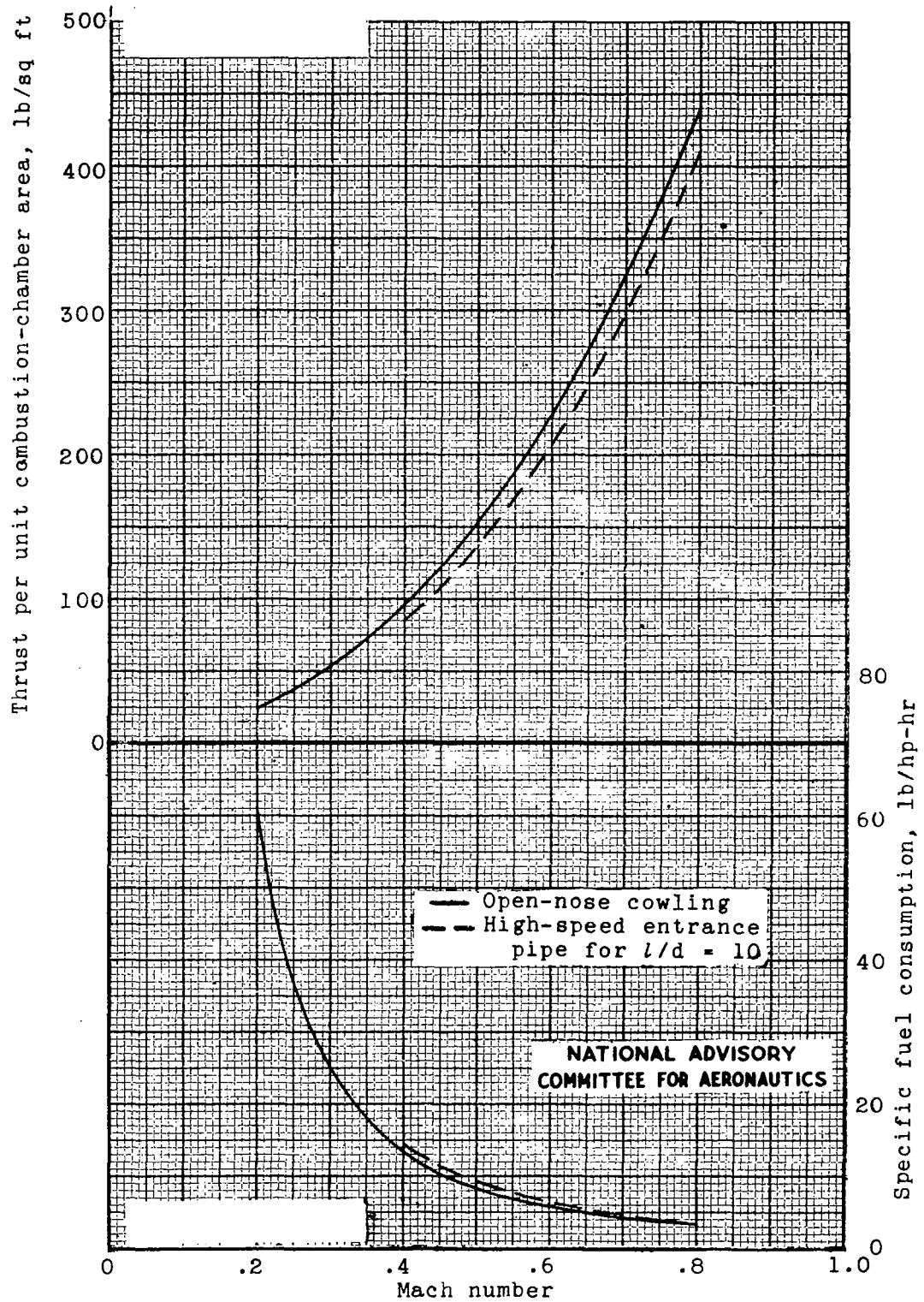

(c) Thrust and economy cross plots.

Figure 14.- Concluded.

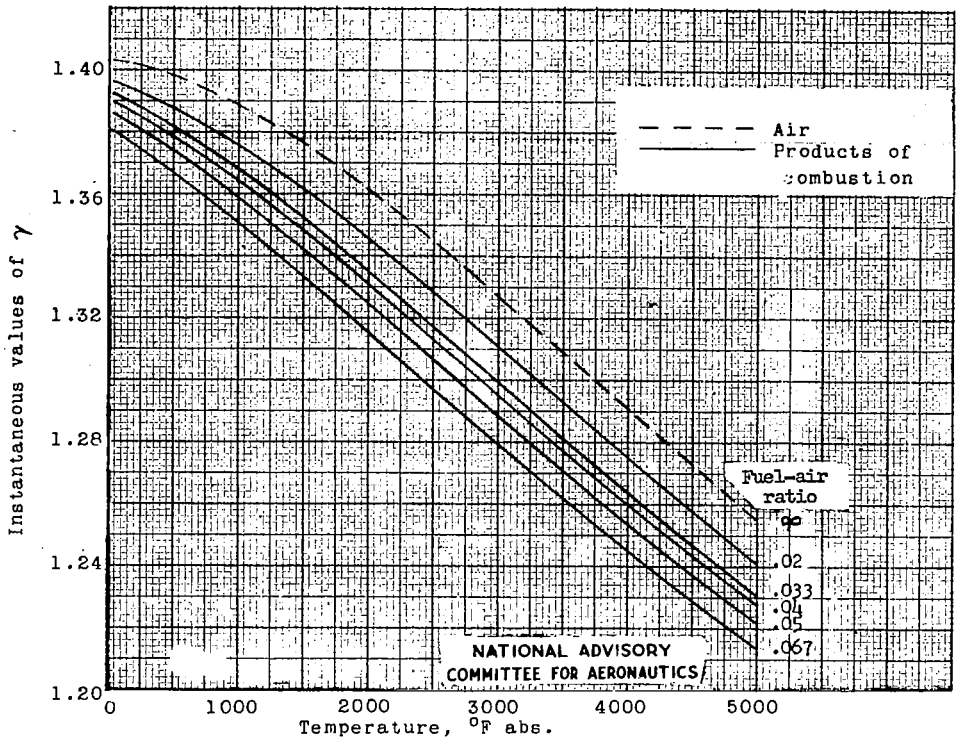

(a) Instantaneous values of the ratio of specific heats.

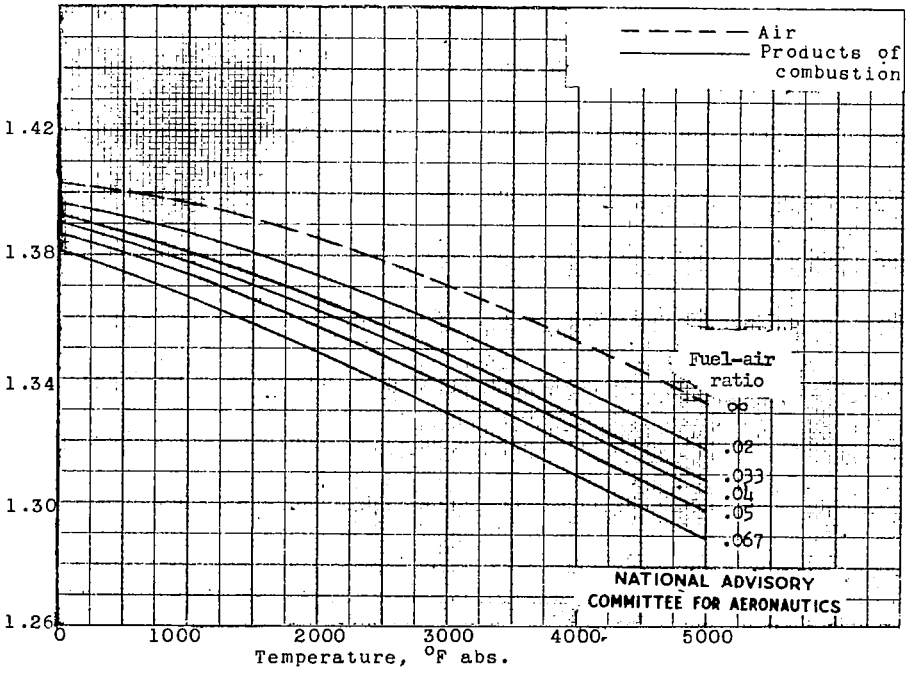

(b) Values of the ratio of specific heats averaged between 0 and T.

Figure 15.- Properties of air and the products of combustion.

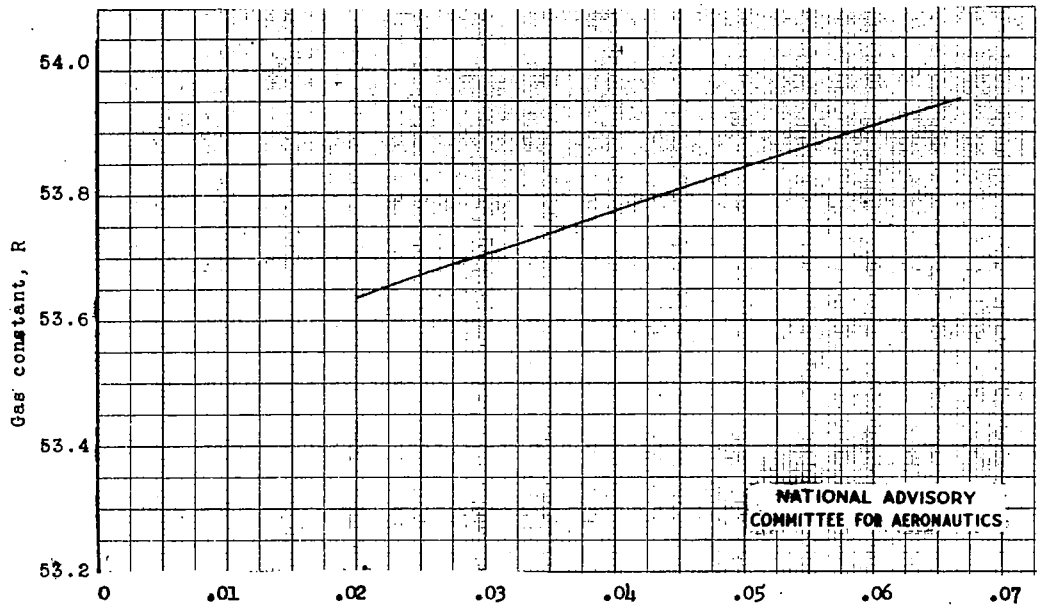

Fuel-Air Ratio
(c) Variation of gas constant with fuel-air ratio.
Figure 15. - Concluded.

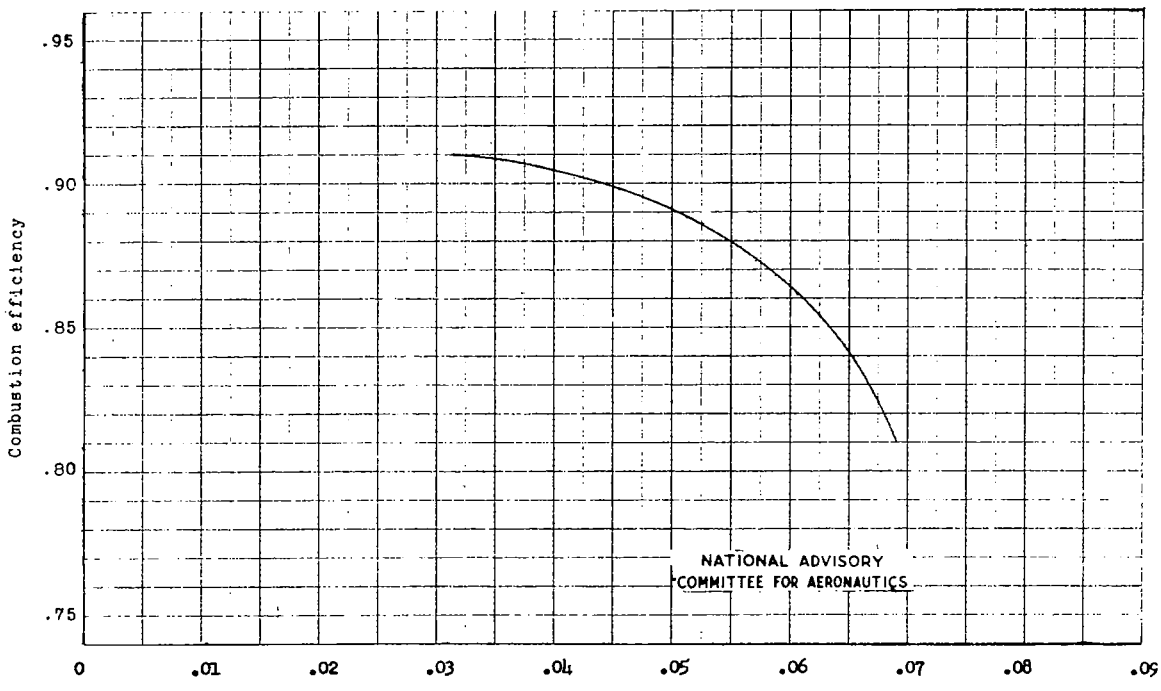

Fuel-air ratio
Figure 16.- Values of combustion efficiency used.

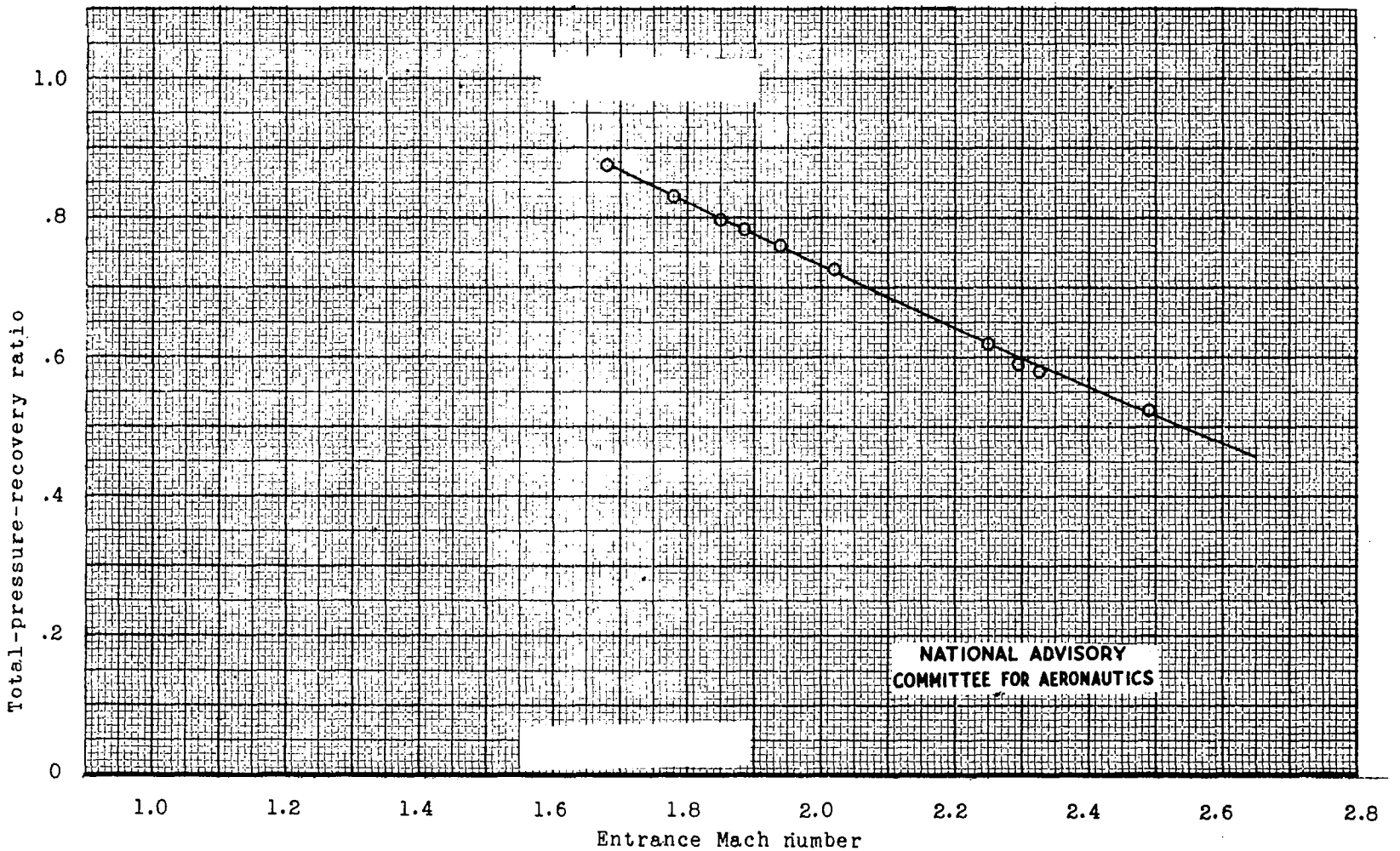

Figure 17.- Performance of supersonic diffuser with exit-cone angle of 3°. Contraction ratio, 1.137. (From fig. 8 of reference 4.)

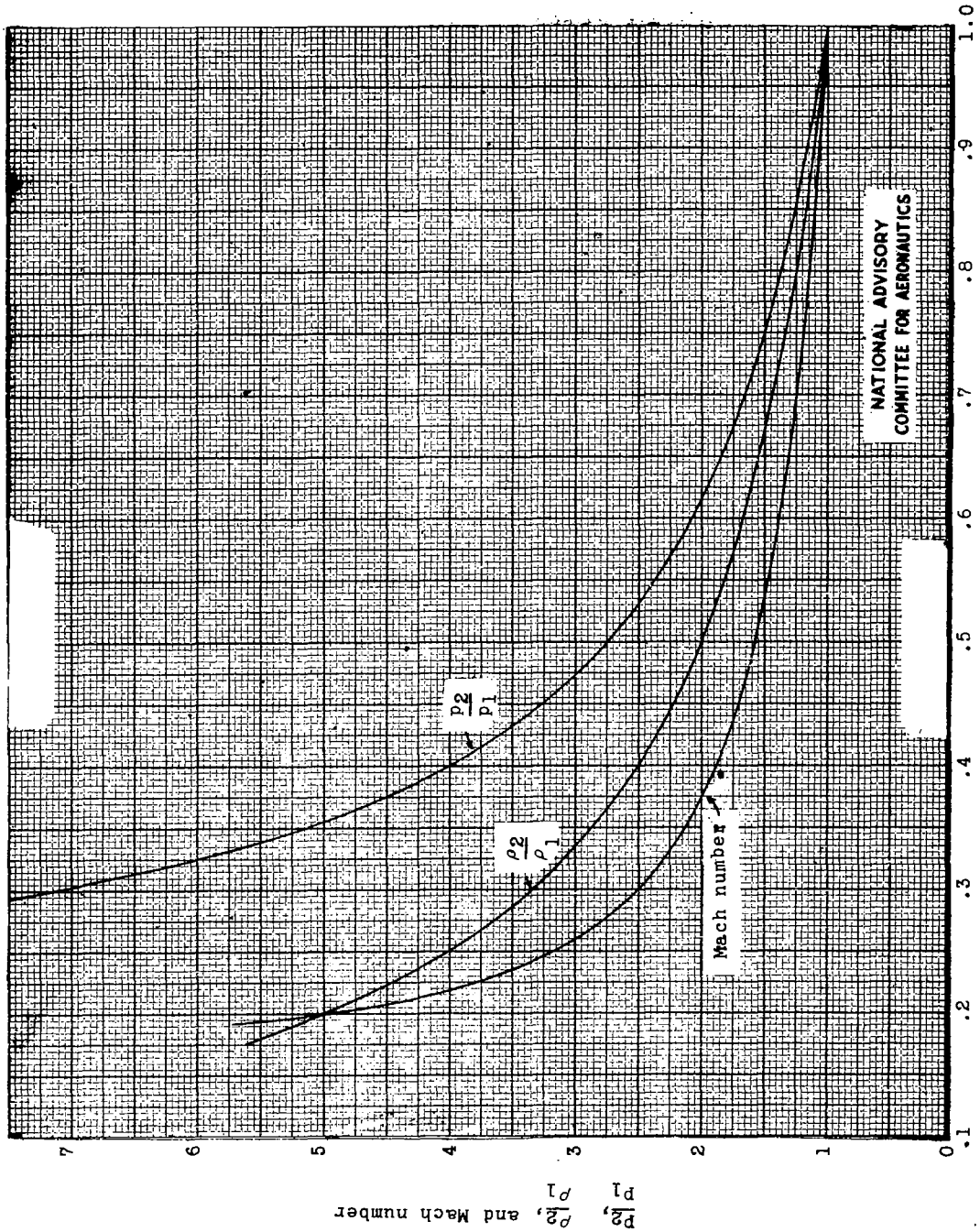

Figure 18.- Changes of velocity, density, and pressure across a shock wave. (From reference 7.)

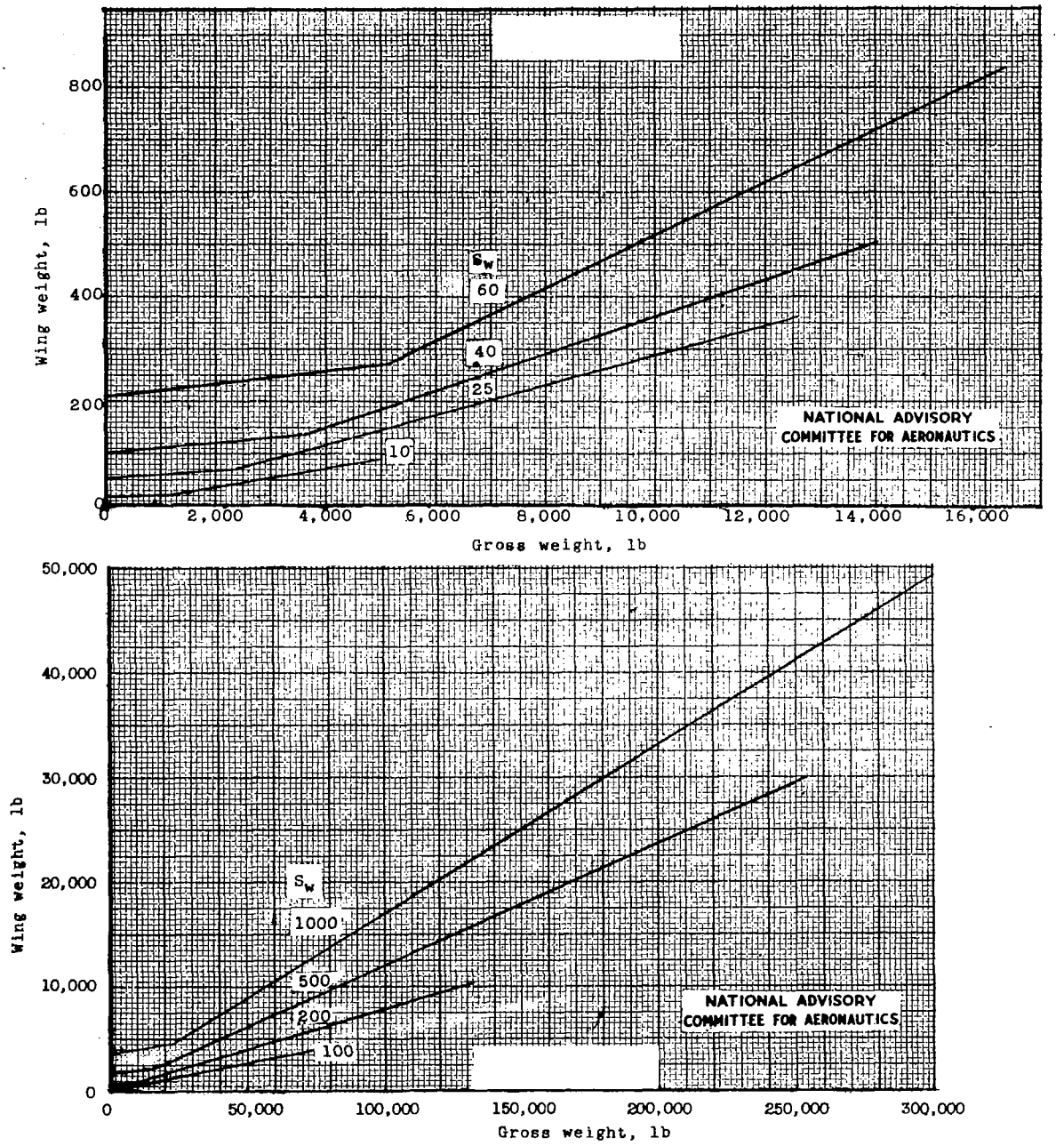

Figure 19.- Weight of double-circular-arc duralumin wings. Thickness ratio, 0.05; aspect ratio, 4.0; load factor, 4.0; taper ratio, 2.5.

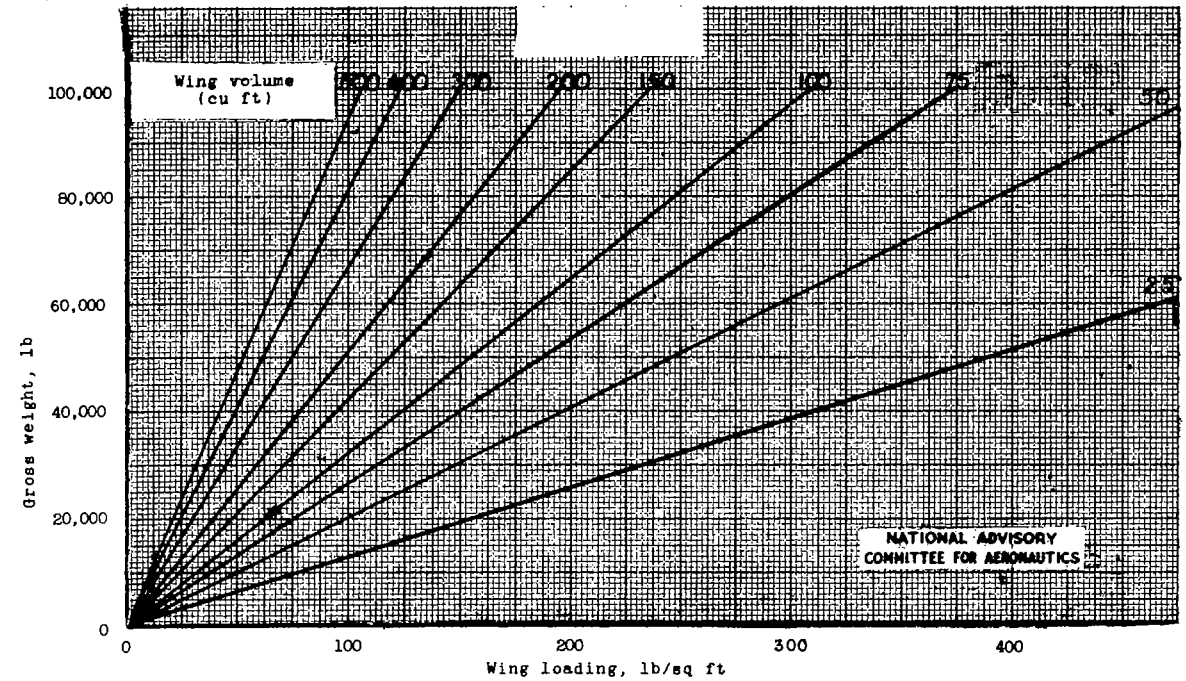

(a) Aspect ratio, 4; taper ratio, 2.5.

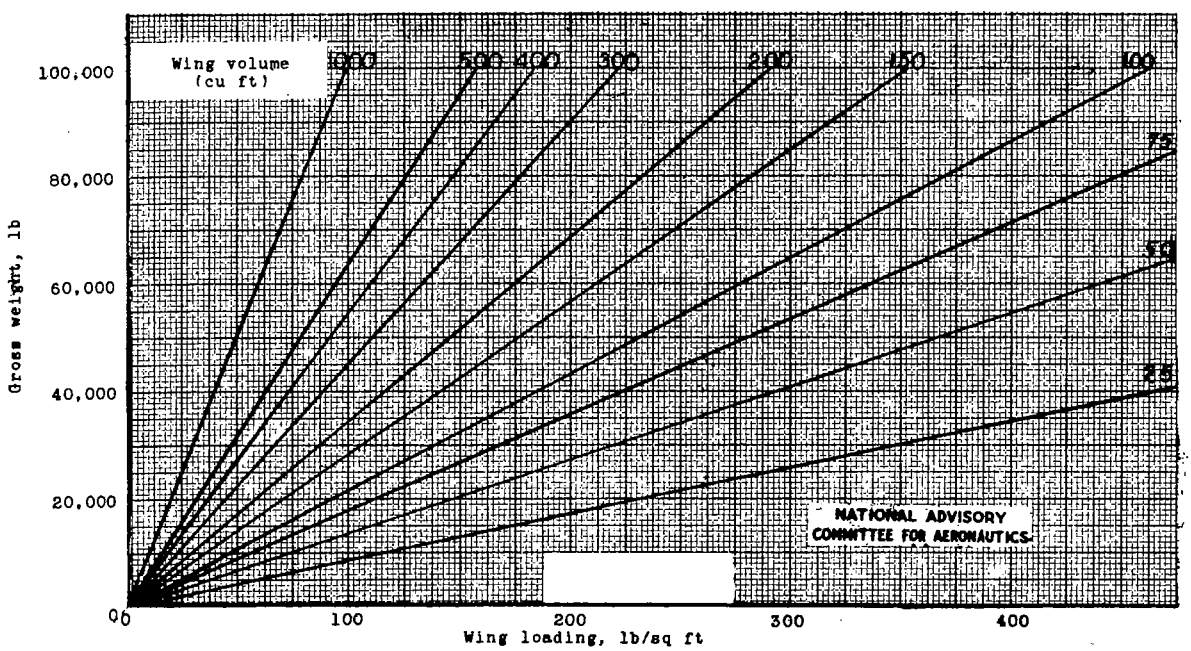

(b) Aspect ratio, 2.0; taper ratio, ∞.

Figure 20.- Volume of double-circular-arc wings. Thickness ratio, 0.05.

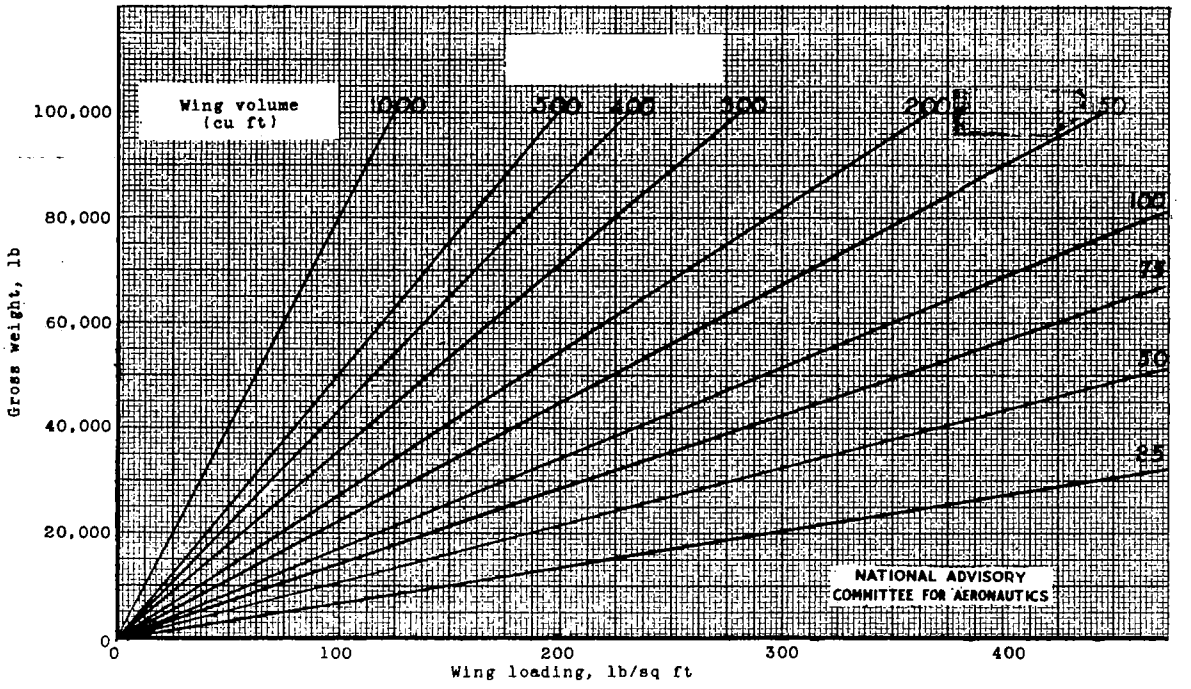

(c) Aspect ratio, 1.0; taper ratio, ∞.

Figure 20.- Concluded.

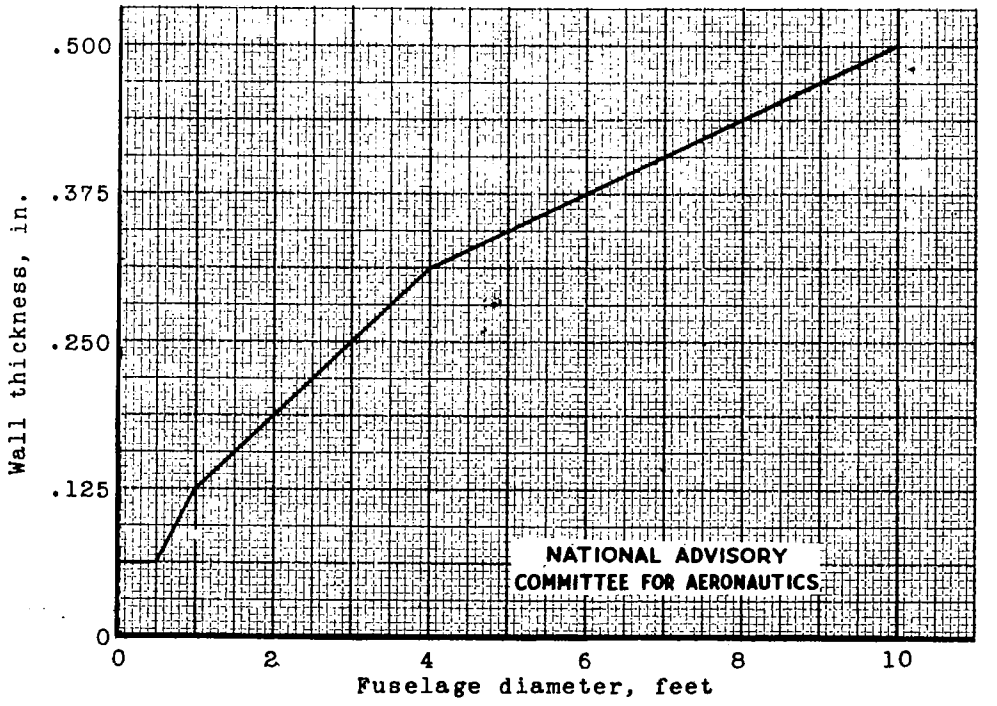

Figure 21.- Values of fuselage-wall thickness.

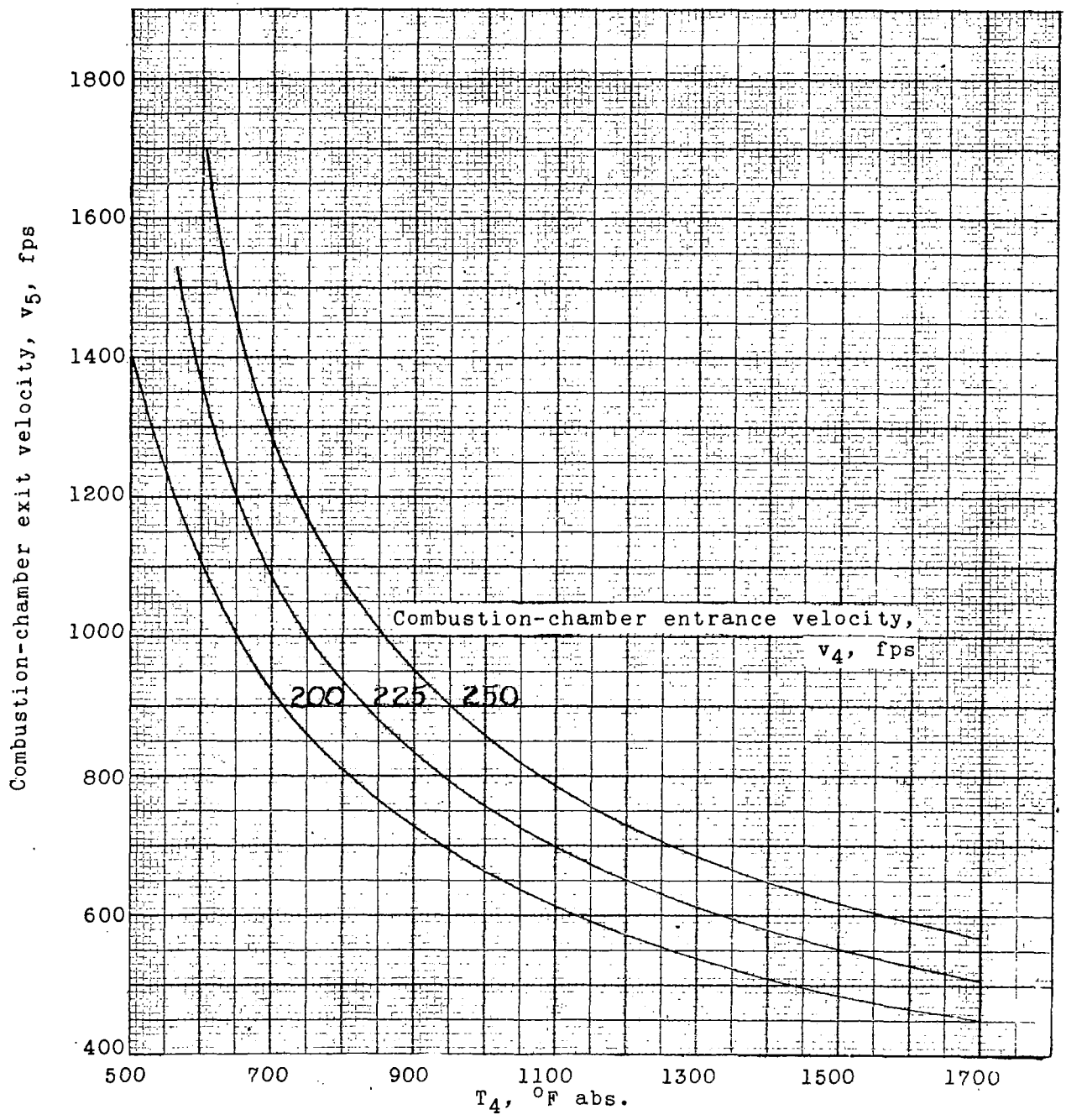

Figure 22.- Solution for combustion-chamber exit velocity. Fuel-air ratio, 0.033.